Stony Brook University

A study of cell death pathways and innate immunity in cancer chemotherapy

A Dissertation Presented

by

Jennifer Lynn Guerriero

to

The Graduate School

in Partial Fulfillment of the

Requirements

for the Degree of

Doctor of Philosophy

in

Molecular and Cellular Biology

(Immunology and Pathology)

Stony Brook University

August 2010

Stony Brook University

The Graduate School

Jennifer Lynn Guerriero

We, the dissertation committee for the above candidate for the

Doctor of Philosophy degree, hereby recommend

acceptance of this dissertation.

Dr. Wei-Xing Zong, Dissertation Advisor
Assistant Professor, Department of Molecular Genetics and Microbiology

Dr. Howard B. Fleit, Chairperson of Defense
Associate Professor, Department of Pathology

Dr. Ute Moll
Professor, Department of Pathology

Dr. Nancy Reich
Professor, Department of Molecular Genetics and Microbiology

Dr. Howard Crawford, Outside Member of Committee
Associate Professor, Department of Pharmacology

This dissertation is accepted by the Graduate School

Lawrence Martin
Dean of the Graduate School

Abstract of the Dissertation

A study of cell death pathways and innate immunity in cancer chemotherapy

by

Jennifer Lynn Guerriero

Doctor of Philosophy

in

Molecular and Cellular Biology

(Immunology and Pathology)

Stony Brook University

2010

Dysregulation of apoptosis is associated with the development of human cancer and resistance to anti-cancer therapy. The ultimate goal of cancer treatment is to selectively induce cancer cell death and to overcome drug resistance. A deeper understanding of how chemotherapy affects tumor cell death is needed in order to develop strategically designed anti-cancer agents. An athymic mouse xenograft tumor system was established utilizing genetically defined cells that are deficient in apoptosis to examine the involvement of multiple forms of cell death induced by a DNA alkylating agent commonly used in chemotherapy. In response to DNA alkylating damage, although apoptosis facilitates a more rapid tumor regression, it is dispensable for complete tumor regression as other forms of cell death such as sporadic necrosis, senescence, autophagy, and mitotic catastrophe are activated. Of these, sporadic necrosis plays a fundamental role in tumor clearance by stimulating the innate immune response in a manner that is dependent upon the high mobility group box 1 (HMGB1) protein. HMGB1 is released from necrotic cells and once outside the cell, it acts as a damage-associated molecular pattern (DAMP) molecule to alert the host of damage by triggering immune responses. Interestingly, while DNA alkylating therapy leads to complete tumor regression in this mouse model, tumors deficient in HMGB1 fail to fully regress. The HMGB1-deficient tumors have an attenuated ability to recruit innate immune cells including macrophages, neutrophils, and natural killer (NK) cells into the treated tumor tissue. Cytokine array analysis reveals that while DNA alkylating treatment leads to suppression of pro-tumor cytokines such as IL-4, IL-10, and IL-13, loss of HMGB1 leads to elevated levels of these cytokines upon treatment. Suppression of innate immunity and HMGB1 using neutralizing antibodies leads to a failure in tumor regression. Taken together, these results indicate that DNA alkylating therapy can induce multiple forms of cell death and extracellular release of cellular contents such as HMGB1, which in turn leads to the activation of innate immunity and tumor regression.

Table of Contents

List of Figures

List of Symbols

3-MA	3-methyladenine
ANT	adenine nucleotide translocase
APAF1	apoptotic peptidase activating factor 1
ATG	autophagy related genes
BH	Bcl-2 homology
CEF	cyclophosphamide/epirubicin/5-fluorouracil therapy
CK-18	cytokeratin-18
CP	cyclophosphamide
DC	dendritic cell
DR	death receptor
Eto	etoposide
FADD	Fas-Associated protein with Death Domain
H & E	hematoxylin and eosin
FISH	fluorescence *in situ* hybridization (FISH)
$GdCl_3$	gadolinium chloride
GFP	green fluorescent protein
GrB	Granzyme B
HCC	hepatoceullular carcinoma
HMGB1	high mobility group box 1
IAP	inhibitor of apoptosis
IHC	immunohistochemistry
IL	interleukin
IP	intraperitoneal
IV	intravenous
JNK	c-Jun N-terminal kinase
LC3 I	microtubule-associated protein 1 light chain 3
MAF	mafosfamide
MEF	mouse embryonic fibroblast
Mip	macrophage inflammatory protein
MNNG	*N*-methyl-*N*′-nitro-*N*-nitrosoguanidine
Nec-1	necrostatin-1
NK	natural killer cell
PAMP	pathogen-associated molecular patterns
PAR	poly(ADP-ribose)
PARP	poly(ADP)-ribose polymerase
PCD	programmed cell death
PDT	photodynamic therapy
PFRN	perforin
PRR	pattern recognition receptors
PTPC	permeability transition pore complex
RAGE	receptor for advanced glycation end products
RIP	receptor interacting protein-1
RFA	radiofrequency ablation

RFP	red fluorescent protein
ROS	reactive oxygen species
SA ß-gal	senescence-associated ß-galactosidase
STS	staurosporine
TAA	tumor-associated antigen
TEM	transmission electron microscopy
TLR	toll-like receptor
TNF	tumor necrosis factor
TNF-R	tumor necrosis factor receptor
TRAF-2	TNFR-associated factor 2
TRAIL	TNF-related apoptosis-inducing ligand
TRAIL-R	TNF-related apoptosis-inducing ligand receptor
TUNEL	terminal transferase dUTP end labeling assay
VDA	vasculature disrupting agent

Acknowledgments

I would like to thank the members of the Zong Lab: Wei-Xing Zong, Erica Ullman, Yongjun Fan, Zhixun Dou, Joseph Catanzaro, Namratha Sheshadri, JiAn Pan, Juei-Suei Chen, and Nadia Jaber for their technical help, scientific discussion, and friendship.

I would like to thank Dr. Dara Ditsworth and Fangping Zhao for providing reagents and some experimental data presented here. I would like to thank Susan Van Horn for assistance on electron microscopy and Dr. Guowei Tian for help with live cell imaging. I would like to thank Dr. Myriam Malet-Martino (Université Paul Sabatier, France) for providing mafosfamide, Dr. Kevin Tracey for the HMGB1 depleting antibody, and Dr. Marco Bianchi for providing *hmgb1*$^{-/-}$ MEFs. I would like to thank Drs. Scott Lowe, Jim Bliska, and Jorge Benach for providing reagents and suggestions. I would like to thank Dr. Christopher Czura, Gregory Sabino, and David Habiel for technical assistance. Additionally, I would like to thank Drs. Craig Thompson, Kevin Tracey, Howard Crawford, Ute Moll, Nancy Reich, and Howard Fleit for discussion and Michael Curato for editing.

I would like to thank the Molecular and Cellular Biology Graduate Program at Stony Brook University for their support and encouragement.

Some material is reprinted with permission from articles published in Cancer Research.

Permission from Cancer Research was granted through the copyright agreement: American Association of Cancer Research (AACR) journals allow authors to reproduce their own articles or portions of their articles in a **doctoral thesis** without requesting permission from the AACR.

Publications

1. **Guerriero, J.L.,** Ditsworth, D., Sabino, G., Furie, M.B., Kew, R., and Zong, W.X. DNA alkylating therapy induces an HMGB1-dependent activation of innate immunity and tumor clearance. (Submitted)

2. Dou, Z., Chattopadhyay, M., Pan, J.A., **Guerriero, J.L.,** Jiang, Y.P., Ballou, L. M., Yue, Z., Lin, R. Z., Zong, W.X. The Class IA phosphatidylinositol 3-kinase p110β subunit is a positive regulator of autophagy. (Submitted)

3. **Guerriero, J.L.,** Ditsworth, D., Fan, Y., Zhao, F., Crawford, H.C., and Zong, W.X. Chemotherapy induces tumor clearance independent of apoptosis. Cancer Res. 2008 Dec 1;68(23):9595-600.

4. Singer, A.J., McClain, S.A., Taira, B.R., **Guerriero, J.L.,** and Zong, W.X. Apoptosis and necrosis in the ischemic zone adjacent to third degree burns. Acad Emerg Med. 2008 Jun;15(6):549-54.

5. Ojima, I., Chen, J., Borella, C.P., Wang, T., Miller, M.L., Lin, S., Geng, X., Kuznetsova, L., Qu, C., Gallager, D., Sun, L., Zhao, X., Zanardi, I., Xia, S., Horwitz, S.B., Mallen-St.Clair, J., **Guerriero, J.L**., Bar-Sagi, D., Veith, J.M., Pera, P., and Bernacki, R.J. Design, synthesis, and biological evaluation of new-generation taxoids. J Med Chem. 2008 Jun 12;51(11):3203-21.

I. Introduction

Cell death plays a fundamental role in all stages of development, viral and bacterial infection, degenerative disease, inflammation, and injury. Programmed cell death (PCD) is an important mechanism in both development and homeostasis in adult tissues for the removal of superfluous, infected, transformed or damaged cells by activation of an intrinsic suicide program, apoptosis. When a cell becomes damaged or transformed the cell triggers apoptosis so that the potentially harmful cell is eliminated. When apoptosis is impaired, the cell may continue to proliferate and divide resulting in tumorigenesis. In fact, the ability of a cell to evade normal apoptotic signaling is considered to be a crucial step in the development of cancer [1-4]. It is widely accepted that most, if not all, human cancer cells harbor defective apoptotic machinery due to mutations in p53 [5-6], deregulation of the Bcl-2 family of proteins [5, 7], oncogenic signaling [8], and/or is acquired from drug resistance during anti-cancer treatment [9].

Despite evidence that apoptosis is blocked in tumor cells, apoptosis has been intensively described to account for chemotherapy-induced cancer cell death and, therefore, anti-cancer agents have been developed to maximize apoptosis. More recently, researchers aiming to circumvent this paradoxical situation have found accumulating evidence that apoptosis may not be the sole mediator of cancer cell death in response to chemotherapy. Other types of cytocidal and cytostatic mechanisms that have gained attention include necrosis, autophagy, senescence, and mitotic catastrophe [4, 7, 10-11]. Among these, necrosis has clinically been reported to occur in numerous cancers following chemotherapy and radiation therapy and has been used as one of the best prognostic factors for a positive outcome [12-15]. The complexities of cell death pathways have been amplified in cancer cells and how much each of these forms of cell death contributes to the anti-cancer activity and how they may interplay remains largely unknown.

An important biological consequence of cell death is the activation of the immune response. A fundamental difference between apoptosis and necrosis is their influence on the immune response. Apoptosis is often characterized by an anti-inflammatory response that is essential during development and for homeostasis in adult organisms to prevent chronic inflammation and autoimmune diseases. In contrast, necrotic cells undergo a rapid loss of membrane integrity that allows the release of intracellular constituents into the extracellular environment producing a pro-inflammatory response. The role of the immune response during cancer progression and anti-cancer therapy is controversial. The immune response has been shown to correlate with both tumor progression and regression. Therefore, it is necessary to utilize simple *in vivo* models, such as the one presented here, to address how cancer cells die in response to anti-cancer therapy. *In vitro* cell death analysis provides a fundamental evaluation of cell death, but to evaluate how tumor cells die in response to chemotherapy, an *in vivo* model is essential. *In vivo* models allow analysis of the complexities of a tumor microenvironment such as cell-to-cell interaction, survival factors, hypoxia, and vasculature, all of which are lacking in an *in vitro* analysis [16]. Additionally, the role of the immune system during chemotherapy can be unveiled. The *in vivo* model described here opens the door for future discovery in the field of tumor cell death. The ability to look at the effects and contributions of anti-cancer therapy on the activation of both non-apoptotic cell pathways and the immune response may reveal novel therapeutic targets.

A. Cell Death Pathways

1. Apoptosis

Apoptosis is an essential process required for maintenance of tissue homeostasis and plays a crucial role in the clearance of cells that have potentially harmful genetic mutations [3]. Apoptosis is the best defined cell death pathway, both molecularly and morphologically. Apoptotic cells undergo a non-inflammatory process that is dependent on ATP and is characterized by blebbing of the cell membrane, reduction of cell size, condensation of chromatin, and fragmentation of the nucleus. The apoptotic pathway often utilizes caspases that have a cysteine residue capable of cleaving aspartic acid-containing motifs and subsequently breaking down cellular organelles and constituents. The activation of caspases in a chain-like fashion results in apoptosis [17-18].

Apoptosis is a delicately regulated process whose deregulation is a hallmark for tumorigenesis [1-2, 19]. A tumor cell's deficiency in apoptosis is often a result of oncogene activation that either directly promotes cell survival signaling pathways or activates aberrant cell cycle and proliferation that impose a selective pressure for anti-apoptotic mutations. Different oncogenes are involved with tumor initiation, progression, and resistance to chemotherapy. Most relevant to the study presented here are K-Ras and E1A (12S). Mutations in one of the three *ras* genes at codon 12, 13, or 61 converts H-*ras*, K-*Ras*, and N-*ras* into active oncogenes. Ras is the most commonly activated oncogene, found in 20-30% of all human cancers [20-21]. Ras mutations occur through point mutations and lead to unregulated proliferation and differentiation [22]. The adenovirus E1A produces two mRNA products, 13S and 12S, through differential splicing. These mRNA products encode two proteins, 289 and 243 amino acids long, respectively. Both of these proteins provide transcriptional regulatory properties for cells, can immortalize primary cells, can cooperate with the activated *ras* gene in primary cell transformations, and can induce host cell proliferation [23]. The major effect of E1A is to force G_0/G_1 cells to S phase and subsequently to mitosis, making it a potent oncogene [24].

A number of genes that directly regulate apoptosis have been found mutated or dysfunctional in human cancers [3, 7, 18, 25-28]. These include the Bcl-2 family of proteins [1], apoptotic peptidase activating factor 1 (APAF1) [9], caspases [29-31], caspase inhibitors such as the inhibitor of apoptosis (IAP) [32], survivin [33-35], and the X-linked inhibitor of apoptosis protein (XIAP) [36-38], death receptor related proteins cellular caspase-8 (FLICE)-like inhibitory protein c-FLIP [39] and Fas [40-42], as well as p53, the most commonly mutated gene in human cancer [43-46]. The vast number of apoptotic mutations found in cancer cells not only attribute to cancer progression but also resistance to chemotherapy.

a. p53

In 1979, p53 was first identified in complex with the large T antigen of SV40 by DeLeo *et.al.* [47]. It was later discovered that p53 functions as a tumor suppressor by inducing apoptosis in cells that may be potentially harmful. The fundamental role of p53 is to induce cell death in response to DNA damage, hypoxia, oncogenic activation, and

other stress signals. It regulates the cell cycle and, therefore, functions as a tumor suppressor that is involved in preventing cancer. Interestingly, p53 is directly inhibited in more than 50% of all human cancers, making it the most commonly mutated gene in cancer. Additionally, in many other cancers, p53 is inhibited due to elevation of p53 inhibitors such as Mdm2 and the E6 protein of HPV, or due to the silencing of the key p53 co-activator ARF [5-6].

b. Bcl-2 family

In 1984, Bcl-2 was identified in follicular lymphoma cells when a gene translocation from chromosome 18 was found at the immunoglobin heavy chain locus. The t(14:18) chromosome translocation results in elevated levels of Bcl-2 [48]. The Bcl-2 family of proteins regulates the efflux of apoptotic factors from the mitochondria. The family contains 1 - 4 Bcl-2 homology (BH) domains. The number and combination of BH domains dictate whether the protein is anti-apoptotic or pro-apoptotic [49]. The anti-apoptotic proteins contain all four BH domains and include proteins such as Bcl-2 and Bcl-xL. The pro-apoptotic family is further divided into BH-3 only members and BH1-3 members such as Bax and Bak. Additionally, more than 25 members of the Bcl-2 family have been identified [18]. Deregulation in the balance between pro-apoptotic and anti-apoptotic proteins within a cell leads to disruption of the balance between cell proliferation and cell death, which can lead to cancer [18, 28]. It has been reported that the t(14:18) chromosomal translocation of Bcl-2 is found in 80-90% of human follicular lymphoma cases. Additionally, Bcl-2 and Bcl-xL are upregulated in other types of hematopoietic and non-hematopoietic malignancies [46, 50]. Other reports show more than 50% of human microsatellite mutator phenotype colon adenocarcinomas [51] and 21% of human hematopoietic malignancies possess mutations of the pro-apoptotic protein Bax [52]. These studies indicate deregulation of the Bcl-2 family of proteins can attribute to the development of human malignancies.

c. Reactivating defective apoptotic machinery for cancer therapy

To circumvent apoptotic mutations in cancer cells, strategies have been implemented to reactivate dysfunctional apoptotic machinery. Some examples include somatic gene transfer to replace lost or inactive p53 [53], pharmacological restoration of p53 [54-57], a p53 peptide that is highly selective for tumors that have high levels of mutant p53 [58], BH3-peptides that act as agonists for Bax and Bak or as inhibitors of anti-apoptotic Bcl-2 family members [59-62], gene transfer of antisense cDNA or RNA interference of the Bcl-2 family of proteins [63], as well as SMAC mimetics to antagonize the apoptosis inhibitory activities of the IAP proteins [64-67].

In addition to targeted therapeutic strategies to restore apoptosis in cancer cells, other cell death pathways have been explored to bypass the mutated apoptotic molecules. Necrosis [68-71], autophagy [72-74], senescence [75-77], and mitotic catastrophe [3, 76, 78-80] are among the best described in their morphological and/or molecular definition. Among these, necrosis, an ancient term formerly used to describe all types of cell death, has been gaining attention owing to the recent advances in its molecular regulation and physiological implication.

2. Necrosis

While apoptosis is well defined at the molecular level, necrosis has long been referred to as a form of cell death that is uncontrolled and pathological. It is short of a molecular signature and is often described morphologically as lacking typical features of apoptosis. However, *in vitro* necrosis has some defining characteristics that include bioenergetic failure, damage to membrane lipids, and loss of function of homeostatic ion pumps/channels, which result in the loss of plasma membrane integrity, swelling of cellular organelles, and the release of cellular constituents into the extracellular environment [81-86]. Necrosis is thought to be a non-programmed cell death pathway that occurs in response to massive cellular insult, is energy independent, and induces an inflammatory response.

a. Necrosis is observed following anti-cancer therapy

Although apoptosis has taken the center stage in the study of cancer cell death, necrosis is also largely associated with human cancer. In solid tumors, necrosis is often observed in areas where vascularization lags behind tumor tissue growth. In clinical settings, due to the lack of molecular definition, characterization of necrosis has mostly relied on morphological features of dead cells or tissue. To determine the extent of chemotherapy induced tumor necrosis, surgically resected tumors are assessed by pathologists. Necrotic tumor tissue is characterized by tumor cell shrinkage, disappearance of cell membranes, fragmented nuclei, and hemorrhage as identified by an increase in red blood cells.

In addition to necrosis resulting from tumor ischemia, chemo- and radio-therapy-induced necrosis has also been observed in many human cancers such as prostate cancer [87], head and neck cancer [88], breast cancer [89], osteosarcoma [14, 90], Kaposi's sarcoma [91-92], soft tissue sarcoma [93], and retinoblastoma [94]. Importantly, favorable clinical outcomes to chemotherapy have been found to correlate with the induction of necrosis. For example, osteosarcoma patients typically receive a combined treatment of preoperative chemotherapy such as doxorubicin, cisplatin, high dose methotrexate, etoposide, cyclophosphamide, or ifosfamide followed by surgery. Analysis of resected osteosarcomas shows that 45% of patients achieve more than 90% tumor necrosis. Patients who achieve levels of 90% or higher of tumor cell necrosis during preoperative chemotherapy have a better prognosis than those whose tumor cells do not respond as favorably [90, 93].

Noninvasive techniques to monitor tumor response to chemotherapy such as determining the percentage of cells undergoing apoptosis versus necrosis using molecular markers found in patient serum are emerging [90-91, 93]. One such molecule is cytokeratin-18 (CK-18). CK-18 is cleaved by caspases 3, 6, 7, and 9 during apoptosis, however during necrosis it remains intact [12, 95-96]. This feature can be used to assess the extent of apoptosis versus necrosis in patients by measuring serum levels of cleaved versus full length CK-18, respectively. In a study where breast cancer patients were treated with cyclophosphamide/epirubicin/5-fluorouracil (CEF) therapy, more necrosis than apoptosis was observed as assessed by the high levels of the full length form of CK-18 in patient serum. Interestingly, the necrotic response correlated with better survival

[89]. In another study, the cleaved form of CK-18 was only a small percentage of the total CK-18 that was found in the serum from prostate cancer patients treated with estamustine and vinorelbine or docetaxel, indicating that apoptosis was not the dominating mode of tumor cell death [97]. These studies provide evidence that necrosis is activated in response to chemotherapy and may in fact mediate tumor regression.

b. Therapeutic approaches for inducing tumor cell necrosis

Targeting necrosis in cancer therapy has lead to the development of vasculature disrupting agents (VDAs). VDAs are a large group of agents that target already established tumor vasculature. Solid tumors must develop a vasculature network to ensure oxygen and other nutrients are delivered into tumor tissue, otherwise tumor cell necrosis may occur in response to ischemic conditions. Tumor vasculature is different than that of normal vessels because tumor vasculature develops rapidly and is characterized by a high rate of endothelial proliferation, absence of pericytes, abnormalities of the basement membrane, and increased vascular permeability. Additionally, tumor vasculature is disorganized, thin-walled, and has long lengths between branches [98]. All of these features make tumor vasculature more susceptible than normal vessels to VDAs. Disruption of tumor vasculature inhibits oxygen and nutrient supply to the tumor and subsequently induces tumor cell necrosis [69, 99-100]. VDAs have been used in combination with other chemotherapeutic agents and have not only led to improvements in cancer treatment, but have also highlighted the importance of tumor cell necrosis.

Necrotic responses have also been shown with radiofrequency ablation (RFA) and photodynamic therapy (PDT). RFA is a procedure that involves nonsurgical, localized induction of radiofrequency energy that produces heat, leading to tumor cell necrosis [101]. RFA is the primary treatment for patients with hepatoceullular carcinoma (HCC) and disease-free survival has been reported [102-104]. RFA has also been used to induce tumor cell necrosis in patients with unresectable intrahepatic cholangiocellular carcinoma, prostate cancer, head and neck cancer, primitive and metastatic lymphomas, breast cancer, and symptom palliation of bone metastasis [101]. PDT relies on the use of photosensitizing drugs that are pharmacologically inactive until they are exposed to light in the presence of oxygen. The photosensitizers are administered either orally or intravenously and accumulate in the tumor. A low-power laser, guided by ultrasound, delivers light directly into the tumor site. The now activated drug forms singlet oxygen and other reactive oxygen species that induce tumor necrosis and subsequently elicits an immune response [87, 105]. PDT has been used in the treatment of skin cancer, head and neck cancer, pancreatic cancer, and prostate cancer [87].

Importantly, the naturally occurring compound shikonin has been shown to induce necrosis in apoptosis deficient tumor cells. Shikonin induces necrosis in both MCF-7 and HEK293 cells and cell death can be blocked pharmacologically with necrostatin-1 (Nec-1; an allosteric inhibitor of receptor interacting protein (RIP)-1, which has been shown to inhibit necrosis [106]), but not overexpression of the P-glycoprotein, Bcl-2 or Bcl-xL [107]. This provides evidence that shikonin induces a programmed form of necrosis, termed necroptosis as described by Degterev *et. al.*, because it is sensitive to nec-1 and proceeds independent of the apoptotic pathway [108]. The mechanism of

shikonin induced necrosis is not well understood, however down regulation of procaspase-8 upon shikonin treatment was identified by western blot and may imply divergence from the apoptotic pathway to necroptosis.

c. Molecular necrotic pathways involved in chemotherapy

Despite the evidence that necrosis takes place in clinical oncology, it remains largely illusive as to what molecular pathways, if any, are involved in necrosis induction in cancer patients and during therapy. Unlike apoptosis, where the Bcl-2 family of proteins and caspases play key roles in the molecular regulation, necrosis is often induced by bioenergetic failure and does not involve the Bcl-2 family of proteins or caspase activation. However, several classes of molecules have been recently described to regulate necrosis and are implicated in cancer development and therapy.

i. Death receptor pathway

The most widely studied programmed necrotic pathway is death receptor (DR) mediated necrosis. Fas, tumor necrosis factor receptor 1 (TNFR1) and TNF-related apoptosis-inducing ligand receptor (TRAIL-R) are death receptors well characterized in the activation of the extrinsic apoptotic pathway that leads to the activation of the caspase cascade. However, when caspases are inhibited, necrosis is elicited in a manner that is dependent on the serine/threonine kinase RIP1 [109]. RIP1 is a death-domain-containing kinase recruited to the death-inducing signaling complex. Activation of RIP1 can mediate various effects, including activation of both apoptosis and necrosis. Interestingly, RIP1 is dispensable for the induction of death-receptor mediated apoptosis but is required for activation of necrosis through death receptors in apoptotic-deficient conditions [109]. This suggests that the death receptors are capable of acting through two separate cell death pathways: 1.) apoptosis, which involves caspase-8 and, 2.) necrosis, which involves the kinase activity of RIP1 [110-111]. RIP1 can be manipulated with genetic knock out and knock down technology or pharmacologically inhibited with necrostatin-1 [106], all of which inhibit necrosis. This provides evidence that necrosis is regulated at a molecular level. Additionally, genetically defined cell systems have been used to show that other molecules such as TNFR-associated factor 2 (TRAF2) and FADD play an essential role in the execution of death-receptor mediated necrosis [109, 112-117].

RIP1 has been shown to regulate necrosis in a variety of ways. When the myelomonocytic U937 and THP-1 cell lines are treated with TNF and apoptosis is blocked with the caspase inhibitor z-VAD, necrosis proceeds in a manner that involves RIP1-dependent suppression of adenine nucleotide translocase (ANT) activity. RIP1 was shown to inhibit ANT-conducted transport of ADP into mitochondria resulting in reduced ATP and cellular necrosis. Inhibiting ANT–conducted ADP/ATP exchange across the mitochondria membrane occurred together with the loss of interaction between ANT and cyclophilin D, a member of the mitochondria permeability transition pore complex (PTPC), and the inability of ANT to adopt the cytosolic conformational state, which prevented cytochrome c release [116]. Additionally, it has been shown that RIP1 is required for the accumulation of pro-necrotic ceramides. Ceramides are one of the major

components in the lipid bilayer and can act as a signaling molecule that regulates differentiation, proliferation, and programmed cell death. Ceramides accumulate in response to apoptotic stimuli and are thought to play a role upstream of the mitochondria, but their exact mechanisms are unknown. To support the role of ceramide in necrosis, it has been shown that TNF induces necrosis in L929 fibrosacroma cells, NIH3T3 fibroblasts, human leukemic Jurkat T cells, and lung fibroblasts in a manner that is dependent on RIP1 and ceramide accumulation in the cell [118]. Therefore, RIP1 may induce necrosis by intermediate generation of ceramides, through direct inhibition of mitochondrial respiration and ROS formation, and/or indirectly by promoting an increase in calcium resulting in a calcium overload for the mitochondria [119].

In three recent papers, RIP3 was identified in complex with RIP1 and was shown to be required for the induction of death receptor mediated necrosis [120-122]. Zhang ***et. al***. identify a role for RIP3 in activating key enzymes of the metabolic pathway that regulates TNF-induced ROS production and promotes necrosis in NIH3T3 cells [122]. He ***et.al.*** reveal that in addition to RIP1, RIP3 forms a necrotic complex with FADD and caspase-8 in HT-29 cells treated with TNF, a Smac mimetic, and z-VAD; and Nec-1 prevents this interaction and subsequently prevents necrosis [121]. Cho ***et.al.*** also identify RIP3 as an essential activator of TNF-induced necrosis. They show that RIP3 forms a complex with RIP1 that is essential to activate their pro-necrotic kinase activity and trigger downstream ROS production to induce necrosis [120].

ii. Poly (ADP-ribose) polymerase (PARP) pathway

DNA alkylating agents are an attractive chemotherapeutic strategy and are one of the most commonly used chemotherapeutics in clinic. Despite the broad usage of DNA alkylating agents in medical oncology, the molecular mechanisms for their anti-tumor activities remain largely elusive. Interestingly, it has been shown that DNA alkylating agents induce necrosis in cells with and without functional apoptosis machinery *in vitro* [86] and *in vivo* [70]. DNA alkylating agents are an attractive strategy for chemotherapy because it has been shown that DNA alkylating agents activate PARP1, which results in cellular ATP and NAD^+ depletion and subsequently necrosis. Since tumor cells are dependent on aerobic glycolysis, they are more susceptible than normal cells to NAD^+ and ATP depletion [86]. Additionally, DNA damage has been shown to increase the expression of Fas and TRAIL receptors on the tumor cells, which make them susceptible to cell death by Fas Ligand, TRAIL therapy, or immune cells [123].

PARP1 is an abundant nuclear protein that is involved in the repair of damaged DNA [124]. Upon DNA damage, PARP-1 facilitates the addition of poly(ADP-ribose) (PAR) chains on acceptor proteins such as histones, DNA polymerases, topoisomerases, DNA ligase-2, high mobility group proteins, and a number of transcription factors. Under homeostatic conditions, PARP1 is capable of facilitating DNA damage repair. However, in some circumstances such as massive DNA damage, excessive PARP activation can cause bioenergetic catastrophe and cellular necrosis. This is due to the depletion of NAD^+, which is essential for glycolysis but is used up by PARP1 as a substrate to facilitate the covalent addition of PAR to accepting proteins to facilitate DNA repair [86]. PARP1 is activated in MEFs in response to the DNA alkylating agent *N*-methyl-*N*′-nitro-*N*-nitrosoguanidine (MNNG) or H_2O_2 treatment and this PARP1

activation mediates reactive oxygen species-induced injury leading to massive consumption of NAD^+ and necrosis [125].

In addition to NAD^+ consumption and energy failure, PARP has been shown to regulate necrosis in a c-Jun N-terminal kinase 1 (JNK1)-dependent manner that also requires RIP1 and TRAF2. MEFs deficient in RIP1 or TRAF2 were resistant to PARP1 mediated cell death in response to MNNG [112]. These findings point to a converging role of PARP in regulating necrosis triggered by DNA damage and death receptors.

iii. Non-caspase proteases

The use of caspase inhibitors have revealed non-caspase proteases such as calpains (calcium-dependent, non-lysosomal cysteine proteases), cathepsins (both cysteine and aspartate proteases), and serine proteases that are capable of inducing caspase-independent apoptotic and necrotic cell death, with the amount of stress dictating the mode of cell death [126]. Under low stress where a limited amount of lysosomal contents are released into the cell, apoptosis proceeds; whereas, under high intensity stress, where the lysosome ruptures, necrosis proceeds. Caplain activation has been linked to ROS formation, which induces necrosis that is independent of PARP [119]. There is evidence that non-caspase proteases are involved in a regulated necrotic cell death pathway that is dependent on p53, cathepsin Q, and ROS [127]. In response to DNA damage induced by etoposide treatment, *bax*$^{-/-}$*bak*$^{-/-}$ MEFs undergo necrosis that correlates with the upregulation of the lysosomal cysteine protease cathepsins. Further investigation reveals that cathepsins cooperate with ROS to induce programmed necrosis [127].

Due to the identification of common molecular regulators of both necrosis and apoptosis it has been suggested that necrosis is an ancestral form of cell death that has been overridden by apoptosis [119] or that necrosis is not due to one cell death pathway, but instead an interplay between multiple pathways [128]. Regardless, with the new findings that necrosis is observed following anti-cancer therapy, there are specific molecular players of necrosis, and pharmacological and/or genetic inhibition of cyclophilin D, AIF, PARP-1, calpains, and cathepsins exhibit cytoprotection in several models of acute cell loss [85], we need to decipher which molecular regulators of necrosis can be targeted to enhance cytotoxicity in apoptotic-deficient cancer cells.

3. Autophagy

Unlike apoptosis and necrosis, autophagy is not synonymous with cell death. It is an adaptive process that cells rely on during differentiation, in response to developmental triggers, and as a means of survival during nutrient starvation. Although autophagy promotes cell adaptation and survival, when excessively activated it can promote cell damage and cell death. Under normal physiologic conditions, autophagy occurs at basal levels in most tissues, contributing to the routine turnover of cytoplasmic components [11, 129-130]. Under metabolic stress, autophagy is utilized to provide energy for the cell [131]. During autophagy, portions of the cytoplasm are encapsulated in a double-membrane structure referred to as an autophagosome. The autophagosome then fuses with lysosomes where the contents are delivered, resulting in their degradation by lysosomal hydrolases. The degraded constituents can be recycled within the cell or utilized for energy [132]. A number of genes that regulate autophagy have been identified in yeast, referred to as autophagy related genes (atg) [133], many of which have mammalian homologues [134].

Autophagy has been implicated in many different human diseases, including cancer [131]. Its role in cancer is controversial, as it may play a role in both tumor progression and tumor prevention. Induction of autophagy can favor tumor growth because as a tumor grows, it may rely on autophagy to survive nutrient poor internal regions, especially where there is poor vascularization [135]. Additionally, autophagy may degrade depolarized mitochondria that would normally initiate cell death [136]. This adaptive process may provide a means of survival during trivial stresses, but under more harsh or prolonged stress, cell death can be induced.

a. Autophagy in cancer

The precise role of autophagy in tumorigenesis is not well characterized, although Yue *et. al.* have shed light on autophagy genes involved in cancer progression. Previously, *beclin 1* (atg 6), has been identified as an autophagy gene that can restore autophagy in yeast cells that are autophagy-defective [137]. Yue *et. al.* generated beclin $1^{-/-}$ and beclin $1^{+/-}$ mutant mice. The group showed that beclin $1^{-/-}$ mice die during embryongenesis and the beclin $1^{+/-}$ mice have a high incidence of spontaneous tumors. Thus, they show *beclin 1* is essential in development and is a haploinsufficient tumor suppressor [138]. Further work on the *beclin 1* gene shows it is located in a tumor susceptibility locus on human chromosome 17q21, where BRCA1 is found frequently mutated in breast and ovarian carcinoma [139]. Due to the proximity of *beclin 1* to BRCA1, Aita *et. al.* performed a screen on 22 human breast carcinoma cell lines utilizing a probe specific for Beclin 1 to identify deletions of the autophagic gene. The group identified 9 of the 22 breast cancer cell lines had deletions of one or more alleles of *beclin 1*. The group also showed that *beclin 1* is ubiquitously expressed at high levels in normal breast epithelia but has decreased levels in human breast carcinomas, which provides further evidence for *beclin 1* as a tumor suppressor [139]. Liang *et. al.* also found that *beclin 1* is down regulated in human breast cancers cells. The group also concluded that *beclin 1* is a tumor suppressor and decreased expression may contribute to the development of breast cancer and other human malignancies [137]. In contrast to the

down regulation of *beclin 1* observed by Aita *et. al.* and Liang *et. al.*, Ahn *et. al.* reported an increased expression of *beclin 1* in gastric and colorectal cancers compared to normal cells [140].

Alva *et. al* show that autophagy is activated during anti-cancer therapy. The group utilized surgical resection specimens examined by transmission electron microscopy to show 7 of 12 primary human tumors studied show evidence of autophagic structures characterized by double- and multi-membrane vacuoles that enclose cytoplasmic content and organelles. The positive tumors include a variety of cancers such as: breast cancer, lung cancer, pancreatic adenocarcinoma, pancreatic islet cell tumor, ganglioneuroma, and pituitary gland cancer [141]. The group concluded that due to their small sample size, it would be reasonable to expect that autophagy occurs in many tumors.

A review by Kondo and Kondo describe various chemotherapeutic agents have been shown to induce autophagy in a variety of different human tumor cells *in vitro* [72]. For example, when tamoxifen is used to induce cell death in MCF-7 cells, the cells succumb to cell death. When autophagy is blocked with addition of the autophagy inhibitor, 3-methyladenine (3-MA), the MCF-7 cells remain viable, providing additional evidence that autophagy is a cell death mechanism [142]. Additionally, DNA alkylating agents have been shown to induce autophagy in malignant gliomas [73] and ionizing radiation has been shown to induce autophagy in breast cancer, prostate cancer, colon cancer, and malignant gliomas [74]. This provides evidence that autophagy is functional in cancer cells and is a plausible target for chemotherapy.

b. Models to assess autophagy induction following chemotherapy

Models to assess tumor cell autophagy i*n vivo* are lacking. Currently, the gold standard to assess autophagy in tumors is through electron microscopy to identify autophagosome structures. Recently, the use of the autophagosome-associated protein microtubule-associated protein 1 (MAP1) light chain 3 (LC3 I) has been described as a marker for autophagy. LC3 I is localized homogeneously in the cytoplasm of normal cells. Upon induction of autophagy, LC3 I is converted to LC3 II and localizes to the membrane of autophagosomes. Tumor cells transfected with LC3 fused with the green fluorescent protein (GFP) are often utilized to visualize the formation of autophagosomes. Using fluorescent microscopy, it is evident by the green punctate pattern if there is induction of autophagy. Another model has been described by Mizushima *et. al.* to understand where and when autophagy occurs *in vivo*. The group generated a transgenic mouse systemically expressing GFP fused to LC3 [143]. Utilizing current *in vivo* models, we can continue to study the effect of autophagy during tumor growth, treatment, resistance to treatment, and regression.

4. Senescence

Replicative senescence is a cytostatic process that occurs from the gradual shortening of telomeres during subsequent cell divisions. Additionally, accelerated senescence is used to describe a type of cell death in the context of cancer therapy. Accelerated senescence induces an irreversible mechanism of cell death in tumor cells with activated oncogenes such as Ras or following DNA damage [144]. These cells appear enlarged, flat, and have increased granularity. Biochemically, there is a metabolic change within the cell that leads to the induction of senescence-associated ß-galactosidase (SA ß-gal) activity as a result of increased lysosomal mass within the senescent cell [3]. It has been reported that cancer cells that undergo senescence in response to DNA alkylating damage undergo permanent growth arrest, but remain metabolically active and are able to secrete proteins [76].

a. Senescence in cancer

Chang *et. al.* measures SA ß-gal activity in 14 solid human cancer cell lines in response to doxorubicin *in vitro*. They found 11 of the 14 cell lines underwent senescence. Under moderate doses of doxorubicin, the human cancer cell lines predominantly underwent senescence and mitotic catastrophe, but not apoptosis; however, the induction of senescence and mitotic catastrophe were independent responses. The group suggests that senescence, unlike mitotic catastrophe, is dependent on p53 because in all three tumor cell lines harboring a p53 mutation, senescence was not observed [80]. Another study by Collado *et. al.* shows senescence is associated with premalignant tumors but not malignant tumors *in vivo*. The group suggests that oncogene induced senescence may help to restrict tumor progression but malignant tumors are unable to do this due to the loss of the oncogene-induced senescence inducer, p53 [145]. There is evidence that senescence plays a role in tumor regression but little is known about its role in cancer therapy. Successful treatment of cancer must take into account the possible tumor promoting effects of senescent cells and the ability of cancer cells to undergo senescence in response to chemotherapy and, therefore, further analysis in this field may offer novel therapeutic strategies.

5. Mitotic Catastrophe

During mitosis cell cycle checkpoints regulate proper cell cycle progression. Activation of cell cycle checkpoints or improper segregation of chromosomes activate cell death through mitotic catastrophe. Mitotic catastrophe occurs as a defense mechanism and is essential to ensure fidelity of daughter cells. Cell death through mitotic catastrophe is characterized by the formation of large cells with multiple micronuclei. The multiple micronuclei arise through the formation of nuclear envelopes around clusters of chromosomes or chromosome fragments during a catastrophic mitosis. Further, faulty mitotic checkpoints can lead to uncontrolled cell proliferation leading to the development of cancer cells.

a. Mitotic catastrophe in cancer

In vitro studies utilizing human cancer cell lines have shown mitotic catastrophe to be the dominant form of cell death in response to ionizing radiation and chemotherapeutic agents such as etoposide, paclitaxel, docetaxel, and cisplatin [3, 76, 78-79]. Morse *et. al*. show *in vitro* that the human breast cancer cell line MCF-7, when treated with docetaxel, undergoes mitotic catastrophe as observed by cytology and transmission electron microscopy. The group suggests that chemotherapeutic agents that target mitotic spindles, such as taxanes, may be the most efficient method to kill apoptotic-resistant tumor cells [146]. Falkvoll *et. al*. uses quantitative histology of tumors taken from a human melanoma xenograft mouse model treated with irradiation to show aberrant mitosis and micronucleation occur, indicating that mitotic catastrophe is the major form of cell death in response to irradiation *in vivo* [75]. Chang *et. al.* tests the effects of γ-irradiation and seven different chemotherapeutic agents including doxorubicin, cisplatin, etoposide, and taxol on the fibrosarcoma cell line HT1080. The group shows that all seven therapies induce mitotic catastrophe at a high fraction. In the same study, they test doxorubicin on 14 different solid human cancer cell lines and reveal 12 out of the 14 cell lines underwent mitotic catastrophe as measured by fluorescence *in situ* hybridization (FISH) with chromosome specific probes that showed fragmented nuclei that contained an increased number of chromosomes [80]. The previously mentioned examples suggest mitotic catastrophe may be involved in tumor cell death but its role is still undefined. Mitotic catastrophe may play an important role in regulating cancer cell death or it may provide a mechanism of drug resistance and, therefore, further examination is needed.

B. Cell death and innate immunity

A fundamental difference between apoptosis and necrosis is that apoptotic cells die in an ordered fashion and are engulfed and cleared by phagocytes or neighboring cells *in vivo*, whereas necrotic cells lose their membrane integrity and release their intracellular content into the extracellular environment. While dead cells are quietly removed during apoptosis so that normal organismal functions are not disturbed, necrosis triggers an inflammatory response to defend against the insult. Suppression of the immune system that arises from apoptotic cells during development and homeostasis is essential to preventing chronic inflammation and autoimmune diseases. Conversely, activation of the immune system by necrosis induced by viral and pathogen infection plays a critical role to warn the host of insult [85, 147-152]. Therefore, proper regulation of apoptosis and necrosis is essential during development and to ensure homeostasis.

Innate immune cells can recognize both apoptotic and necrotic cells through a number of different bridging molecules and receptors that facilitate engulfment of the cell or cell debris [153]. Engulfment of apoptotic cells has been considered to be an anti-inflammatory process because upon engulfment, phagocytes secrete anti-inflammatory cytokines such as IL-10, TGF-β, prostaglandin E2, and platelet activating factor [153-159], and suppress the synthesis and secretion of pro-inflammatory cytokines such as macrophage inflammatory protein-2 (Mip-2), MIP-1α, and IL-12 [148, 160]. The production of anti-inflammatory cytokines and the suppression of pro-inflammatory cytokines ensure apoptotic cell phagocytosis without activation of the immune system. In contrast to apoptotic cells, necrotic cells release many intracellular substances that stimulate a pro-inflammatory response [149, 161]. These include mRNA, genomic DNA, nucleotides, and nucleosides that induce transient activation of the immune system [162]. A number of other, more stable molecules have been identified that elicit a potent immune response. These include S100 family molecules [163], HMGB1 [164], purine metabolites [165], uric acid [166], and heat shock proteins [149, 167].

1. Innate immunity in cancer therapy

Innate immune cells make up one component of the immune system that protects the host against infectious organisms and other invaders. Innate immune cells such as macrophages, neutrophils, natural killer (NK) cells, and dendritic cells (DC) use receptors termed pattern recognition receptors (PRR) to identify potentially dangerous organisms by pathogen-associated molecular patterns (PAMPs) that are unique to bacteria, viruses, or other invaders. Innate immune cells can also identify pre-cancerous cells by ectopic or mutated molecules on the cell surface that are acquired during transformation, referred to as tumor-associated antigens (TAAs). In addition to expression of TAAs on the cell membrane, TAAs can be secreted by transformed cells due to cellular stress [168]. The body is on constant surveillance for TAAs to identify and destroy cells that have the potential to become tumorogenic [169-170]. The role the immune system plays in the elimination of potentially harmful cells is crucial to prevent tumorigenesis [19, 171]. In fact, it has been shown that immunodeficient patients, such as transplant recipients, develop tumors more frequently than immunocompetent patients, validating the essential role of the immune system in cancer prevention [172].

In addition to the role of innate immune cells in immunosurvalience, they have also been shown to play an important role in cancer biology [173-174]. However, their physiological consequence in cancer biology remains unclear and controversial. For example, the innate immune response has been found to be activated in response to chemotherapy-induced tumor cell death and may be involved with tumor cell clearance leading to tumor regression [70, 175]. In contrast, involvement of the innate immune system in cancer may facilitate tissue repair and remodeling and further promote tumor growth [176]. Additionally, chronic inflammation has been shown to promote cancer cell survival and growth [177-178] and spontaneous tumor necrosis has been found to correlate with accelerated tumorigenesis [179].

Clinically, innate immune cells have been shown to infiltrate into both mouse and human cancers [180-184] and to have anti-tumor activity [70, 175]. Specifically, it has been shown that NK cells themselves can kill tumor cells, and infiltration of NK cells into human gastric or colorectal cancers is also associated with better prognosis [177, 185-186]. Additionally, other innate immune cells such as neutrophils have been shown to be highly cytolytic and cytostatic against tumor cells [187-191]. Conversely, there have been reports that infiltration of neutrophils, macrophages, and mast cells have been shown to promote tumor development by facilitating tissue repair and remodeling [173, 176-177, 192-195]. Clinically, it has been reported that increased infiltration of macrophages in breast tumors and increased number of infiltrating mast cells in lung adenocarcinoma and melanoma are associated with unfavorable clinical prognosis [196-198]. Yet, it remains to be determined whether conventional chemotherapy can induce immune-stimulating cell death *in vivo*, and if so, how the pro-inflammatory response can affect the outcome of the anti-cancer treatment.

2. Activation of the pro-inflammatory response during cancer therapy

The immune response can be activated in response to tumor cell necrosis because not only is the tumor mass destroyed, but intracellular molecules are released from the necrotic tumor cell. For example, it has been shown that during RFA, pro-inflammatory molecules such as IL-1, IL-6, TNF-α, and Hsp are released from necrotic tumor cells and help activate an anti-tumor immune response. Other experimental anti-cancer therapies with the potential to be immunomodulatory are microwave coagulation [199], laser, high frequency ultrasonic hyperthermia [200], and magnetic embolization hyperthermia [101].

Tumor cell induction of apoptosis or necrosis stimulates the recruitment of innate immune cells towards dying cells [201-203]. Therefore, the pro- versus anti-tumor effects of the immune response depends on the type of therapy administered and the type of cell death triggered by the therapy (apoptotic versus necrotic). For example, *in vitro*, when macrophages are subjected to necrotic tumor cells, they exert anti-tumor properties whereas exposure of macrophages to apoptotic cells does not results in anti-tumor effects and, interestingly, stimulates re-growth of the tumor cells that are not committed to cell death [204]. This provides evidence that different chemotherapeutic agents have different effects on the immune system and the response may be determined by the type of cell death, suggesting the consequences of cell death may be more important than the actual mode of cell death. Activation of the innate immune system may be a sustainable resource that is capable of being harnessed for anti-cancer treatment. Therefore, further characterization of the role necrosis and the molecules associated with inflammation is warranted in cancer therapeutics.

3. Adaptive immune response

Another type of cell death induced anti-tumor activity is due to the convergence of innate to adaptive immunity. Indeed, innate immune cells such as macrophages, DC, and neutrophils are the first line of defense against an insult. They react to tissue injury rapidly without memory of a previous insult and play an essential role in initiation and regulation of the immune response. When innate immune cells remove dying tumor cells through phagocytosis, they are subsequently capable of presenting antigens to T cells, which induces an immunogenic response [205-207]. The T cell response is dependent upon additional signals such as co-stimulatory molecules and cytokines [208-210]. For example, DC can efficiently phagocytose both apoptotic and necrotic cells, however only late apoptotic and necrotic cells induce DC maturation, which includes up regulation of chemokine receptors and co-stimulatory molecules. Immunogenic activation of T cells and activation of the adaptive immune response has been shown to promote long term tumor surveillance and immunity [149, 167, 211-213]. For example, when animals are immunized with the high mobility group box 1 protein (HMGB1) released from tumor cells killed *in vitro*, they become resistant to the formation of newly inoculated xenograft tumors [214-215]. Therefore, chemotherapy induced tumor cell necrosis may be an optimal strategy for the activation of an anti-tumor immune response.

C. The high mobility group box 1 protein (HMGB1)

HMGB1 is one of the most abundant proteins in the nucleus whose functions include binding and bending DNA to facilitate transcription factor binding and the assembly of site-specific DNA binding proteins including p53, stabilizing nucleosomes, and facilitating DNA repair processes [216-217]. HMGB1 binds loosely to chromatin in living cells [218], however during apoptosis histones H3 and H4 are deacetylated and, due to this generalized underacetylation, HMGB1 binds firmly to chromatin [218-219]. In contrast, during necrosis HMGB1 is mobilized from chromatin and, due to the breakdown of the cell membrane, can escape from the cell into the extracellular milieu.

HMGB1 can be released from cells by at least two distinct pathways including necrotic and damaged cells with compromised plasma membranes or through active secretion by stimulated immune cells such as macrophages, monocytes, NK cells, dendritic cells, endothelial cells, and platelets [220-224]. Monocytes may have adapted the use of HMGB1 secretion as a danger signal to "talk" with nearby immune cells. In activated immune cells, HMGB1 secretion is a regulated event and begins with the post-translational modification of HMGB1. Acetlyation and phosphorylation induce translocation of HMGB1 from the nucleus to the cytoplasm and increase HMGB1 secretion from macrophages [218, 225]. In neutrophils, post-translational methylation of HMGB1 causes its translocation to the cytosol [226]. This modification changes HMGB1's charge, which reduces its interaction with chromatin and causes translocation into the cytoplasm. Once in the cytoplasm, HMGB1 is taken up by specialized vesicles called endolysosomes and brought to the plasma membrane for secretion [225, 227-231]. Additionally, calcium and ROS-dependent mechanisms have also been shown to induce HMGB1 release [232-233]. Interestingly, another post-translational modification, its redox status, has been shown to be important for its immunological potential outside the cell [234].

Outside the cell, HMGB1 acts as a damage-associated molecular pattern (DAMP) molecule to alert the host of damage by triggering immune responses. It binds with high affinity to at least eight separate receptors including receptor for advanced glycation end products (RAGE), toll-like receptor (TLR) 2, TLR4, and TLR9 [235-236], which are expressed on a wide variety of cells including immune cells and endothelial cells. HMGB1 binding to its receptors induces a pro-inflammatory response that results in the recruitment of inflammatory cells, stem cell migration, angiogenesis, and dendritic cell maturation [237-240].

In necrotic, damaged, or dying cells, HMGB1 can dissociate from chromatin and be released into the extracellular environment due to loss of plasma membrane integrity [218]. Generally, this is considered a passive process, but it has also been shown to be regulated by the activation of PARP. PARP is a nuclear enzyme that catalyzes the transfer of ADP-ribose moieties from NAD^+ to itself and other acceptor proteins in response to DNA damage [241]. In *parp*$^{-/-}$ cells, HMGB1 remains nuclear upon treatment with the DNA alkylating agent MNNG, whereas HMGB1 is released from WT cells with the same treatment. It was shown that displacement of HMGB1 from the nucleus following PARP activation requires the presence of its C-terminus because it is required to destabilize HMGB1 with the chromatin [164]. This demonstrates an active

mechanism of PARP-dependent nuclear-to-cytoplasmic translocation of HMGB1 in cells that have sustained DNA damage.

1. HMGB1 in cancer

HMGB1 plays a complex role in cancer. The observed overexpression of HMGB1 in tumors, particularly in conjunction with its receptor RAGE, has been associated with the proliferation and metastasis of many tumor types [237-238]. Blockade of RAGE-HMGB1 signaling has been shown to inhibit tumor growth and metastasis in both xenograft and endogenously formed tumors [242]. Conversely, when animals are immunized with HMGB1 released from cells killed *in vitro*, they become resistant to the formation of newly inoculated xenograft tumors [214-215]. HMGB1 released by dying tumor cells can stimulate antigen presentation on dendritic cells through its interaction with TLR2 or TLR4, which subsequently activates an adaptive anti-cancer immune response [215, 243].

Showing an anti-tumor role for HMGB1, breast cancer patients that harbor the loss-of-function TLR4 Asp299Gly polymorphism relapse more quickly after anthracycline-based therapy [215, 244]. Tumors implanted into *tlr4*$^{-/-}$ mice do not respond to therapy, whereas the same tumors implanted in wild-type mice respond to therapy [215, 245]. The anti-tumor role of HMGB1 is further supported by work that reveals when apoptotic cells are injected into mice, they are poorly immunogenic. However, when apoptotic cells mixed together with necrotic wild-type cells, but not necrotic *hmgb1*$^{-/-}$ cells, are injected into mice, the mice become resistant to the formation of newly inoculated xenograft tumors [214]. These studies point to an anti-tumor role for therapy-induced HMGB1 release and the activation of the adaptive immune system. However, it remains to be determined whether conventional chemotherapy can induce immune-stimulating cell death *in vivo*, and if the innate immune system plays a role in tumor regression.

II. Results

1. DNA alkylating agents induce tumor regression *in vivo* independent of key apoptosis regulators.

Despite the fact that human cancers are defective in their apoptotic pathways, DNA alkylating agents remain among the most effective chemotherapeutic agents used clinically [246], suggesting that alternative cell death pathways are activated. Presently, most mechanistic studies of the anti-cancer activities of DNA alkylating agents have been conducted using cultured cells and, therefore, a comprehensive understanding of tumor cell death has been lacking. Due to the complexity of a tumor's response to chemotherapy, it is important to use an *in vivo* system to evaluate the contribution of the alternative cell death pathways in anti-cancer therapy. Therefore, for the study presented here, an *in vivo* animal tumor model was developed to study non-apoptotic tumor cell death in response to DNA alkylating therapy.

E1A and K-Ras oncoproteins were used to transform genetically defined mouse embryonic fibroblasts (MEFs) isolated from wild-type, *bax*$^{-/-}$*bak*$^{-/-}$, and *p53*$^{-/-}$ mice. Stable tumor cell lines were generated from these MEFs, which maintained their respective genotypes (Fig. 1A) and grew at similar rates in cell culture (Fig. 1B). The stable *bax*$^{-/-}$*bak*$^{-/-}$ tumor cells were injected into nude mice to test for their response to doxorubicin and ortataxol, two agents commonly prescribed in the clinic. The *bax*$^{-/-}$*bak*$^{-/-}$ tumors were resistant to both treatments (Fig. 2). Since previous results showed that *bax*$^{-/-}$*bak*$^{-/-}$ cells were sensitive to DNA alkylating damage [86], the wild-type, *bax*$^{-/-}$*bak*$^{-/-}$, and *p53*$^{-/-}$ tumor cells were tested for the *in vivo* sensitivity to the DNA alkylating agent, cyclophosphamide (CP). CP is a clinically prescribed pro-drug that is converted into an active DNA alkylating agent in the liver. Tumors developed from all three cell lines (Fig. 3A). Nine days after tumor implantation, CP was injected into the tumor-bearing mice intraperitoneally (IP) at 170 mg/kg every 5 days. In response to CP, tumors derived from all three MEF tumor lines stopped growing and progressively regressed, indicating that *in vivo*, DNA alkylating damage possesses anti-tumor activity independent of key apoptosis regulators Bax, Bak, and p53 (Fig 3A and 3B).

In order to compare the response of apoptosis-proficient and -deficient tumors to CP treatment in the same environment, the wild-type and *bax*$^{-/-}$*bak*$^{-/-}$ tumor cells were labeled with GFP and RFP, respectively, and injected bilaterally into the same animal. When tumors formed, the mice were either left untreated or treated with 170 mg/kg of CP by IP injections every five days. The treated wild-type and *bax*$^{-/-}$*bak*$^{-/-}$ tumors both grew for an additional 3 to 4 days after the first CP treatment, then began to regress. The treated *bax*$^{-/-}$*bak*$^{-/-}$ tumors showed an initial delay in response to CP compared to the wild-type tumors, but most of these tumors eventually resolved to undetectable limits by both caliper measurement (Fig. 4A) and by a fluorescence imaging (Fig. 4B). Overall, in two separate experiments, 92% (11 out of 12) of the wild-type tumors and 50% (6 out of 12) of the *bax*$^{-/-}$*bak*$^{-/-}$ tumors regressed to a size that was not detectable by caliper or fluorescence imaging. The 6 remaining treated *bax*$^{-/-}$*bak*$^{-/-}$ tumors were still detectable by caliper measurement and RFP fluorescence at the end of the study (after day 50) but had progressively decreased from their peak volume. Importantly, when CP was discontinued on 3 mice whose wild-type and *bax*$^{-/-}$*bak*$^{-/-}$ tumors regressed to a non-detectable limit, these mice remained tumor free for 5 months before they died due to natural causes at one year of age (data not shown).

Clinically, in addition to p53 mutations found in human cancers, overexpression of anti-apoptotic proteins is also responsible for disabling cellular apoptotic machinery. Therefore, the anti-apoptotic protein, Bcl-xL was expressed in the transformed wild-type MEF tumor cells. The Bcl-xL overexpressing tumor cells show resistance to apoptotic inducers such as staurosporine (STS) and etoposide (Eto) *in vitro*, indicating apoptosis is sufficiently inhibited in these tumor cells (Fig. 5A). Wild-type (vector) and Bcl-xL overexpressing tumor cells were injected into athymic nude animals. When tumors formed, the mice were either left untreated or treated with 170 mg/kg of CP every 5 days, as indicated by the arrows (Fig. 5B). Both tumors regressed in response to CP treatment (Fig. 5A and 5B). These results demonstrate that: 1.) Bax/Bak-mediated apoptosis contributes to a more rapid tumor regression, as the $bax^{-/-}bak^{-/-}$ tumors showed a delay in response (Fig. 4A and 4B); and, that 2.) the apoptosis machinery may be dispensable for tumor regression in response to DNA alkylating agents, as the $bax^{-/-}bak^{-/-}$, $p53^{-/-}$ and Bcl-xL overexpressing tumors still regressed despite their defect in the apoptotic pathway.

2. Apoptosis is not the sole mediator for cyclophosphamide-induced tumor regression.

To demonstrate that apoptosis was not responsible for tumor regression in apoptosis-deficient tumor cells following CP treatment, paraffin embedded tumor sections were subjected to immunohistochemistry (IHC) analysis for cleaved caspase 3 and terminal transferase dUTP end labeling (TUNEL) assay, both hallmarks for caspase-dependent apoptosis. The treated wild-type tumor cells displayed positive staining for cleaved caspase 3 and TUNEL, whereas the treated $bax^{-/-}bak^{-/-}$ tumor cells showed virtually no positive staining (Fig. 6A-C). The same effect was observed by immunoblot analysis for cleaved caspase 3 using tumor lysates prepared from the excised tumor tissues (Fig. 6D). An antibody against phosphorylated H2A.X (γH2A.X) revealed that both wild-type and $bax^{-/-}bak^{-/-}$ tumors incurred a similar extent of DNA damage following CP treatment (Fig. 6D). Taken together, these results indicate that while apoptosis contributes to CP-induced tumor regression in apoptosis-proficient tumors, tumor cells deficient in apoptosis do not undergo apoptosis and, therefore, must rely on alternative forms of cell death.

3. Senescence and autophagy may contribute to tumor regression when apoptosis is not functional.

In addition to apoptosis and necrosis, several other cytocidal and cytostatic mechanisms have been implicated in the anti-tumor activity of chemotherapy including necrosis, autophagy, senescence, and mitotic catastrophe [4, 7, 10-11, 114]. To evaluate the involvement of these anti-cancer activities in response to CP, transmission electron microscopy (TEM) analysis was performed to examine morphological features of CP-treated tumor cells (Fig. 7). After CP treatment, both apoptotic cells (indicated by condensed chromatin) and necrotic cells at various stages (indicated by disruption of cell structure, lack of chromatin condensation, and formation of a large amount of vacuoles) were observed in the wild-type tumors. In $bax^{-/-}bak^{-/-}$ tumors, no apoptotic cells were apparent, while necrotic cells were commonly observed in CP-treated tumors. Some nuclei in the treated cells appeared to be larger and pleomorphic, indicative of senescence

and/or mitotic catastrophe [247]. In both wild-type and *bax*$^{-/-}$*bak*$^{-/-}$ tumors treated with CP, leukocytes, characterized by an electron dense cell body and high nucleus/cytoplasm ratio [248], were also observed (Fig. 7). Additionally, hematoxylin and eosin (H & E) staining revealed that both wild-type and *bax*$^{-/-}$*bak*$^{-/-}$ tumor tissues treated with CP displayed a significant morphological difference compared to the untreated tumor tissues. The majority of cells in the treated tumors had larger nuclei than the cells in the untreated tumors (Fig. 8A). This suggests that alternative cell death pathways such as mitotic catastrophe or senescence, which are often characterized by a "giant cell" or large nuclei phenomenon, may also be triggered in response to CP therapy. To characterize the mitotic capabilities of the treated tumor cells, the untreated and treated tumor tissues were subjected to IHC for Ki67, a molecular marker that identifies actively proliferating cells. In both the untreated wild-type and *bax*$^{-/-}$*bak*$^{-/-}$ tumors, the majority of the cells stained positive for Ki67. Following CP treatment, both wild-type and *bax*$^{-/-}$*bak*$^{-/-}$ tumors showed a decreased level of Ki67 staining, indicating that CP treatment can arrest cell proliferation (Fig. 8B and 8C).

Other possible forms of cell death in response to chemotherapy are senescence and autophagy. TEM analysis suggested that both may be occurring in the treated tumor tissue (data not shown). Frozen tumor sections from untreated and treated mice were assessed for senescence-associated ß-galactosidase (SA-ß-gal) activity. SA-ß-gal activity was observed in the *bax*$^{-/-}$*bak*$^{-/-}$ tumor tissue and increased significantly upon CP treatment (Fig. 9A). Surprisingly, neither the untreated nor the treated wild-type tumor tissue showed SA-ß-gal activity. To evaluate whether autophagy is involved in CP-induced tumor response, GFP-tagged microtubule-associated protein 1 (MAP1) light chain 3 (LC3) was retrovirally introduced into the wild-type and *bax*$^{-/-}$*bak*$^{-/-}$ tumors. The induction of autophagy can be revealed by the conversion of the cytosolic form of LC3 (LC3-I) to an autophagosomal membrane-bound form (LC3-II) [249]. In unstressed cells LC3 diffusely distributes throughout the cytoplasm, as indicated by diffuse green fluorescence observed in the untreated tumor tissue cells. Cells undergoing autophagy display a punctate GFP-LC3 pattern because LC3 translocates to autophagosomes. Upon CP-treatment, autophagy is induced in both wild-type and *bax*$^{-/-}$*bak*$^{-/-}$ tumors, indicating that autophagy may also play a role in CP-induced tumor response (Fig. 9B). Interestingly, the amount of autophagic cells increased progressively in *bax*$^{-/-}$*bak*$^{-/-}$ tumors upon subsequent rounds of treatment with CP. In contrast, the number of autophagic cells were much fewer in wild-type tumors, and did not seem to further increase upon longer CP treatment (Fig. 9B and 9D). This phenomenon is similar to that observed in SA-β-gal staining, where senescent cells were preferentially observed in *bax*$^{-/-}$*bak*$^{-/-}$ cells (Fig. 9A and 9C). These results indicate that either the molecular signaling pathways leading to senescence (such as p53 and p19Arf) and autophagy (such as Atg proteins) have been impaired in wild-type cells or enhanced in *bax*$^{-/-}$*bak*$^{-/-}$ cells or, more likely, apoptosis is the preferred cell fate when cells are subjected to irresolvable stress or damage. However, when the apoptosis machinery is impaired, cells must rely on alternative forms of cell death such as senescence and/or autophagy. Whether senescence and autophagy act as active death mechanisms under these circumstances remains to be determined.

4. DNA alkylating damage triggers sporadic necrosis *in vivo*.

TEM analysis indicated that necrosis may occur in CP-treated tumors (Fig. 7). To further examine this, IHC was performed on CP-treated tumor tissues using an antibody against the high mobility group box 1 (HMGB1) protein. HMGB1 is a nuclear protein that binds tightly to chromatin in apoptotic cells, whereas during necrosis it is released into the extracellular environment [218]. IHC analysis revealed nuclear staining of HMGB1 in untreated tumor tissues. In contrast, extracellular HMGB1 staining was observed in both wild-type and *bax*$^{-/-}$*bak*$^{-/-}$ CP-treated tumor tissues (Fig. 10), indicating that necrosis occurs in response to CP in both apoptosis-proficient and -deficient tumors. It is interesting to note that this CP-induced necrosis is different from necrosis that is often observed in solid tumors with overgrowth. The latter constitutes the "necrotic centers" comprised of large amounts of necrotic cells resulting from limited oxygen and nutrient supplies due to tumor overgrowth and lack of vascularization. CP-induced necrotic cells were scattered and evenly distributed throughout the tumor mass, as judged by both TEM and HMGB1 staining (Fig. 7 and 10), thus is referred to as "sporadic necrosis".

To further confirm that CP can induce necrosis, a biologically active metabolite of CP, mafosfamide (MAF) [250], was used for *in vitro* cell culture studies. Treatment of wild-type, Bcl-xL-expressing, and *bax*$^{-/-}$*bak*$^{-/-}$ tumor cells with MAF induced cell death in all three cell lines (Fig. 11A). Microscopic analysis revealed that the dead cells displayed features of necrosis such as plasma membrane dilation and disruption in all three cell lines (Fig. 11B). Wild-type cells were more sensitive than Bcl-xL-expressing cells, which were more sensitive than *bax*$^{-/-}$*bak*$^{-/-}$ cells, indicating that Bax/Bak deficiency suppresses apoptosis more efficiently than Bcl-xL overexpression (Fig. 11A and 11B). Similar to CP *in vivo*, MAF induced DNA damage was indicated by the increase of γH2A.X (Fig. 11C). This was also indicated by the levels of caspase 3 cleavage, which correlated to a cell's ability to die by apoptosis (Fig. 11D). While apoptosis was virtually blocked in *bax*$^{-/-}$*bak*$^{-/-}$ cells, Bcl-xL only shifts the balance between the anti- and pro-apoptotic Bcl-2 proteins and, therefore, did not completely block apoptosis (Fig. 11D). Additionally, HMGB1 was found in the cell culture medium from both MAF-treated apoptosis-proficient and -deficient cells, indicative of necrosis (Fig. 11D). The more rapid release of HMGB1 in wild-type cells is probably due to "secondary necrosis", since apoptotic cells are not engulfed and cleared as they are *in vivo*.

5. CP-induced cell death activates the innate immune response.

A fundamental feature of apoptosis is that apoptotic cells are quickly engulfed as an intact corpse *in vivo* and, thus, do not trigger pro-inflammatory responses. In contrast, cells dying by necrosis release intracellular contents into the extracellular environment and cause pro-inflammatory responses. In TEM analysis, the presence of leukocytes in both wild-type and *bax*$^{-/-}$*bak*$^{-/-}$ CP-treated tumors was observed, suggesting infiltration of innate immune cells (Fig. 7). To confirm that this is the case, IHC was performed using an antibody against F4/80, a pan macrophage marker, and an antibody against an allotypic marker of neutrophils on untreated and treated tumor tissue. The untreated tumor tissue showed minimal positive staining for either macrophages (Fig. 12A) or

neutrophils (Fig. 13A). However, the treated tumor tissue showed significantly increased amounts of both macrophages (Fig. 12A) and neutrophils (Fig. 13A). To demonstrate this effect more quantitatively, single cell suspensions were prepared from the tumor tissues. The cell suspensions were stained for Mac-1 and F4/80 to identify macrophages or a neutrophil specific marker and subjected to flow cytometry analysis (12B and 13B). Both wild-type and *bax*$^{-/-}$*bak*$^{-/-}$ treated tumor tissues showed a significant increase of both macrophages and neutrophils over the untreated tumor tissues (Fig. 12B and 13B). Taken together, these results indicate that infiltration of innate immune cells occurs in response to chemotherapy, regardless of the tumors cell's ability to die by apoptosis.

Both apoptotic and necrotic cells can attract phagocytes. However, it is generally accepted that phagocytes, such as macrophages, secrete immune-suppressive cytokines upon engulfing apoptotic cells, whereas those encountering necrotic cells secrete pro-inflammatory cytokines [155, 251]. To examine this issue, it was determined whether the leukocytes recruited to the tumor tissue produced pro-inflammatory cytokines. In both wild-type and *bax*$^{-/-}$*bak*$^{-/-}$ tumor tissues, CP treatment increased the number of interleukin-1β (IL-1β) positive cells and the levels of both IL-1β and TNFα (Fig. 14A-C). This suggests a critical role of the innate immunity in DNA alkylating damage-induced tumor clearance. Taken together, these results strongly indicate that CP-induced tumor cell death is not exclusively apoptotic, but includes necrosis and can activate a pro-inflammatory response.

6. HMGB1 plays an essential role in tumor regression in response to chemotherapy *in vivo*.

DNA alkylating therapy induced tumor regression in athymic nude mice that lack an adaptive immune response. This tumor regression is associated with sporadic tumor cell necrosis, HMGB1 release, and infiltration of innate immune cells into the treated tumor tissue [70]. To determine the role of HMGB1 in tumor response to chemotherapy, *hmgb1*$^{-/-}$ MEFs [252] were transformed with E1A and K-Ras oncoproteins. To ensure a fair comparison of cells with an isogenic background, Flag-tagged HMGB1 was introduced into the *hmgb1*$^{-/-}$ MEFs to restore HMGB1 at comparable levels to the wild-type cells (Fig. 15A). Bcl-xL was expressed in both the Flag-HMGB1 and *hmgb1*$^{-/-}$ E1A/K-Ras transformed cells to suppress apoptosis to mimic apoptosis-deficient human cancers (Fig. 15A). The cells were injected into athymic nude mice. After tumors formed, the tumors were taken out of the mice and tumor cells were recovered and cultured as stable tumor cell lines. The Flag-HMGB1 and *hmgb1*$^{-/-}$ tumor cells grew in culture at similar rates (Fig. 15B) and had comparable sensitivity to treatment with the DNA alkylating agent mafosfamide (MAF; Fig. 16A and 16B). Upon MAF treatment, the Flag-HMGB1 tumor cells released HMGB1 into the culture media in a dose-dependent manner (Fig. 16C). Additionally, time lapse video imaging was performed to capture the release of HMGB1 from cells during necrosis. GFP-tagged HMGB1 was introduced into *hmgb1*$^{-/-}$ MEFs and treated with MAF in the presence of propidium iodide (PI) and a live cell permeant DNA dye Hoechst 33342. Simultaneous decrease of cellular GFP-HMGB1 and loss of plasma membrane integrity indicated by PI positive staining was observed. Representative images are shown in Figure 17. This is consistent with previous reports that DNA alkylating damage can induce tumor cell necrosis [70, 86] and

that HMGB1 is released from necrotic cells [86, 164, 218]. Hence, a transformed MEF tumor cell line was established to study the role of HMGB1 in response to chemotherapy.

To study the effect of HMGB1 in response to chemotherapy *in vivo* the green fluorescent protein (GFP) was expressed in the Flag-HMGB1 and *hmgb1*$^{-/-}$ tumor cells. The Flag-HMGB1 and *hmgb1*$^{-/-}$ tumor cells were then injected bilaterally into the left side and right side, respectively, of 20 athymic nude mice. Both cell lines formed tumors that grew at similar rates (Fig. 18A and 18B). Fourteen of these animals were then compared side-by-side for their susceptibility to cyclophosphamide (CP), a DNA alkylating agent that is commonly prescribed in the clinic. All 14 tumors with restored HMGB1 showed a virtually complete regression in response to CP treatment by day 22, as they were no longer detectable by either caliper measurement or fluorescence imaging (Fig. 18A and 18B). In sharp contrast, while *hmgb1*$^{-/-}$ tumors initially responded to treatment, all 14 tumors failed to regress to non-detectable means. Instead, around day 30 these tumors began to increase in size. Further, at day 35, 3 of the 14 mice were taken off of CP. While the tumors with reconstituted HMGB1 remained undetectable, the *hmgb1*$^{-/-}$ tumors recurred to form large tumors (Fig. 18A red lines and Fig. 18B bottom panel). Taken together, these results indicate that HMGB1 plays an essential role in tumor regression induced by DNA alkylating therapy.

7. HMGB1 released from chemotherapy-induced necrotic tumor cells is a chemoattractant.

CP treatment induces sporadic tumor cell necrosis and HMGB1 extracellular release *in vivo* [70]. To determine if Flag-HMGB1 changed subcellular localization in response to CP treatment, tumors were extracted from untreated and CP-treated mice and subjected to immunohistochemistry (IHC) using an antibody against Flag. The *hmgb1*$^{-/-}$ tumors showed no positive staining for HMGB1. In tumors with restored HMGB1, the untreated tumor cells showed nuclear HMGB1 localization and the CP-treated tumors showed extracellular localization, indicating Flag-HMGB1 is released into the extracellular environment upon tumor cell necrosis in response to CP-treatment (Fig. 19A).

A prominent hallmark associated with HMGB1 released from damaged tissue or from immune cells in response to endotoxin exposure is leukocyte recruitment [227]. As HMGB1 was released upon CP-treatment, it was next determined if leukocytes were recruited to CP-treated tumors. An increase in macrophage infiltration was observed in CP-treated Flag-HMGB1 tumors, while the increased infiltration of macrophages upon CP treatment was significantly lower in *hmgb1*$^{-/-}$ tumors shown by both IHC using an antibody against Mac-2 (Fig. 19A) and flow cytometry using antibodies against CD11b and F4/80 (Fig. 19B). The percentage of macrophages in the CP-treated Flag-HMGB1 tumors is seemingly high, reaching over 60% of the total cell population. The difference between the IHC and flow cytometery results may be due to antibody specificity. Mac-1 and F4/80 have been found to label other immune cells besides macrophages. Additionally, while generating a single cell suspension from treated tumor tissue, immune cells may be more easily dislodged then the tumor cells, generating an immune cell rich population for analysis. Hematoxylin and eosin (H &E) staining reveals the presence of immune cells within the treated tumor tissue although quantitation is difficult

based solely on H & E staining (data not shown). Strikingly, Flag-HMGB1 but not *hmgb1*$^{-/-}$ tumors had a significant infiltration of neutrophils detected by an antibody against an allotypic marker of neutrophils (Fig. 19A), despite a reduced number of neutrophils in the peripheral blood upon CP treatment as previously reported (Fig. 19C) [253]. Similar to macrophages and neutrophils, an anti-natural killer (NK) cell antibody (NKp46) revealed that while CP treatment induced a drastic infiltration of NK cells, the levels were markedly reduced in the CP-treated *hmgb1*$^{-/-}$ tumors compared to the HMGB1 restored tumors (Fig. 19A).

A molecular marker for activated NK cells is granzymes, which mediate NK cell killing activities via its delivery into the target cell through perforin (PFRN) [254]. The presence of Granzyme B (GrB) and PFRN was assessed by IHC. Upon CP treatment, there was a significant increase of both GrB and PFRN in the Flag-HMGB1 tumors, whereas both markers were virtually absent in *hmgb1*$^{-/-}$ tumors (Fig. 20A and 20B). The enhanced GrB and PFRN levels were associated with increased caspase 3 cleavage (Fig. 20B), which has been shown to be activated through proteolytic cleavage by GrB, independent of the mitochondrial apoptosis pathway [254-255]. Taken together, these results indicate that HMGB1 released during chemotherapy can act as a chemoattractant to activate the innate immune system including macrophages, neutrophils, and NK cells, and that granzyme-mediated cell killing may be a mechanism for tumor clearance.

8. Activation of innate immunity plays an anti-tumor role in chemotherapy.

It has been shown that the activation of innate immunity contributes to tumor regression mediated by activation of p53 [175]. As compromised infiltration of macrophages, neutrophils, and NK cells were observed in *hmgb1*$^{-/-}$ CP-treated tumors (Fig. 19), the role of innate immune cells in anti-cancer therapy was assessed. To further investigate if macrophage activation contributes to tumor clearance, gadolinium chloride ($GdCl_3$) was used to deplete macrophages. $GdCl_3$ has been shown to deplete peripheral blood macrophages, most of the liver Kupffer cells, and some spleen macrophages in mice [256-257]. The effect of $GdCl_3$ was tested on E1A/K-Ras transformed Bcl-xL-expressing tumor cells expressing endogenous HMGB1. Animals bearing these tumors were treated with CP only or in combination with $GdCl_3$ every 3 days by intravenous (IV) injection. A significant level of macrophage depletion in the peripheral blood was achieved in animals treated with $GdCl_3$ (Fig. 21A). Around day 25, the tumors in mice treated with both CP and $GdCl_3$ began to increase in size (Fig. 21B). Similarly, to determine the effects of neutrophils, an anti-neutrophil antibody (Ly-6G) was used to deplete neutrophils. Successful depletion was achieved, as indicated by lower counts of neutrophils in peripheral blood (Fig. 22A). Animals bearing tumors were treated with CP only or CP in combination with intraperitoneal (IP) injections of the anti-neutrophil depletion antibody. While tumors in mice receiving only CP showed complete regression by day 40, those in mice receiving CP along with the anti-neutrophil depletion antibody initially exhibited tumor regression, but then became resistant to the treatment (Fig. 22B). Similarly, to study the effect of NK cells during tumor response to CP, an anti-NK cell antibody (anti-Asialo GM1) was administered to tumor bearing mice. Successful depletion was achieved, as indicated by lower counts of NK cells in peripheral blood (Fig. 23A). Tumor bearing mice were treated with CP-only or CP plus intravenous (IV)

injections of the anti-NK depletion antibody. Similar to the neutrophil and macrophage depletion studies, mice with NK cell depletion could not achieve complete tumor regression and their tumors continued to grow after an initial delay of growth (Fig. 23B).

9. HMGB1 suppresses an M2 immune response.

Circulating immature monocytes are attracted by tumor-derived chemokines to migrate from the blood into the tumor tissue and differentiate into macrophages. Once inside the tumor, differentiation and polarization of the monocytes into activated (M1) or alternatively activated (M2) cells depend on the cytokines present in the tumor microenvironment [258]. Recently it has been suggested that tumor-associated macrophages (TAMs) are generally characterized by the M2 type cytokine profile and facilitate tissue repair and remodeling, and tumor progression, whereas the M1 type is usually associated with anti-tumor activity [259-260]. Therefore, switching TAMs from M2 to M1 may have significant therapeutic value. Since macrophage infiltration was enhanced in both Flag-HMGB1 and *hmgb1*$^{-/-}$ tumors upon CP treatment (Fig. 19), and *hmgb1*$^{-/-}$ tumors failed to activate an anti-tumor immune response (Fig. 18), the effect of HMGB1 on M1/M2 polarization was tested. Indeed, IHC revealed that production of the pro-inflammatory cytokine IL-1β, an M1 cytokine, was stimulated by CP treatment in Flag-HMGB1 tumors but not in *hmgb1*$^{-/-}$ tumors (Fig. 24A). Tissue cytokine array and immunoblot analysis revealed that the production of M2-type immune tolerant cytokines such as IL-4, IL-10, and IL-13 was enhanced in *hmgb1*$^{-/-}$ tumors upon CP treatment. Strikingly, expression of Flag-HMGB1 resulted in decreased levels of these immune tolerant cytokines (Fig. 24B and 24C; Fig. 25A and 25B). This is consistent with previous reports showing that HMGB1 can activate innate immune cells to produce a number of pro-inflammatory cytokines but not anti-inflammatory cytokines [222, 261]. These results indicate that HMGB1 may facilitate tumor regression in response to chemotherapy by suppressing the production of the pro-tumor M2 cytokines in the tumor tissue.

10. HMGB1 is essential for activation of innate immunity and tumor regression.

To further confirm the importance of HMGB1 during chemotherapy-induced activation of the innate immune system and subsequent tumor regression, an HMGB1 neutralizing antibody [221, 262] was used to block HMGB1 activity. Flag-HMGB1 and *hmgb1*$^{-/-}$ tumor cells were injected bilaterally into the left and right side of athymic nude mice, respectively. When tumors formed, mice were divided into two groups. One group received CP-treatment alone and the other received both CP and the HMGB1 neutralizing antibody. As anticipated, *hmgb1*$^{-/-}$ tumors failed to regress in response to both treatment regimens (Fig. 26A). The Flag-HMGB1 tumors initially responded to both treatments. However, the tumors in mice receiving CP in combination with the HMGB1 neutralizing antibody started to grow around day 35 (Fig. 26A and 26B). IHC analysis showed that the HMGB1 neutralizing antibody suppressed Mac-2 positive macrophages and GrB positive NK cells in CP-treated Flag-HMGB1 tumors to similar levels as in *hmgb1*$^{-/-}$ tumors (Fig. 27A and 27B).

HMGB1 was knocked down in the human breast cancer cell line, MDA-MB-231, to test if HMGB1-mediated tumor regression was limited to the mouse embryonic fibroblast cell line. MDA-MB-231 cells with and without HMGB1 expression (Fig. 28A) were injected into athymic nude animals. When tumors formed, the mice were treated with CP. Tumors that lacked HMGB1 were resistant to treatment (Fig. 28B and 28C), similar to the results obtained with the *hmgb1*$^{-/-}$ MEFs (Fig. 18) and wild-type MEFs in which HMGB1 was blocked with an antibody (Fig. 26). Further analysis on the effect of the innate immune response using MDA-MB-231 cells is warranted. Taken together, these results demonstrate that HMGB1 plays an essential role in activation of innate immunity and tumor regression during chemotherapy.

III. Discussion

The enormous efforts spent investigating basic signaling mechanisms involved in cell death pathways will ultimately allow us to design strategically targeted cancer therapies. A greater understanding of how tumor cells die in response to chemotherapy and subsequently activate the immune response is likely to reveal new approaches to induce tumor regression while possibly providing greater protection to normal cells. A xenograft mouse tumor model was generated using apoptosis-proficient and -deficient tumor cells to examine the contribution of the known forms of cell death in tumor regression induced by cyclophosphamide, a DNA alkylating agent and one of the most commonly prescribed chemotherapeutic drugs. Interestingly, while apoptosis facilitates a more rapid tumor regression, it is dispensable for complete tumor regression. Other forms of cell death, including necrosis, autophagy, senescence, and mitotic catastrophe are all initiated in response to CP treatment. Specifically, sporadic necrosis played a critical role in stimulating the innate immune system that contributes substantially to tumor regression. The activation of the innate immune system required the release of HMGB1 from chemotherapy-induced necrotic tumor cells. The use of the *in vivo* animal system provided evidence, for the first time, that necrosis and the innate immune response were necessary for tumor regression.

1. Chemotherapy induces sporadic necrosis in both apoptosis-proficient and -deficient tumor cells.

Necrosis is often observed in solid tumor areas where vascularization lags behind tumor tissue growth. Necrosis has been reported to occur in numerous cancers following chemotherapy and radiation therapy, and has been used as one of the best prognostic factors for a positive outcome [12-15, 88, 92, 94, 263-265]. However, these occasional reports have been overwhelmed by the amount of literature suggesting that apoptosis is the main death mechanism in response to radiation treatment or chemotherapy. It is unclear whether necrosis in human tumors is: 1.) the result of a "secondary necrosis" where apoptotic cells are not efficiently removed and begin to show necrotic qualities; 2.) a mechanism of cell death apparent only when apoptosis becomes unavailable; or, 3.) an active, independent form of cell death. Tumor cells derived from *bax*$^{-/-}$*bak*$^{-/-}$, *p53*$^{-/-}$, and Bcl-xL overexpressing cells, provided evidence that necrotic death is an active response to chemotherapy and is apoptosis-independent. Tumor cells undergo necrosis, shown by TEM morphology (Fig. 7), HMGB1 extracellular release (Fig. 10), and activation innate immune cells in the treated tumor tissue (Fig. 14). Importantly, the features of necrosis are present in both apoptosis-deficient and -proficient tumor cells. Despite clear signs of apoptosis, necrotic cells were also observed in CP-treated wild-type tumor cells. Thus, necrosis is not merely a death mechanism observed in the absence of apoptosis. Rather, it may play an important physiological role even in apoptosis-proficient cells by directly inducing tumor cell death and by triggering a pro-inflammatory response.

Several molecular pathways have been described to induce necrosis under physiological settings. These include RIP1-mediated necrosis in response to death receptor ligation, generation of reactive oxygen species (ROS), Ca^{2+}-dependent activation of non-caspase proteases, and hyperactivation of PARP [84-86, 151, 266]. These pathways are not mutually exclusive. Although cell culture results indicate that DNA alkylation-induced necrosis is a tumor cell autonomous response (Fig. 11), the increased

levels of TNFα and IL-1β (Fig. 14) and the recruitment of innate immune cells (Fig. 12 and 13) that can lead to higher ROS production may all contribute to CP-induced necrosis *in vivo*, singly or jointly.

2. Crosstalk among multiple cell death pathways.

While these findings demonstrate that necrosis plays a critical role, apoptosis was also found to be vital in CP-induced tumor regression. While apoptosis-deficient *bax*$^{-/-}$ *bak*$^{-/-}$ and Bcl-xL-expressing cells do not survive long term treatment of mafosfamide in cell culture (Fig. 11), the deficiency in Bax and Bak results in delayed tumor regression and remission in nearly 50% of the animals treated with CP (Fig. 4). This is consistent with previous studies using an Eμ-myc lymphoma model expressing Bcl-2 treated with CP [267], indicating that deficiency in apoptosis can contribute to chemoresistance. Interestingly, CP-resistance was not observed in Bcl-xL-overexpressing tumors (Fig. 5B). It is possible that in fibrosarcomas generated from MEFs the threshold for apoptosis inhibition required for the resistance to CP treatment is higher than that in the lymphoma system. *bax*$^{-/-}$*bak*$^{-/-}$ cells displayed better resistance than the Bcl-xL-expressing cells to DNA alkylating damage *in vitro* (Fig. 11) and *in vivo* (Fig. 4 compared to Fig. 5B). Thus it is likely that there exists a critical threshold in a cell's ability to die by apoptosis in order to acquire chemoresistance *in vivo*, and this threshold may vary depending on the types of cancer and the nature of the chemotherapeutic agents.

In addition to apoptosis and necrosis, treated tumor cells showed evidence of cell cycle arrest (Fig. 8B), autophagy (Fig. 9B), premature senescence (Fig. 9A), and mitotic catastrophe (Fig. 8A). Unlike necrosis and cell cycle arrest, which occurred at similar levels in apoptosis-proficient and -deficient cells, premature senescence and autophagy were more commonly observed in apoptosis-deficient cells. This suggests two possible scenarios: 1.) either these events are alternative active cell death mechanisms that are amplified in apoptosis-deficient cells or, 2.) they are cellular defense mechanisms against stress imposed by chemotherapy whose existence is more easily visualized in the absence of apoptosis. Literature exists supporting both possibilities. In an Eμ-myc lymphoma mouse model where Bcl-2 was over expressed, senescence was the main form of tumor response to the DNA alkylating agent, CP [71]. Conversely, although a senescent cell cannot divide even if stimulated by mitogens, it remains metabolically active and able to secrete proteins with potential tumor-promoting activities [76-77]. Finally, various chemotherapeutic agents have been shown to induce autophagy in a variety of different human tumor cells *in vitro* [72]. DNA damaging agents induce autophagy in numerous cancer lines [73]. Autophagy has been described to be either a death mechanism or a survival mechanism in response to chemotherapy [74, 268-272]. The outcome of autophagy induction or inhibition in cancer cells may depend on the cell's ability to resolve the stressing condition and/or to die by apoptosis, which vary depending on the nature of the insults and the cancer type [268, 273-274].

3. Therapy-induced tumor cell necrosis induces innate immune cell recruitment and activation.

Apoptotic cells are generally thought to be recognized and cleared by phagocytes and neighboring cells, avoiding activation of immune cells, whereas necrotic cells are pro-inflammatory [275-276]. Phagocytes recruited by apoptotic cells often express immune-suppressive cytokines [154-155]. In contrast, inflammation-associated macrophages secrete pro-inflammatory cytokines [177]. Due to the difficulty in characterizing non-apoptotic forms of cell death *in vivo* and the lack of animal models that can separate different forms of cell death, how chemotherapy-induced cell death may modulate the immune response remained largely unclear. Shown here, CP treatment can induce recruitment of innate immune cells into the treated tumor tissue, as indicated by macrophage and neutrophil infiltration (Fig. 12 and 13). The ability of cells to die by apoptosis does not seem to have a significant influence on this effect, as the infiltration of innate immune cells was observed in both wild-type and *bax*$^{-/-}$*bak*$^{-/-}$ tumors. Since innate immune cells respond to both apoptotic and necrotic tumor cells, it was necessary to characterize the status of the response as either anti-inflammatory or pro-inflammatory, respectively. Interestingly, the pro-inflammatory cytokines IL-1β and TNFα were up regulated in both CP-treated apoptosis-proficient and -deficient tumors (Fig. 14). These findings strongly suggest that: 1.) cell death occurring by a non-apoptotic mechanism is the trigger for the immune cell infiltration; and, 2.) immune cell infiltration is not just a phenomenon observed in apoptosis-deficient cells, but may have important physiological relevance even in apoptosis-proficient cells.

Of the potential alternative cell death mechanisms that might trigger the pro-inflammatory response in CP-treated tumors, necrosis plays a major role due to the release of intracellular constituents. p53-mediated senescence has also been recently shown to trigger tumor clearance by activating the innate immune response [175]. Consistent with this, there were increased senescent cells (SA-β-gal positive) in *bax*$^{-/-}$ *bak*$^{-/-}$ tumors upon CP treatment (Fig. 9A), thus the possibility that the macrophage and neutrophil infiltration is mediated by premature senescence in *bax*$^{-/-}$*bak*$^{-/-}$ cells cannot be ruled out. However, a similar amount of immune cell infiltration was observed in wild-type tumors (Fig. 12 and 13), where SA-β-gal positive cells were not present (Fig. 9A). Thus, CP-induced immune-stimulation does not seem to require senescence. Further analysis reveals that chemotherapy-induced necrosis not only causes the recruitment of innate immune cells into the tumor tissue (Fig. 12 and 13), but does so in a manner that stimulates a pro-inflammatory response (Fig. 14). This is consistent with other reports that show necrotic cell death activates the pro-inflammatory response, whereas other cell death types such as apoptosis or autophagy do not [85, 147-152, 214, 227, 251, 275, 277].

Immune responses play an important role in cancer development and therapy. While chronic inflammation has been shown to promote tumor growth, inflammation under certain circumstances has been shown to promote tumor clearance [177]. Chronic inflammation has been found to be induced by necrosis resulting from tumor overgrowth, and is associated with accelerated tumor growth [179]. On the other hand, therapy-induced immune responses may act as an anti-tumor mechanism. Activation of the innate immune system facilitates tumor clearance in a xenograft model where senescence is

induced by p53 reactivation in p53 null tumors [175]. Boosting the innate immune response may be a promising approach for adjuvant treatment of cancer.

4. Activation of the innate immune response is mediated by HMGB1.

Induction of necrosis is associated with the release of the pro-inflammatory molecule HMGB1. It has previously been reported that HMGB1 plays an important role in the tumor microenvironment. HMGB1 has been shown to mediate inflammation, cell migration, metastasis, activate macrophages and DC, and promote neutrophil recruitment [227, 278-281]. Therefore, in an effort to link tumor cell necrosis with the activation of the innate immune response and tumor regression, HMGB1-defecient tumors were generated using the *in vivo* animal model presented here. While tumor cells generated from HMGB1-defecient MEFs did not have survival advantages in response to DNA alkylating treatment in cell culture (Fig. 16), they were surprisingly resistant to chemotherapy *in vivo* (Fig. 18). This resistance correlated with impaired innate immunity, indicated by lower levels of macrophage, neutrophil, and NK cell infiltration into the HMGB1-deficient tumor tissues upon CP-treatment (Fig. 19A). Showing for the first time that a protein not directly involved in the execution of cell death plays an essential role *in vivo* for tumor response to chemotherapy.

While chemotherapy has long been known to induce cancer cell death, it is becoming appreciated that tumor response to chemotherapy is not simply cytotoxic or cytostatic [282]. Both innate and adaptive immune responses can be activated by dying cells, pointing to an important question as to whether the immune response also plays a significant role in therapy. In this study, macrophages, neutrophils, and NK cells were individually found to be required for tumor regression (Fig. 21-23). These findings point to an important role of the innate immune response in therapy-induced tumor clearance. It has been shown that cells killed by chemotherapeutic agents *in vitro* can immunize animals against newly inoculated tumors via antigen cross-presentation to activate cytolytic T cells in an HMGB1/TLR4-dependent manner [215]. Here by using immune-compromised athymic nude mice, it was demonstrated that the innate immune response can also play a major role in tumor clearance in response to chemotherapy. This is consistent with a previous report showing that innate immunity is essential for tumor clearance in a p53 restoration mouse model [175]. In the clinic, CP has been shown to affect both the T cell and B cell compartments, and to block antibody production [283-284]. The findings presented here provide an explanation for why CP, which is often used as an immune suppressant, works efficiently in cancer treatment by blocking humoral immunity and allowing cellular tumor immunity to predominate.

The mechanism by which the innate immune system kills cancer cells remains to be determined. The leukocyte depletion results indicate that macrophages, neutrophils, and NK cells play an anti-tumor role (Fig. 21, 22, and 23) [70, 175]. However, it remains to be determined whether there exists a cross dependence of these innate immune cells to be recruited or activated. In addition, consistent with impaired NK cell recruitment, markedly lower levels of perforin and granzyme B were detected in *hmgb1*$^{-/-}$ tumors, suggesting that perforin/granzyme-mediated cytotoxicity may contribute to tumor cell death (Fig. 20). This can also explain why tumor cells deficient in mitochondrial apoptosis are susceptible to alkylating chemotherapy *in vivo*, as perforin and granzymes

have been shown to mediate cell death independent of the mitochondrial apoptotic pathway [254-255].

5. HMGB1 induces monocyte polarization.

The results presented here suggest that HMGB1 may contribute to tumor regression by regulating monocyte polarization. Macrophages have been shown to facilitate both tumor cell death and growth. Macrophages that mediate these opposing functions have been classified as M1 (anti-tumor) and M2 (pro-tumor). While M1 macrophages are characterized by classic cytotoxic cytokines, the pro-tumor M2 macrophages are classified by elevated production of cytokines including IL-4, IL-10, and IL-13. Interestingly, the cytokine array analysis revealed that while CP treatment stimulated the production of certain cytokines such as MIP-1α and RANTES (Fig. 24 and 25), levels of the M2 cytokines IL-4, IL-10, and IL-13 are higher in CP-treated *hmgb1*$^{-/-}$ tumors but are markedly suppressed in the presence of HMGB1 (Fig. 24 and 25). The elevated levels of M2 cytokines correlate with the tumor regrowth observed in *hmgb1*$^{-/-}$ tumors (Fig. 18A and 18B). Hence, HMGB1 released by dying tumor cells may suppress M2 polarization of macrophages and prevent tumor regrowth and resistance to treatment. Modalities aimed at inducing tumor cell necrosis may likely result in final eradication of tumors as a consequence of nonspecific activation of the innate immune system. While elevated levels of HMGB1 have been detected in various types of cancers [237, 285-286], boosting the innate immune response by inducing necrotic release of HMGB1 may be a promising approach for adjuvant treatment of cancer.

In the fight against cancer, cell death pathways that remain active in cancer cells have great therapeutic potential. The work presented here utilizing the *in vivo* animal system demonstrates that DNA alkylating damage induces a complex cell death response, and that sporadic tumor cell necrosis plays a critical role in tumor regression. HMGB1 released from chemotherapy-induced necrotic tumor cells was found to be necessary not only for recruitment of innate immune cells into the treated tumor tissue but also for complete tumor regression. Therefore, necrosis is an attractive strategy for cancer therapy because not only does it induce tumor cell death, but it also activates the innate immune response to induce subsequent tumor cell clearance. Additionally, HMGB1 was found to be an important mediator of the pro- versus anti-tumor effect mediated by the innate immune response (Fig. 29). In genetically heterogeneous human tumors, cells that are apoptosis-competent will regress quickly in response to conventional chemotherapy, leaving behind apoptosis-resistant populations. The finding represented here suggest that if we can design therapies to deliberately induce necrosis early in cancer therapy, we will effectively target apoptosis-competent and -resistant cells equally and will avoid selecting for more aggressive tumor cell populations, increasing the chances for a positive outcome of therapy. Further characterization of the molecular players in necrosis and the immune response will create new opportunities for chemotherapeutic targets.

.

IV. Current and Future Perspectives

The mechanism of how chemotherapy induces tumor cell death *in vivo* remains a controversial issue despite many years of research. The work presented here provides evidence as to how chemotherapy may work in the clinic. First, cyclophosphamide (CP), which has been described to suppress both B and T cells in the clinic, induced tumor regression in immunodeficient animals. Interestingly, this study shows that CP-induced tumor regression was dependent on activation of the innate immune response. This provides evidence as to how chemotherapy may work in the clinic when chemotherapy suppresses the adaptive immune response. Second, this study provides evidence that HMGB1 is important in activating the innate immune response and facilitating tumor clearance. This study is the first to show that HMGB1, a protein not directly involved in the execution of cell death per se, mediates the tumor clearance. Third, there is evidence that multiple forms of cell death are activated in response to chemotherapy in apoptosis deficient tumor cells. Interestingly, necrosis is activated in both apoptotic-proficient and deficient tumor systems indicating necrosis may be a general cell death mechanism in response to chemotherapy.

Research like this is necessary to work towards strategically targeted therapy. The results presented here indicate that boosting the innate immune response by inducing necrotic release of HMGB1 may be a promising approach for adjuvant treatment of cancer. However, some remaining questions include: 1.) the post-translational modification status of HMGB1. Recent reports have shown that its modification status can change the way it activates the immune response. 2.) Whether NK cells directly induce tumor cell killing and through which mechanisms. 3.) How HMGB1 would mediate tumor regression in an immunocompetent animal. 4.) How an orthotopic tumor animal model would change the outcome of tumor regression mediated by HMGB1. It is interesting to speculate that the immune response would be altered in different organs/tumor locations. 5.) The status of the immune cells that have infiltrated into the tumor tissue. Specific markers have been characterized for M1 versus M2 macrophages which could be used on single cell suspensions of the treated tumor tissue for flow cytometry. 6.) Which innate immune cells are making cytokines such as IL-4, IL-10, and IL-13 that are involved in the pro-tumor response in the *hmgb1*$^{-/-}$ CP-treated tumor tissue. 7.) How IL-4, IL-10, and IL-13 are suppressed in the presence of HMGB1.

V. Figures

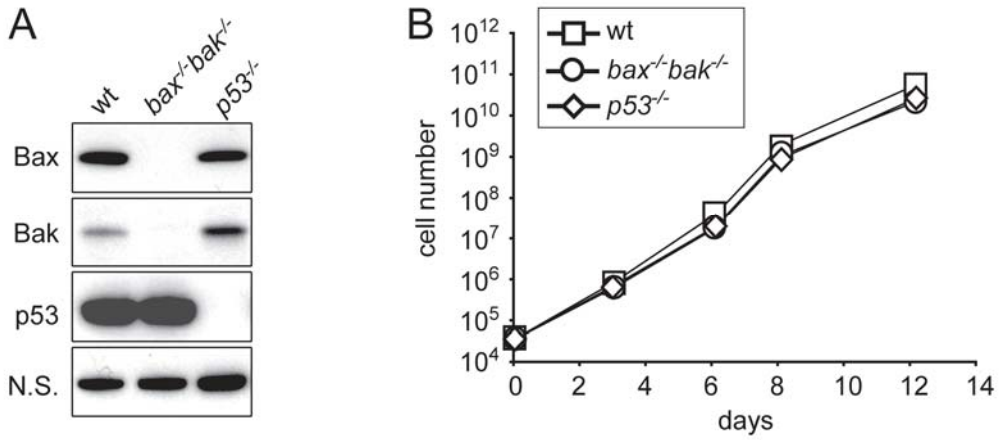

Figure 1. Mouse embryonic fibroblasts derived from *bax*$^{-/-}$*bak*$^{-/-}$ and *p53*$^{-/-}$ mice do not have proliferation defects.

Mouse embryonic fibroblasts (MEFs) were obtained from wild-type, *bax*$^{-/-}$*bak*$^{-/-}$, and *p53*$^{-/-}$ mice. (A) Cell lysates were made and probed for Bax, Bak, and p53 by immunoblotting analysis. N.S., a non-specific band to verify equal loading. (B) Wild-type, *bax*$^{-/-}$*bak*$^{-/-}$, and *p53*$^{-/-}$ MEFs were plated and the cell number was determined on the indicated days. Data shown are the averages of four independent countings ± S.E.M. (error bars are too small to be seen).

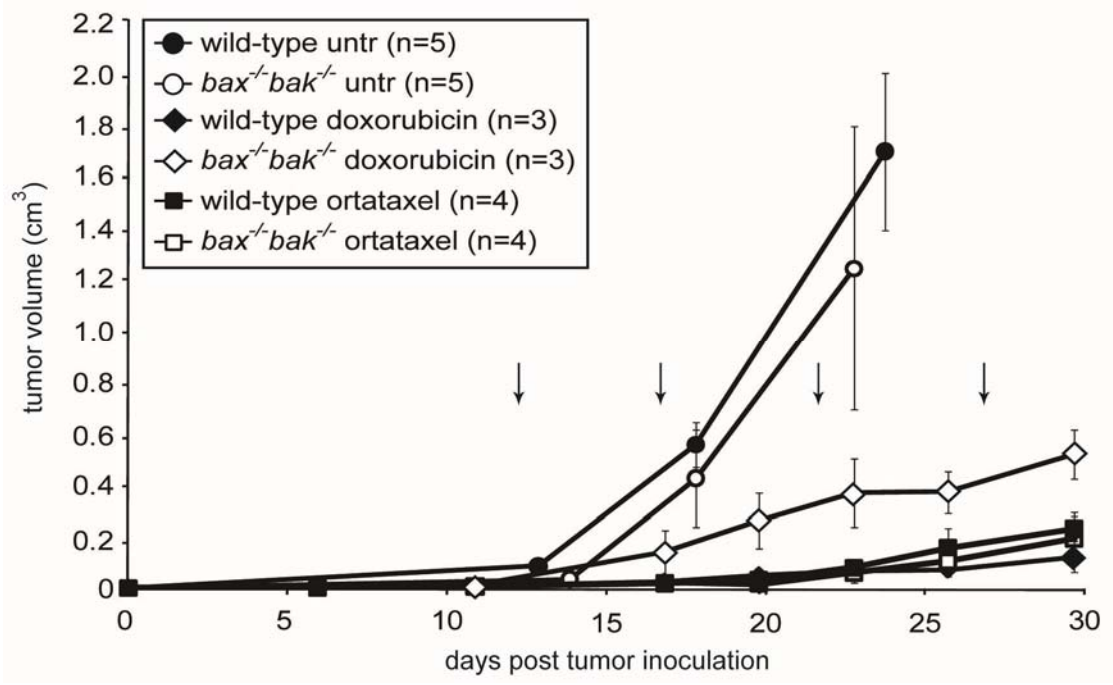

Figure 2. Apoptosis-proficient and -deficient tumors are resistant to chemotherapy.

Mouse embryonic fibroblasts (MEFs) were obtained from wild-type and *bax*$^{-/-}$*bak*$^{-/-}$ mice, transformed with E1A and K-Ras, and injected into athymic nude mice. The tumors were excised from the mice to generate stable tumor cell cultures. One million of the established tumor cells were injected subcutaneously into nude mice. When tumors formed, mice were treated with IV injections of either 5 mg/kg of doxorubicin or 50 mg/kg of ortataxol, every 5 days, as indicated by the arrows. The tumor volume was calculated based on caliper measurement and plotted. Note that the tumors are resistant to treatment by common chemotherapeutic agents.

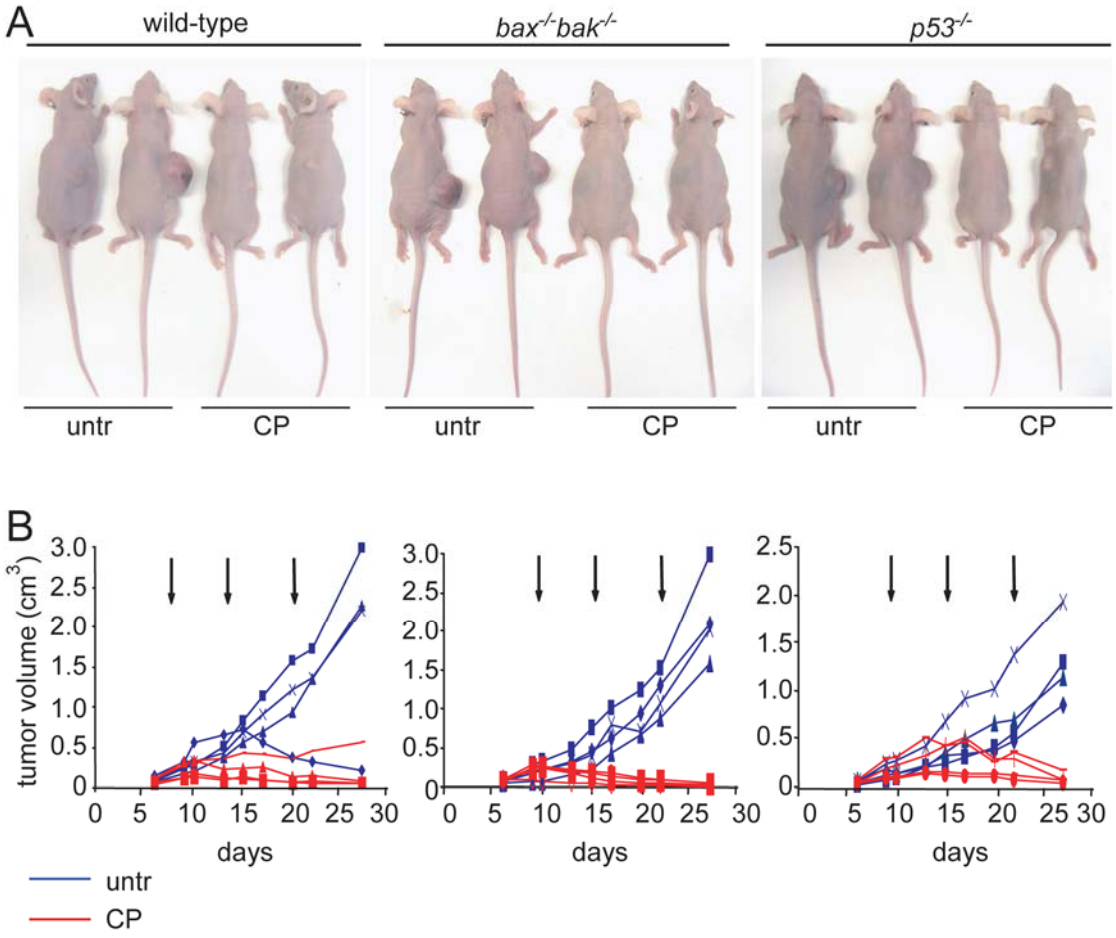

Figure 3. Apoptosis is dispensable in response to chemotherapy.

Mouse embryonic fibroblasts (MEFs) were obtained from wild-type, *bax*$^{-/-}$*bak*$^{-/-}$, and *p53*$^{-/-}$ mice, transformed with E1A and K-Ras, and injected into athymic nude mice. The tumors were excised from the mice to generate stable tumor cell cultures. One million of the established tumor cells were injected subcutaneously into nude mice. When tumors formed, mice were treated with 170 mg/kg of cyclophosphamide (CP) every 5 days, as indicated by the arrows (B). (A) Representative untreated and CP-treated mice are shown. (B) Tumor volume was calculated based on caliper measurement and plotted. Note that tumors of all three genotypes regressed after CP treatment, regardless of their ability to die by apoptosis.

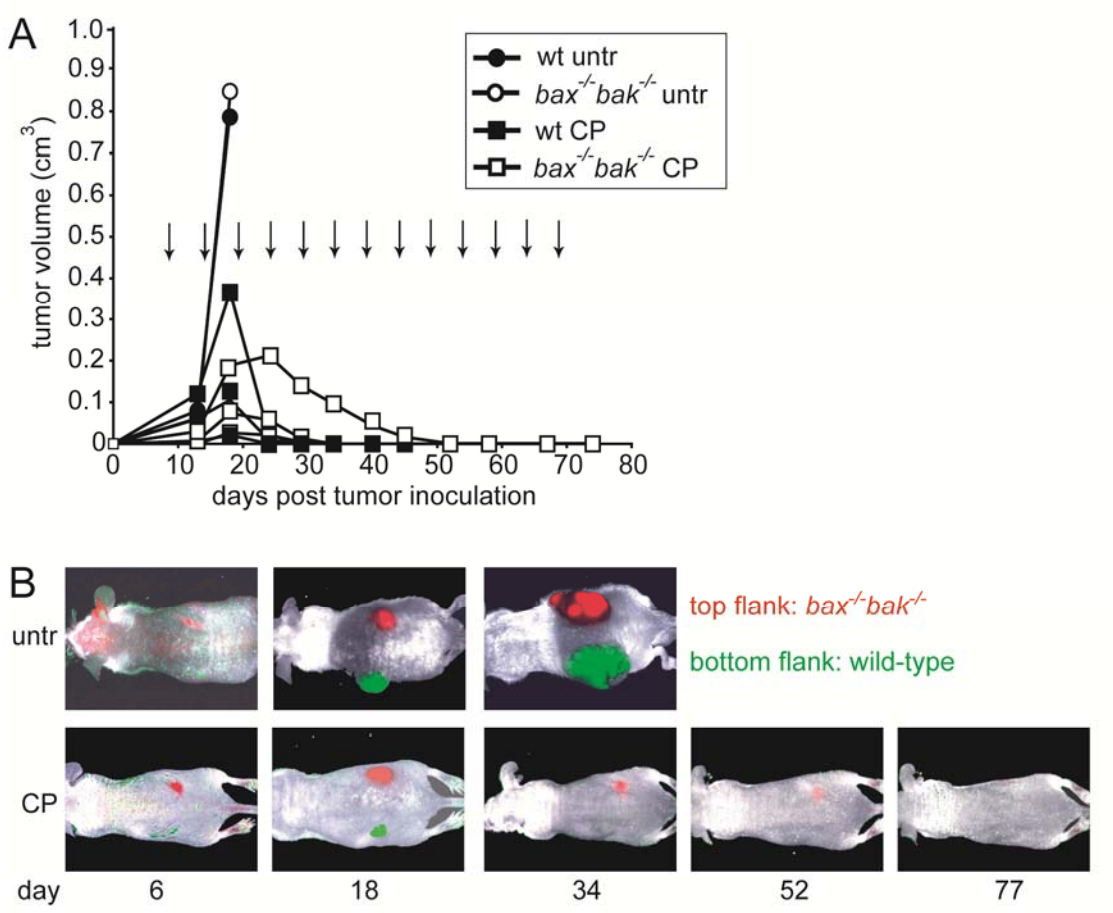

Figure 4. Bilateral comparison of wild-type and *bax*$^{-/-}$*bak*$^{-/-}$ tumors.

One million of the established wild-type and *bax*$^{-/-}$*bak*$^{-/-}$ tumor cells were injected subcutaneously into the left and right side, respectively, of athymic nude mice. (A) Mice were either left untreated (n = 5) or treated (n = 12) with 170 mg/kg of CP every 5 days, as indicated by the arrows. Tumor volume was calculated based on caliper measurement and plotted. Note that tumors of both genotypes regressed after CP treatment, regardless of their ability to die by apoptosis. (B) E1A and K-Ras-transformed wild-type and *bax*$^{-/-}$*bak*$^{-/-}$ tumor cells were transfected with GFP and RFP, respectively. Tumors were visualized by the Maestro small animal imaging system. Representative mice are shown.

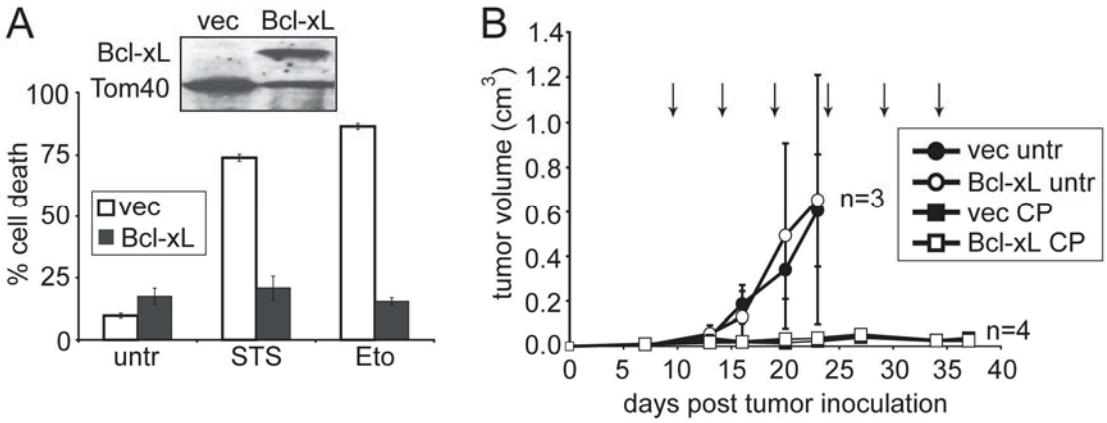

Figure 5. Bcl-xL overexpression does not inhibit tumor regression in response to CP.

(A) Bcl-xL was expressed in the wild-type E1A and K-Ras-transformed MEFs. Lysates from vector control and Bcl-xL expressing cells were probed for Bcl-xL. Tom40 was used as a loading control. Wild-type and Bcl-xL-expressing cells were treated with staurosporine (STS, 0.5 μM) or etoposide (Eto, 25 μM) for 24 hours. Cell viability was measured by trypan blue exclusion. Data shown are the averages of three independent experiments ± S.E.M. (B) Vector and Bcl-xL-expressing tumor cells were injected bilaterally into nude mice. The mice were treated with 170 mg/kg of CP every 5 days, as shown by the arrows, or left untreated. Note that both tumors regressed after CP treatment regardless of their ability to die by apoptosis.

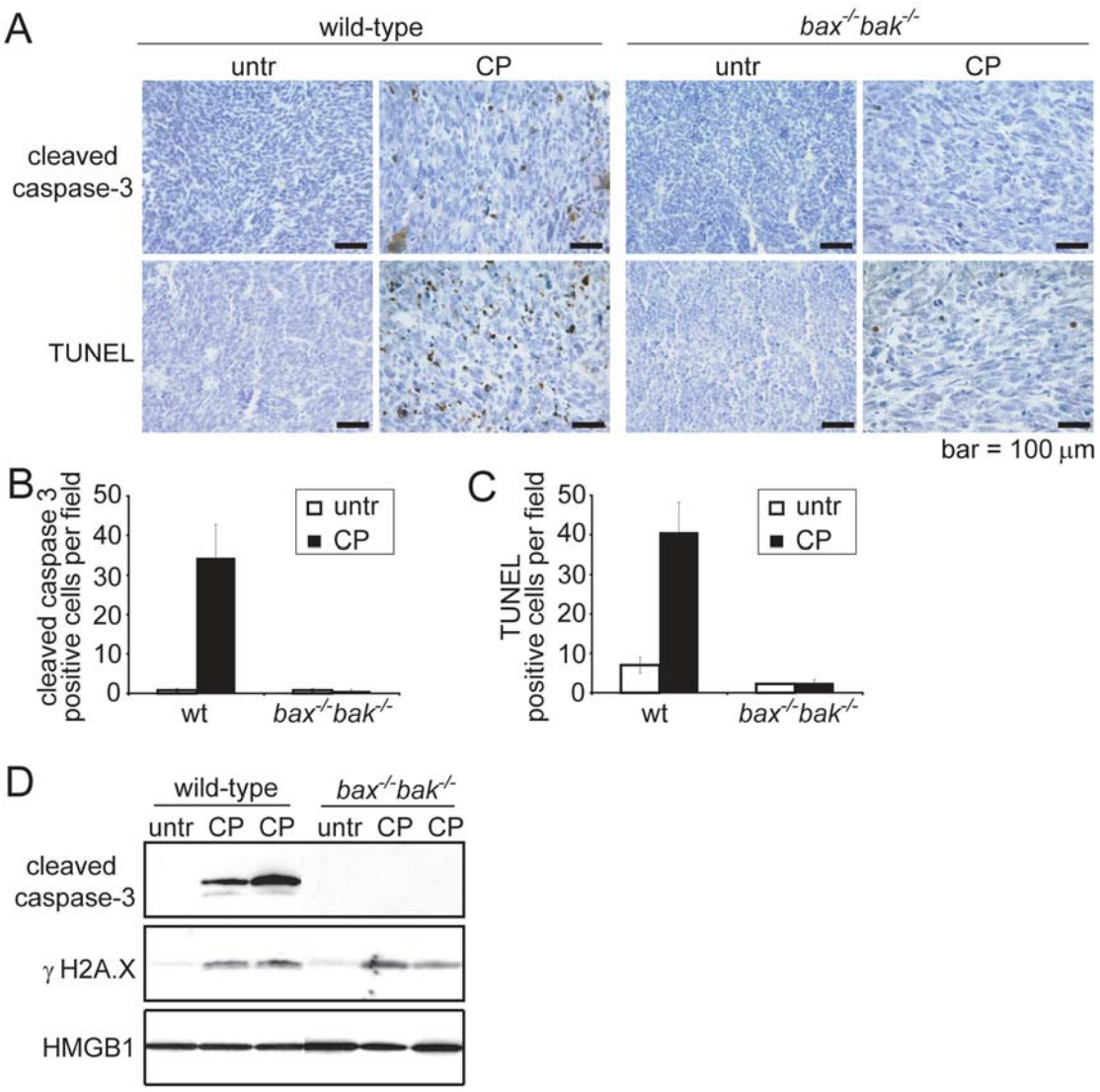

Figure 6. CP treatment does not induce apoptosis in *bax*$^{-/-}$*bak*$^{-/-}$ tumors.

Animals bearing wild-type and *bax*$^{-/-}$*bak*$^{-/-}$ tumors were either left untreated or treated with 170 mg/kg of CP every 5 days. Tumors were obtained from the untreated and treated animals and subjected to immunohistochemistry (A-C) and immunoblot analysis (D). (A) Sections from tumors untreated or treated with CP were assayed for cleaved caspase 3, and for apoptotic DNA fragmentation using a TUNEL assay. The dark brown staining indicates apoptotic cells. Representative pictures of untreated tumors and tumors treated with CP for 1 day are shown. Similar results were obtained from tumors treated with CP 2, 3, 4, and 5 times and are not shown. Quantitation was performed by counting positive cells under a microscope in randomly selected areas for (B) caspase 3 cleavage and (C) DNA fragmentation. Data shown represents averages of 5 independent countings ± S.E.M. (D) Tumor lysates from one untreated and two independent CP-treated animals (each received one treatment) were prepared and subjected to immunoblotting analysis for cleaved caspase 3 and phosphorylated H2A.X (γH2A.X) to compare the extent of DNA damage. HMGB1 was probed as a control for equal loading.

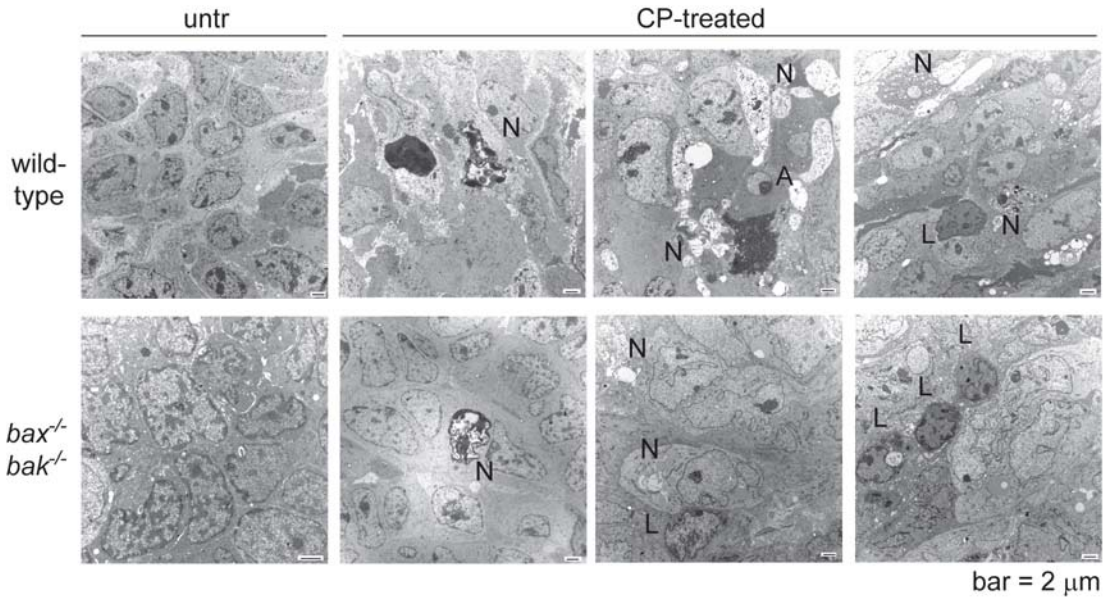

Figure 7. Morphological analysis of untreated and CP-treated tumors.

E1A and K-Ras-transformed wild-type and *bax*$^{-/-}$*bak*$^{-/-}$ tumor cells were injected into athymic nude mice to allow tumors to form. When palpable tumors formed, the mice were either left untreated or treated with 170 mg/kg of CP every 5 days. Tumors were obtained at various time points after CP treatment and subjected to transmission electron microscopic (TEM) analysis. Representative pictures are shown (A, apoptotic cells; L, leukocytes; N, necrotic cells). Note that cells with large and pleomorphic nuclei indicative of senescence or mitotic catastrophe are also present in the CP-treated tumors. Scale bar represents 2 μm.

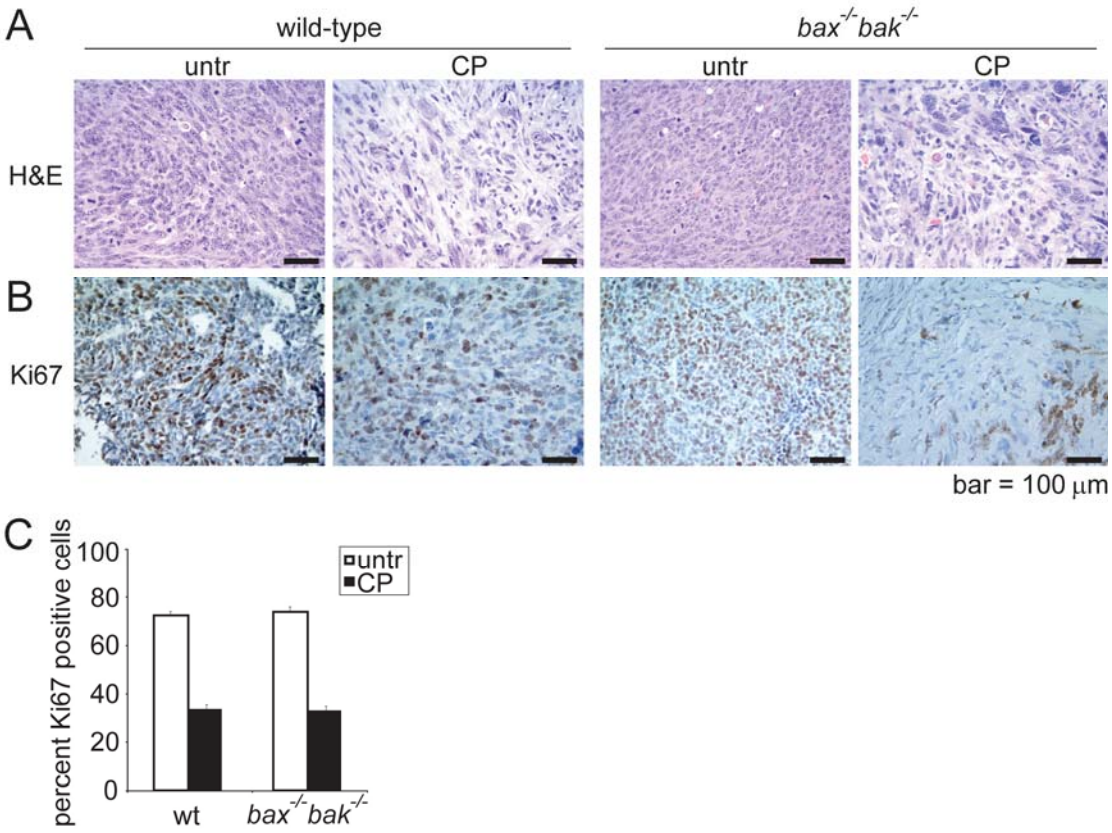

Figure 8. Evaluation of mitosis in apoptosis-proficient and -deficient tumors in response to CP-treatment.

Animals bearing wild-type and *bax*$^{-/-}$*bak*$^{-/-}$ tumors were left untreated or treated with CP one time. Paraffin-embedded sections were made and subjected to IHC. (A) Hematoxylin and eosin (H & E) staining of paraffin-embedded sections; (B) Ki67 staining of paraffin-embedded sections. Scale bar represents 100 μm. (C) Ki67 positive cells were counted per 100 cells in 5 randomly selected fields.

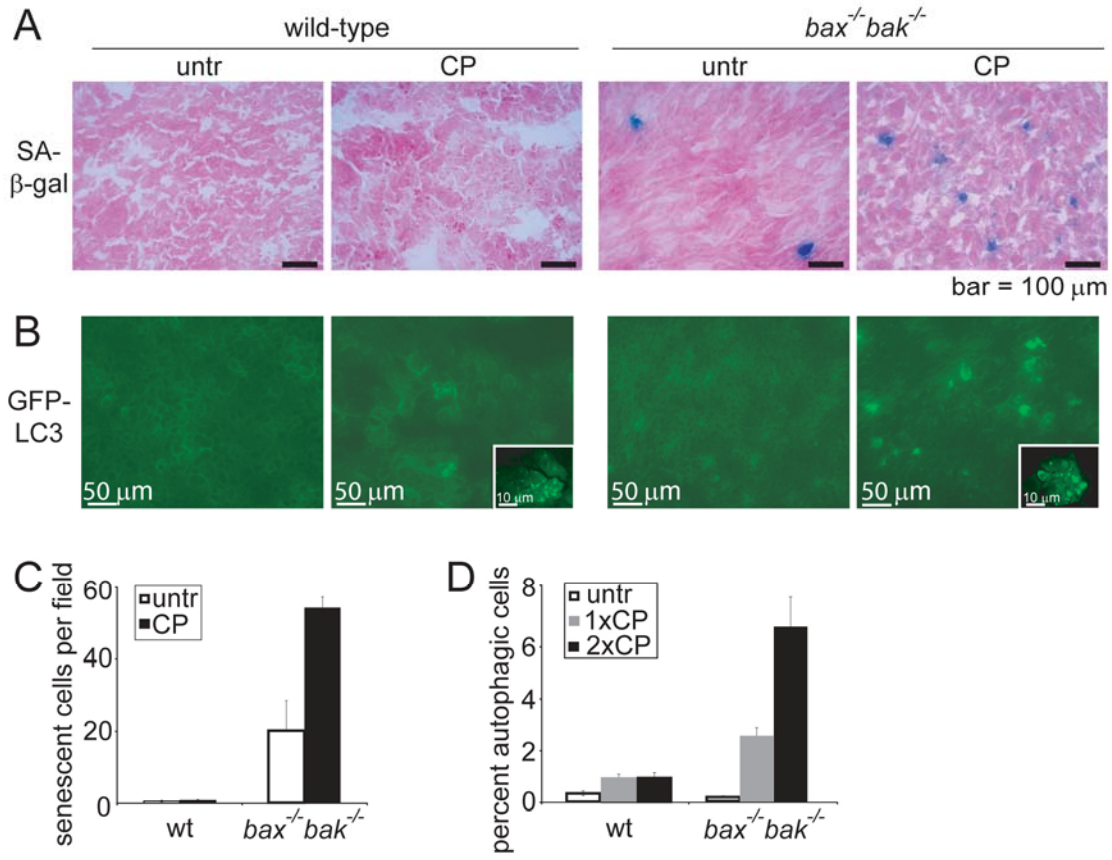

Figure 9. Evaluation of senescence and autophagy in apoptosis-proficient and -deficient tumors in response to CP treatment.

Animals bearing wild-type and *bax*$^{-/-}$*bak*$^{-/-}$ tumors were left untreated or treated with 170 mg/kg of CP one time. Frozen sections were made. (A) Sections were subjected to senescence associated β-galactosidase (SA-β-gal) analysis at pH 6.0 and were counterstained with eosin. Scale bar represents 100 μm. Senescent cells were quantitated by counting SA-β-gal positive cells (blue cells) in 5 randomly selected fields (C). (B) GFP-LC3 was expressed in both wild-type and *bax*$^{-/-}$*bak*$^{-/-}$ tumor cells. Mice bearing tumors derived from these cells were treated with CP (170 mg/kg) every 5 days once (1X) or twice (2X). Cryosections of the tumors were visualized under a fluorescent microscope. Induction of autophagy is revealed by the formation of the bright and punctate GFP signal. Scale bar represents 50 μm and 10 μm in the inset. Cells were considered autophagic if they had more than 5 GFP-LC3 puncta. The percentage of cells undergoing autophagy were determined by counting the total number of autophagic cells compared to the total number of cells in 10 random fields (D).

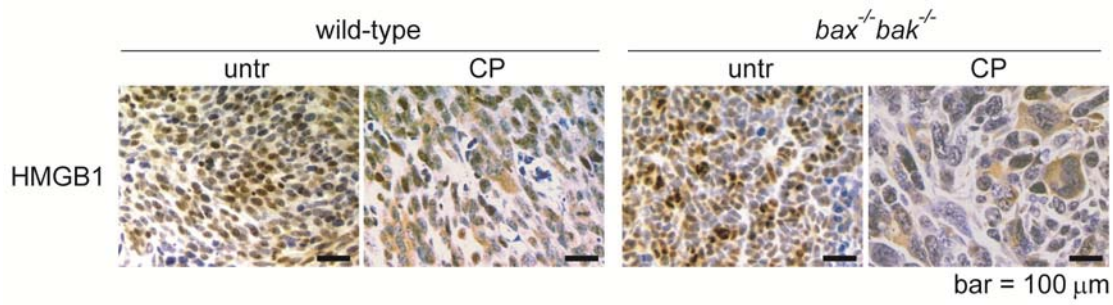

Figure 10. CP treatment induces sporadic tumor cell necrosis.

Animals bearing wild-type and *bax*$^{-/-}$*bak*$^{-/-}$ tumors were left untreated or treated with 170 mg/kg of CP every 5 days for two treatments. Paraffin-embedded sections were made and assessed by IHC using an anti-HMGB1 antibody. Nuclear staining is present in the untreated tissue whereas cytoplasmic and extranuclear staining of HMGB1 is found in the tumor tissue treated twice with CP, indicative of necrosis. Similar results were obtained from tumors treated with CP 1, 3, 4, and 5 times and are not shown. Scale bar represents 100 μm.

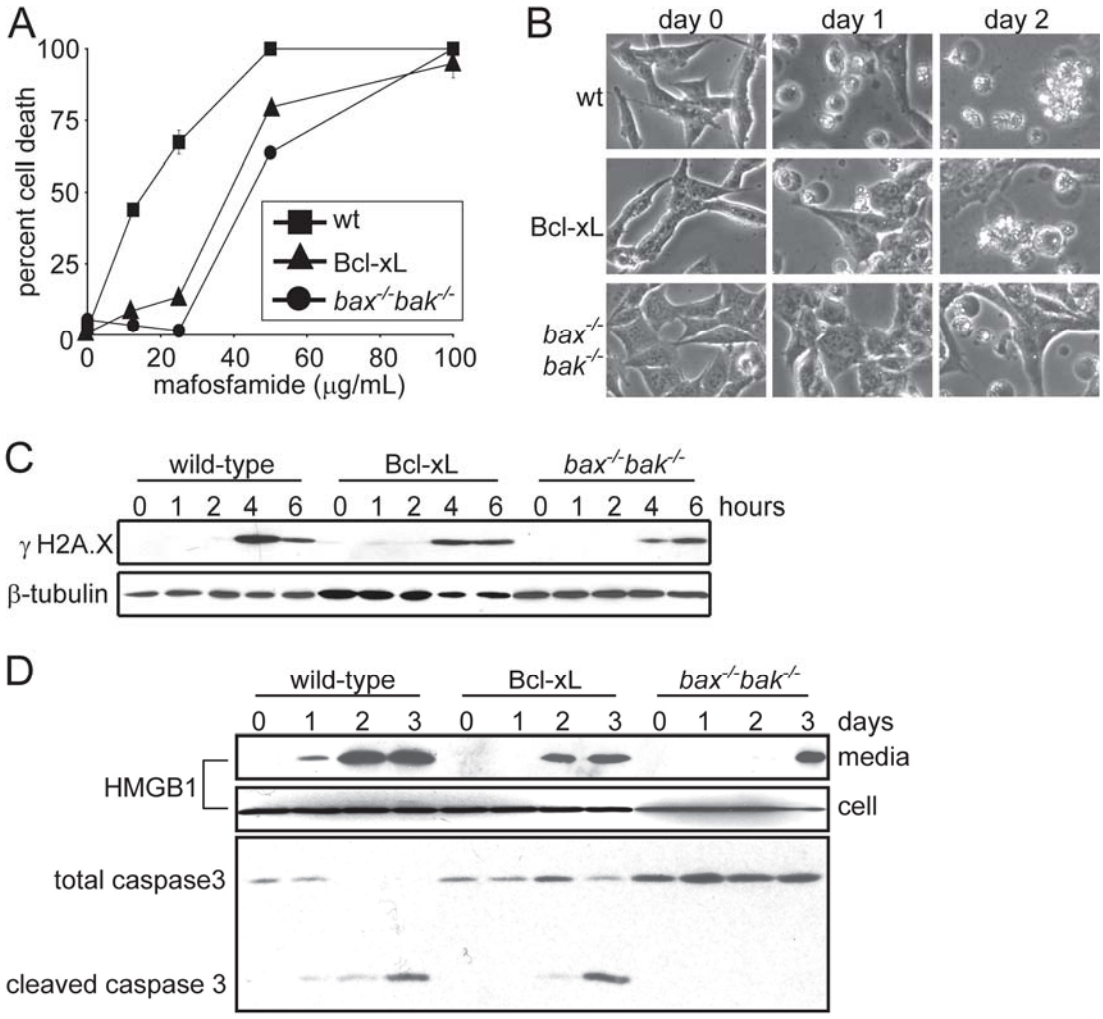

Figure 11. HMGB1 is released from tumor cells in response to DNA alkylating damage.

(A) Wild-type, Bcl-xL-expressing, and *bax*$^{-/-}$*bak*$^{-/-}$ tumor cells were treated for 24 hours with increasing concentrations of mafosfamide (MAF). Cell death was measured by trypan blue staining and expressed as average of 2 independent experiments ± S.E.M. (B) Wild-type, Bcl-xL-expressing, and *bax*$^{-/-}$*bak*$^{-/-}$ tumor cells were treated with 12.5 μg/mL of MAF for the indicated days. Cells were photographed under a phase-contrast filter. (C) Wild-type, Bcl-xL-expressing, and *bax*$^{-/-}$*bak*$^{-/-}$ tumor cells were treated with 12.5 μg/mL of MAF for the indicated hours. Cell lysates were made and immunoblotting was performed using an anti-γH2A.X antibody to determine the extent of DNA damage. (D) Wild-type, Bcl-xL-expressing, and *bax*$^{-/-}$*bak*$^{-/-}$ tumor cells were treated with 12.5 μg/mL of MAF for the indicated days. The cells and the cell culture media were collected separately and subjected to immunoblot analysis using an anti-HMGB1 antibody. Note that HMGB1 is retained inside untreated cells, whereas it is found in the cell culture media of treated cells. The cell lysates were also probed with an antibody recognizing both pro-and cleaved caspase 3.

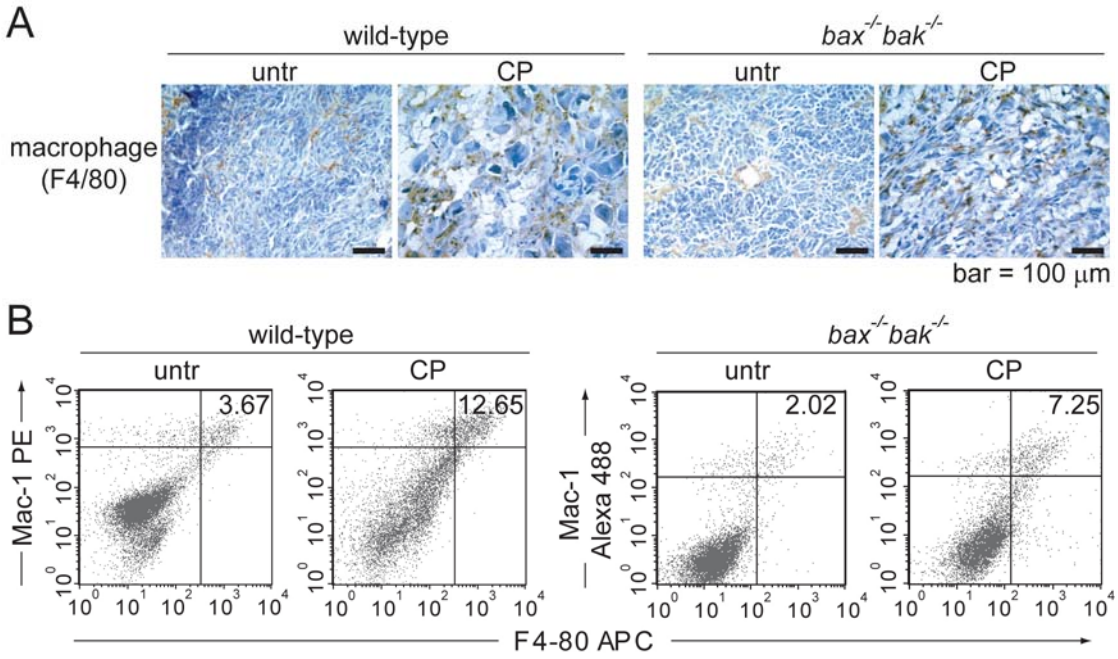

Figure 12. CP-induced sporadic tumor cell necrosis induces macrophage infiltration.

Wild-type and *bax*$^{-/-}$*bak*$^{-/-}$ untreated and CP-treated tumor tissue was assessed for innate immune cell infiltration. IHC and flow cytometry were used to detect the infiltration of macrophages. (A) IHC was performed using an antibody against F4/80 to assess macrophage infiltration in the tumor tissue. Tissue sections from animals that received 1, 2, 3, 4, or 5 CP-treatments were assessed for macrophage infiltration. Similar results were obtained at the various treatment points. Photographs of tissues from untreated or CP-treated (twice) mice are shown. Scale bar represents 100 μm. (B) Single tumor cell suspensions were obtained from the untreated and treated tumors and subjected to flow cytometry analysis. Due to the expression of GFP and RFP in the wild-type and *bax*$^{-/-}$ *bak*$^{-/-}$ tumors, respectively, PE-conjugated Mac-1 was used for the wild-type, and Alexa-488-conjugated Mac-1 was used for the *bax*$^{-/-}$*bak*$^{-/-}$ tumor cells. Both samples were co-stained with APC-conjugated F4/80.

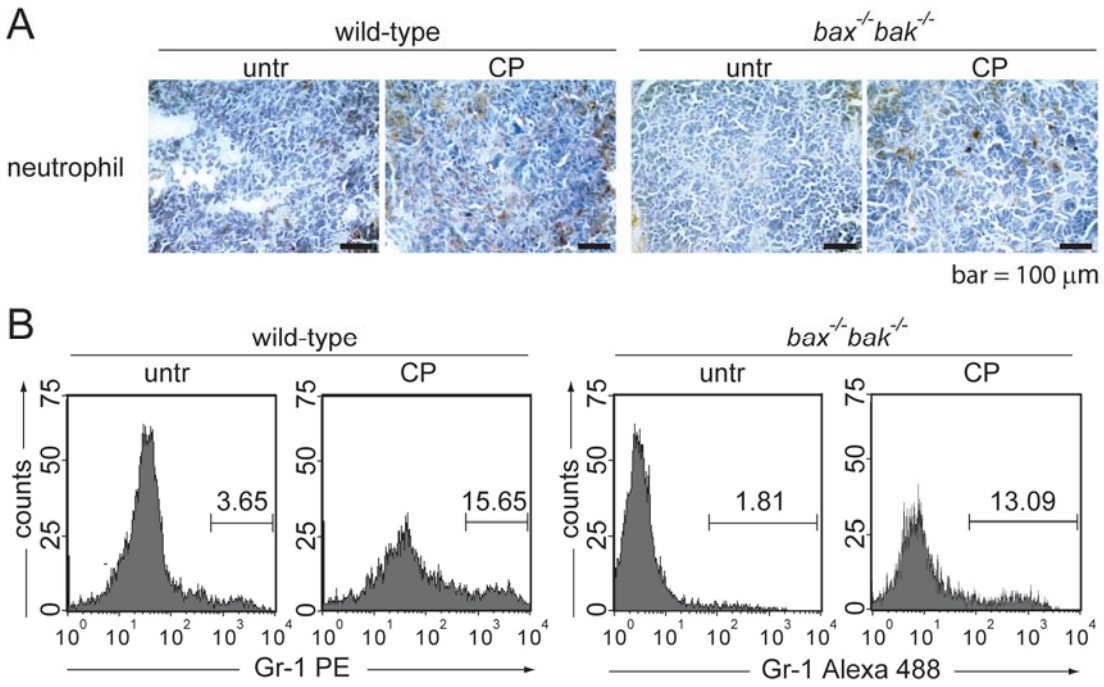

Figure 13. CP-induced sporadic tumor cell necrosis induces neutrophil infiltration.

Wild-type and *bax*$^{-/-}$*bak*$^{-/-}$ untreated and CP-treated tumor tissue was assessed for innate immune cell infiltration. IHC and flow cytometry were used to detect the infiltration of neutrophils. (A) IHC was performed using an antibody against an allotypic marker of neutrophils to detect neutrophils in the tumor tissue. Tissue sections from animals that received 1, 2, 3, 4, or 5 CP-treatments were assessed for neutrophil infiltration. Similar results were obtained at the various treatment points. Photographs of tissues from untreated or CP-treated (twice) mice are shown. Scale bar represents 100 μm. (B) Single tumor cell suspensions were obtained from the untreated and treated tumors and subjected to flow cytometry analysis. Due to the expression of GFP and RFP in the wild-type and *bax*$^{-/-}$*bak*$^{-/-}$ tumors, respectively, PE-conjugated Gr-1 was used for the wild-type, and Alexa-488-conjugated Gr-1 was used for the *bax*$^{-/-}$*bak*$^{-/-}$ tumor cells.

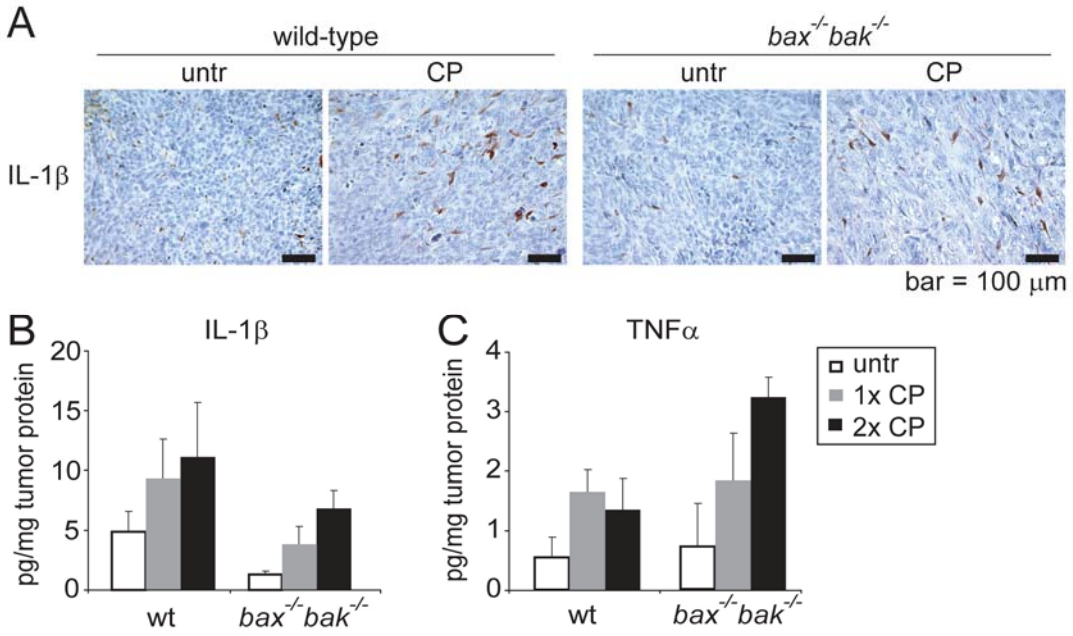

Figure 14. CP-induced tumor cell necrosis activates a pro-inflammatory response.

Wild-type and *bax*$^{-/-}$*bak*$^{-/-}$ untreated and CP-treated tumor tissue was assessed for activation of innate immune cells. (A) IHC was performed using an anti-IL-1β antibody to detect activated leukocytes in the tumor tissue. Scale bar represents 100 μm. (B-C) Tissue lysates were made from both wild-type and *bax*$^{-/-}$*bak*$^{-/-}$ tumors that were left untreated or treated once (1x) or twice (2x) with CP. One-hundred μg of tumor lysates were run on an enzyme-linked immuno sorbent assay (ELISA) to determine the levels of IL-1β (B) and tumor necrosis factor α (TNFα) (C). The amount of IL-1β and TNFα in tumor tissues were calculated and expressed as picogram per milligram of tumor protein. Each data point represents tumors isolated from two independent mice and each sample was run in duplicate. Shown is the average ± S.E.M.

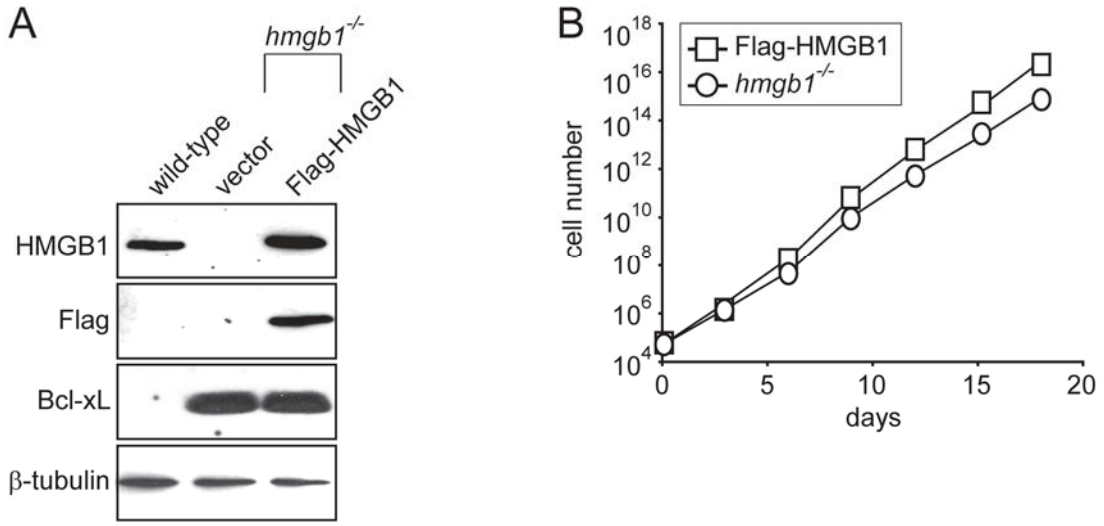

Figure 15. Restoration of HMGB1 in *hmgb1*$^{-/-}$ tumor cells does not affect cell proliferation *in vitro*.

Wild-type and *hmgb1*$^{-/-}$ mouse embryonic fibroblasts (MEFs) were transformed into apoptosis-deficient tumor cells using E1A, K-Ras, and Bcl-xL. Subsequently a pool of these cells was transfected with Flag-tagged HMGB1 to restore HMGB1 in *hmgb1*$^{-/-}$ cells. These cells were injected into athymic nude animals. When tumors formed, they were extracted from the animals and used to generate stable tumor cell lines. (A) Cell lysates were subjected to immunoblot analysis using antibodies against HMGB1, Flag, Bcl-xL, and β-tubulin. (B) The Flag-HMGB1 and *hmgb1*$^{-/-}$ tumor cells were plated and cell number was determined on the indicated days. Data shown are the average of four independent counts ± S.E.M. (S.E.M. is narrower than symbols to be seen).

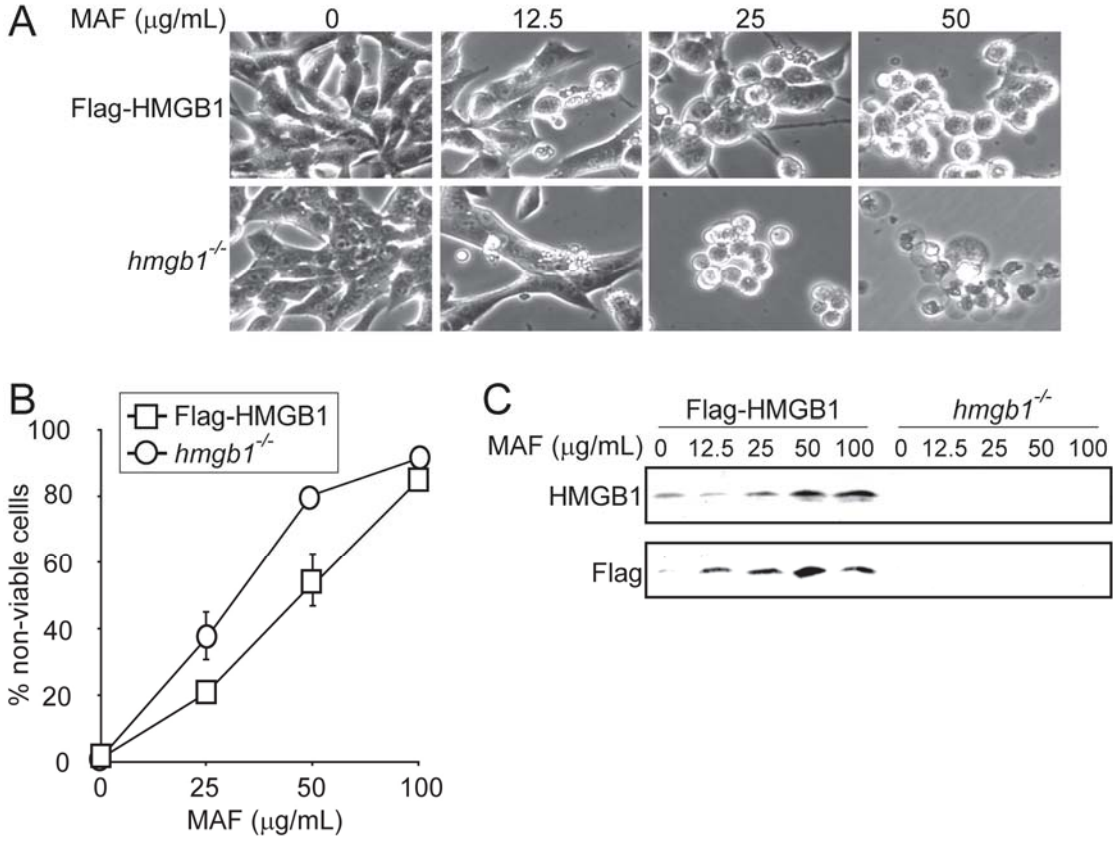

Figure 16. Restoration of HMGB1 in *hmgb1*$^{-/-}$ tumor cells does not affect cell sensitivity to chemotherapy *in vitro*.

The Flag-HMGB1 and *hmgb1*$^{-/-}$ tumor cells were treated with the DNA alkylating agent mafosfamide (MAF) at the indicated concentrations for 24 h. (A) Cells were photographed under a phase-contrast filter and representative images are shown. (B) Cell death was measured by propidium iodide (PI) exclusion and expressed as an average of 3 independent experiments ± S.E.M. (C) Cell culture medium was collected from the untreated and treated cells and assessed for HMGB1 by immunoblot analysis using antibodies against HMGB1 and Flag. Note that HMGB1 is found in the cell culture media from Flag-HMGB1 but not *hmgb1*$^{-/-}$ cells.

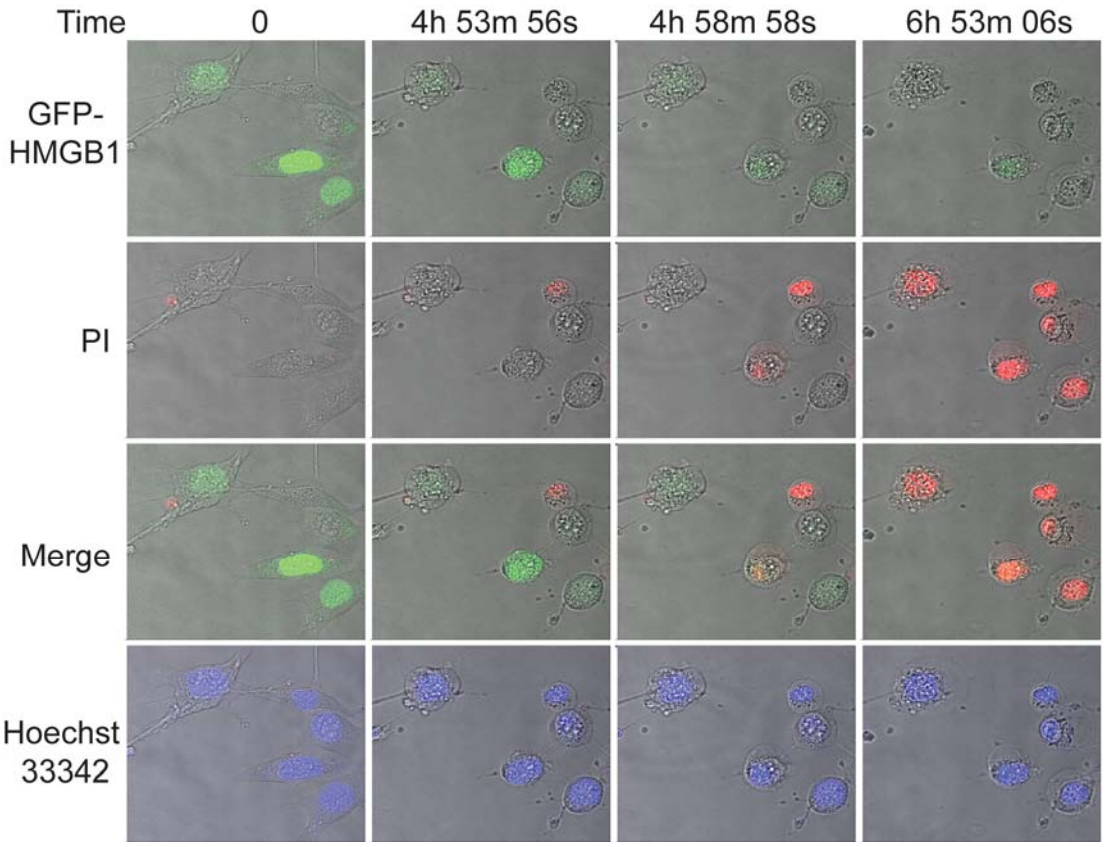

Figure 17. HMGB1 is released from dying cells after DNA alkylating treatment *in vitro*.

hmgb1$^{-/-}$ MEFs were transfected with GFP-HMGB1 and treated with MAF in the presence of PI and the live cell permeant DNA dye Hoechst 33342. Live cell imaging was performed and representative pictures are shown for GFP-HMGB1, propidum iodide (PI) for plasma membrane integrity, merged images with GFP-HMGB1 and PI, and Hoechst 33342 for nuclear staining. Note the simultaneous decrease of cellular GFP-HMGB1 and loss of plasma membrane integrity indicated by PI positive staining.

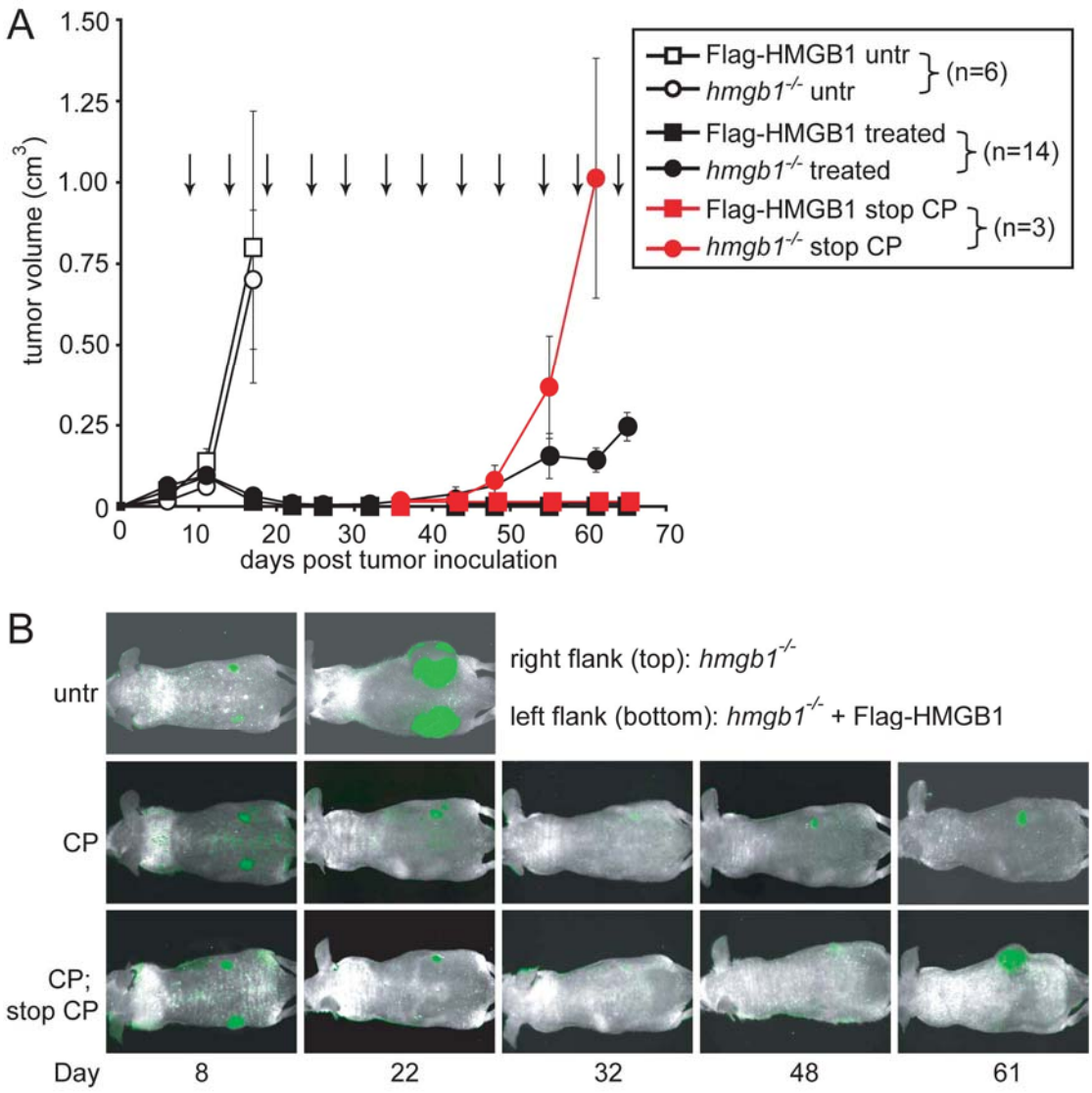

Figure 18. HMGB1 mediates tumor regression upon CP treatment *in vivo.*

Both Flag-HMGB1 and *hmgb1*$^{-/-}$ tumor cells were labeled with GFP and injected bilaterally into the same mouse to allow tumors to form. When palpable tumors formed, the mice were left untreated or treated with 170 mg/kg of CP every 5 days as indicated by arrows. Thirty days after the initial CP treatment, CP was discontinued on 3 mice (red symbols). (A) Tumor volume was determined by caliper measurement and the average tumor volume was plotted with S.E.M. (B) Tumors were monitored by *in vivo* imaging and representative images are shown.

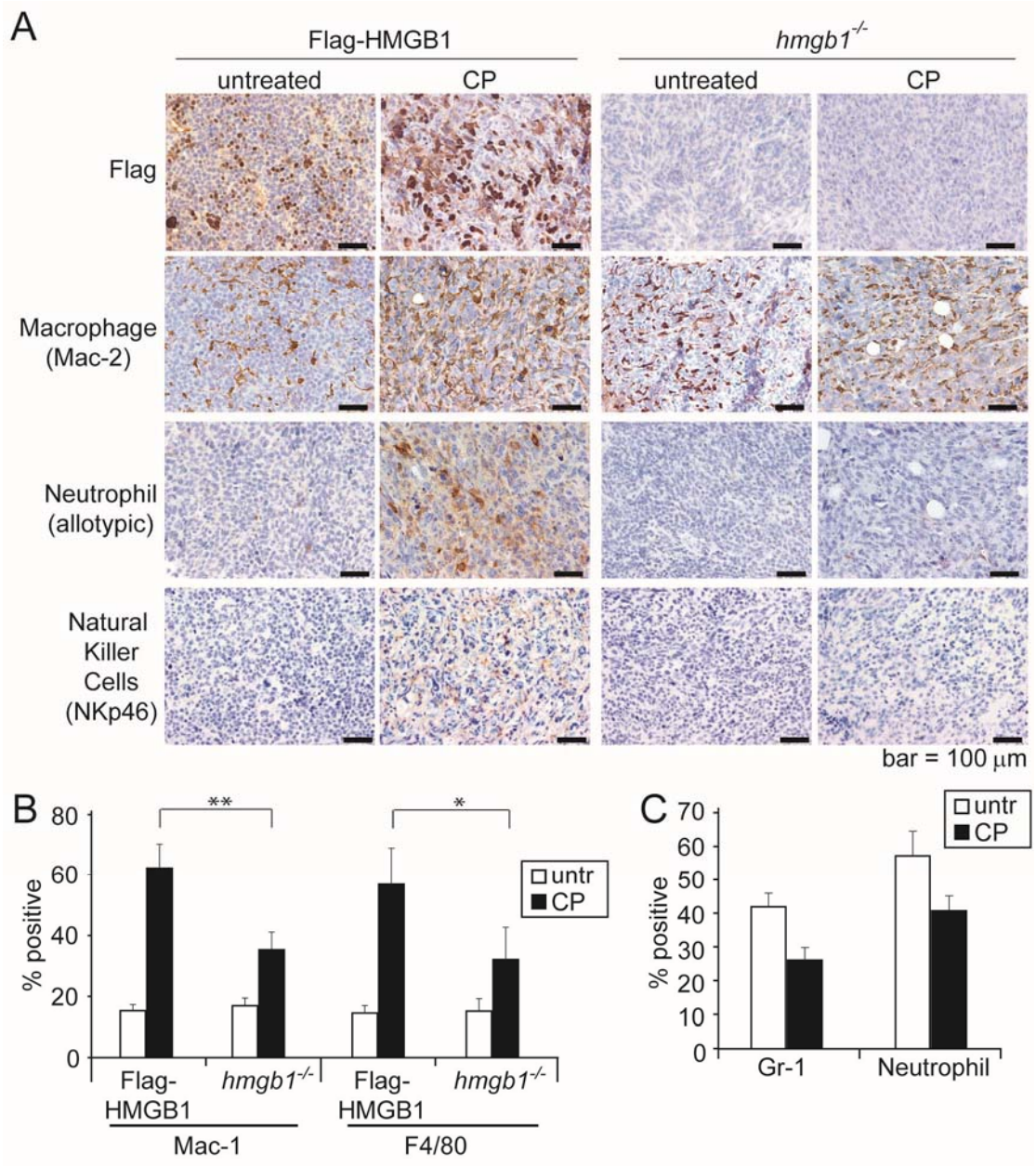

Figure 19. HMGB1 induces innate immune cell infiltration following CP treatment regardless of CP's ability to deplete peripheral neutrophils.

Mice bearing Flag-HMGB1 or *hmgb1*$^{-/-}$ tumors were either left untreated or treated twice with IP injections of 170 mg/kg of CP. Tumors were excised. (A) Tumors were embedded in paraffin, sectioned, and subjected to IHC. Cellular localization of HMGB1 was assessed using a Flag antibody and infiltration of macrophages, neutrophils, and NK cells was assessed using antibodies against Mac-2, an allotypic marker of neutrophils, and NKp46, respectively. (B) Single cell suspensions were prepared from untreated and treated tumor tissues and subjected to flow cytometry using anti-CD11b and anti-F4/80 antibodies to quantitate macrophage infiltration (*, $p<0.05$; **, $p<0.005$). (C) Peripheral blood was collected and subjected to flow cytometry analysis using anti-Gr-1 or an allotypic anti-neutrophil antibody.

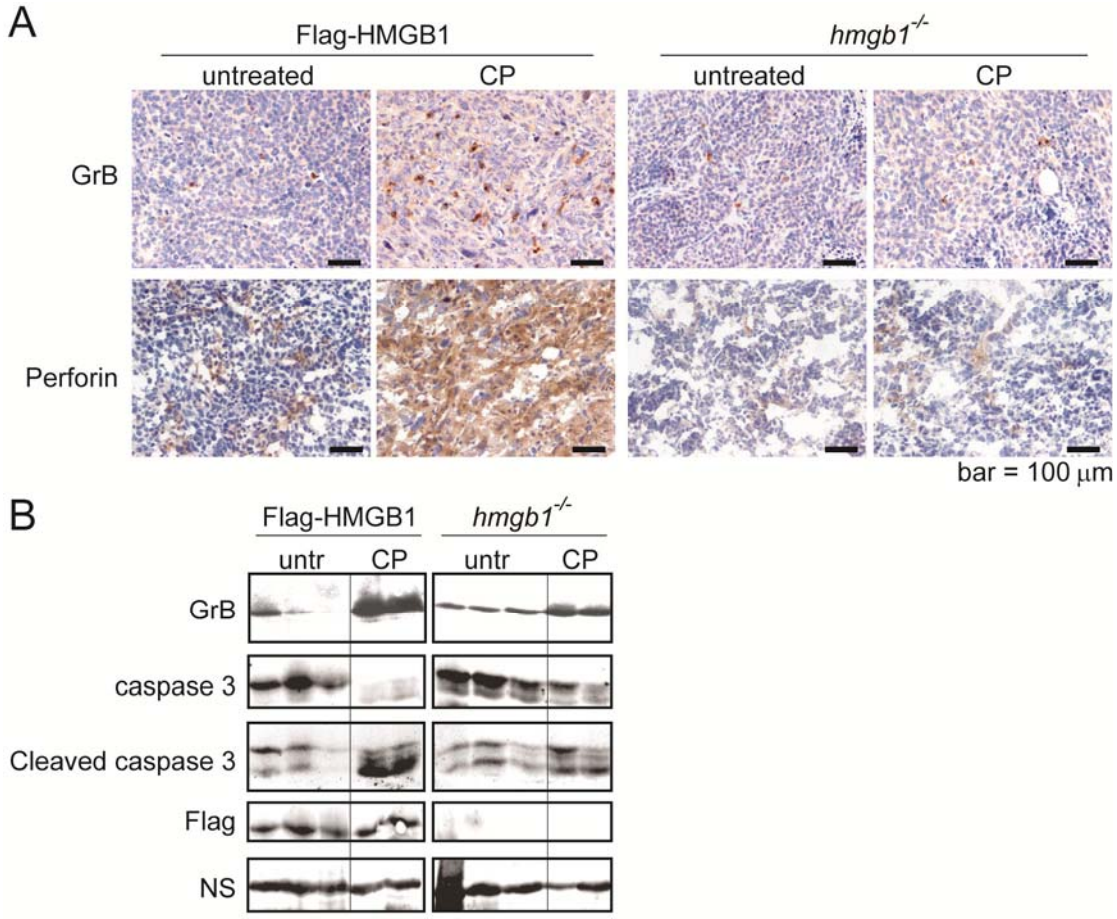

Figure 20. HMGB1 activates NK cells following CP treatment.

Mice bearing Flag-HMGB1 or *hmgb1*$^{-/-}$ tumors were either left untreated or treated twice with IP injections with 170 mg/kg of CP. Tumors were excised. (A) Tumors were embedded in paraffin, sectioned, and subjected to IHC. Activation of NK cells were examined using antibodies against granzyme B (GrB) or perforin (PFRN). (B) Immunoblot analysis was performed for GrB, caspase 3, cleaved caspase 3, and Flag on three independent Flag-HMGB1 and *hmgb1*$^{-/-}$ untreated tumors and two independent Flag-HMGB1 and *hmgb1*$^{-/-}$ CP-treated tumors.

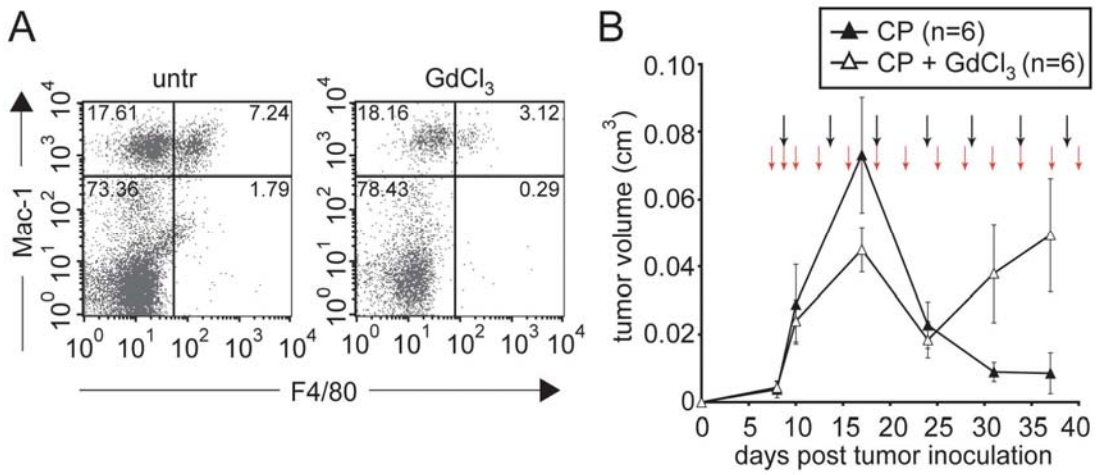

Figure 21. Neutralization of macrophages leads to tumor resistance to CP treatment.

E1A and K-Ras transformed Bcl-xL-expressing tumor cells with endogenous HMGB1 were injected into 6 mice. When palpable tumors formed, mice were either left untreated, treated with IP injections of 170 mg/kg of CP every 5 days (black arrows) with or without IV injections of 10 mg/kg of $GdCl_3$ to deplete macrophages (red arrows). (A) Peripheral blood from mice that were left untreated or treated with 10 mg/kg of $GdCl_3$ for 5 days was collected and subjected to flow cytometry using antibodies against Mac-1 and F4/80 to confirm macrophage depletion. (B) Tumor volumes were measured by caliper and graphed. Tumors were measured by caliper and the average volume of tumors with S.E.M was plotted.

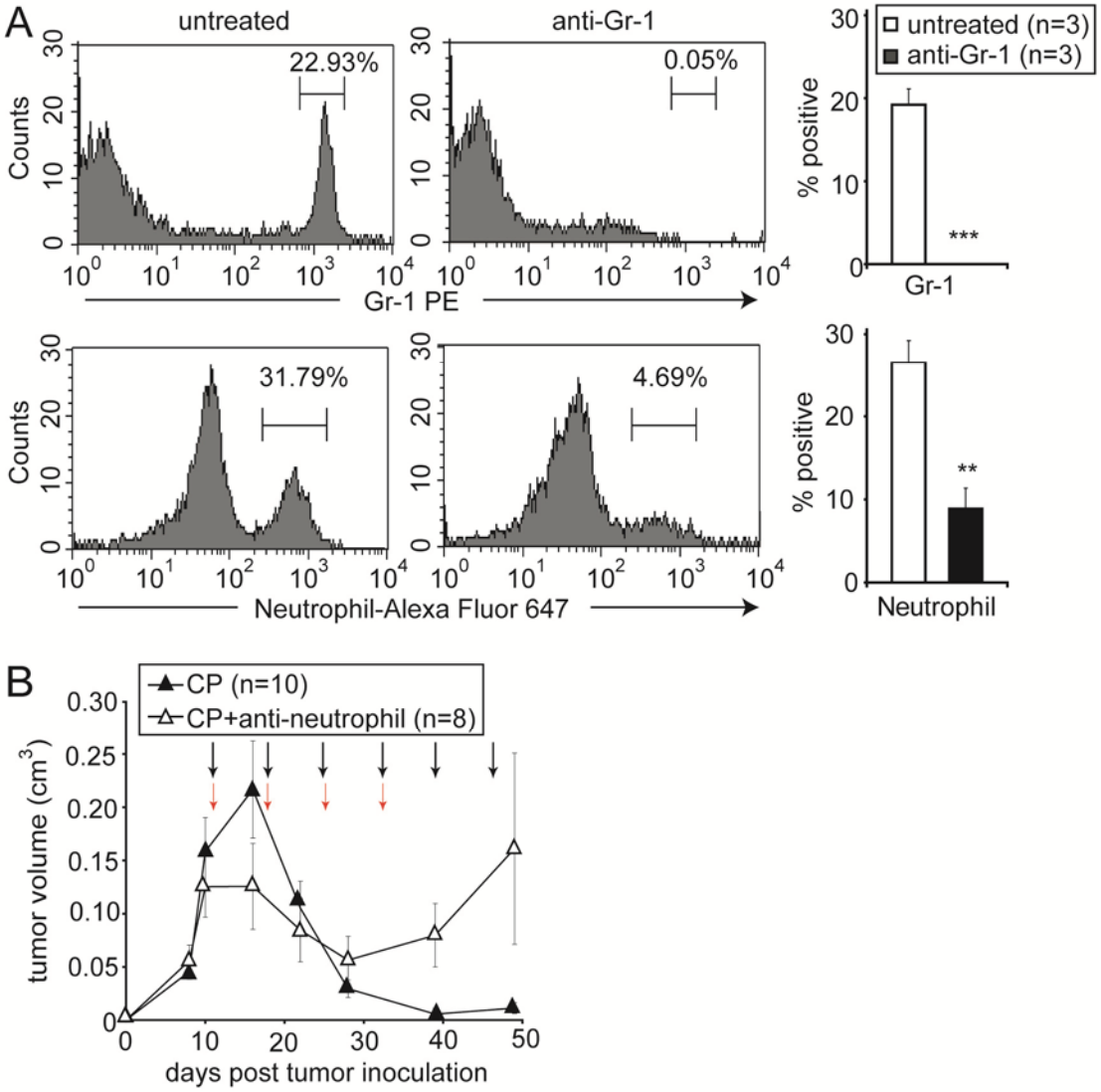

Figure 22. Neutralization of neutrophils leads to tumor resistance to chemotherapy.

E1A and K-Ras transformed Bcl-xL-expressing tumor cells with endogenous HMGB1 were injected into athymic nude mice. (A) Mice were left untreated or treated with one IP injection of 150 μg of the anti-Gr-1 neutrophil depleting antibody for 3 days. Peripheral blood was collected and analyzed by flow cytometry using indicated antibodies. Shown on the right are the averages from three animals in each group ± S.E.M. (**, $p<0.005$; ***, $p<0.0005$). (B) Mice were treated by IP injections with 170 mg/kg of CP every 5 days (black arrows) alone, or in combination with IP injections with 150 μg of the anti-Gr-1 neutrophil depleting antibody in combination with the first four CP treatments (red arrows). Tumors were measured by caliper and the average volume of tumors with S.E.M was plotted.

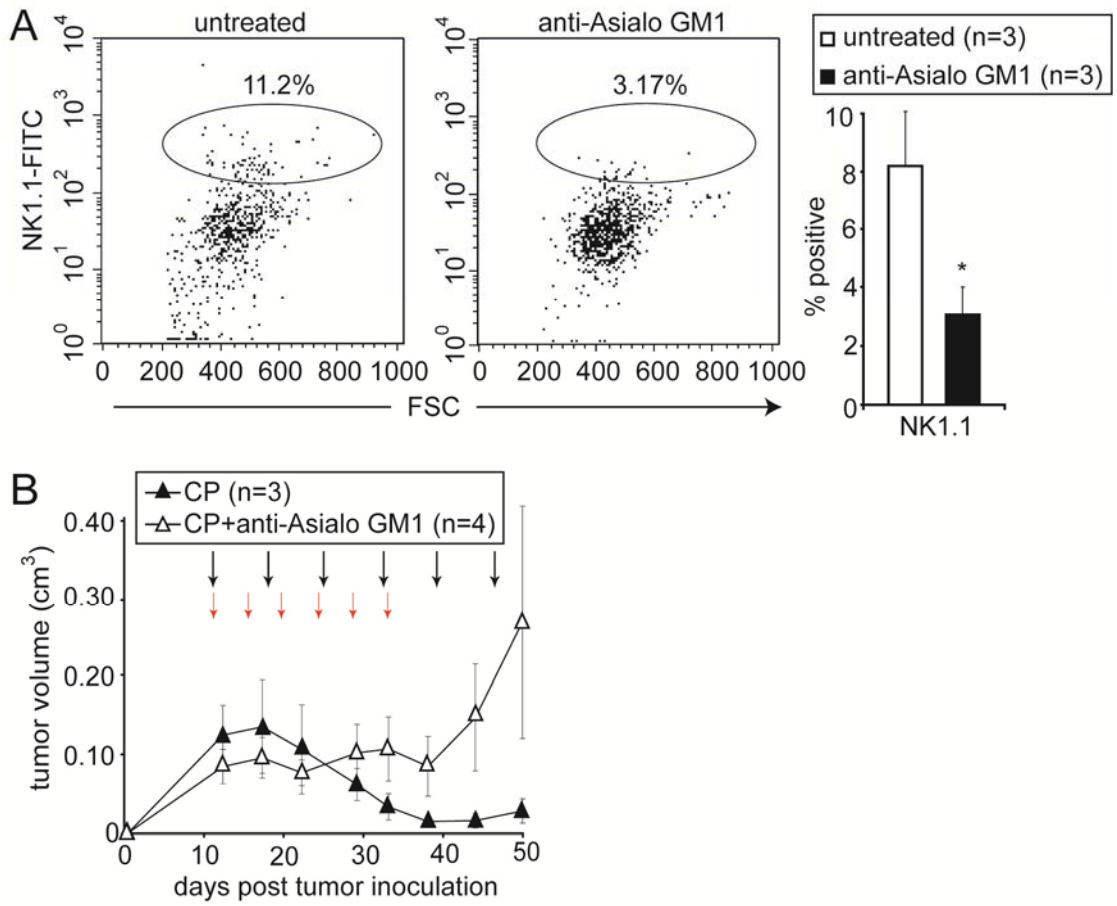

Figure 23. Neutralization of NK cells leads to tumor resistance to chemotherapy.

E1A and K-Ras transformed Bcl-xL-expressing tumor cells with endogenous HMGB1 were injected into athymic nude mice. (A) Mice were left untreated or treated with IV injections of 25 μL of the anti-Asialo GM1 NK depleting antibody for 6 days. Peripheral blood was collected and analyzed by flow cytometry using indicated antibodies. Shown on the right are the averages from three animals in each group ± S.E.M. (*, $p<0.05$). (B) Mice were treated by IP injections with 170 mg/kg of CP every 5 days (black arrows) alone, or in combination with IV injections with 25 μL of the NK cell depleting antibody every 3 days (red arrows). Tumors were measured by caliper and the average volume of tumors with S.E.M was plotted.

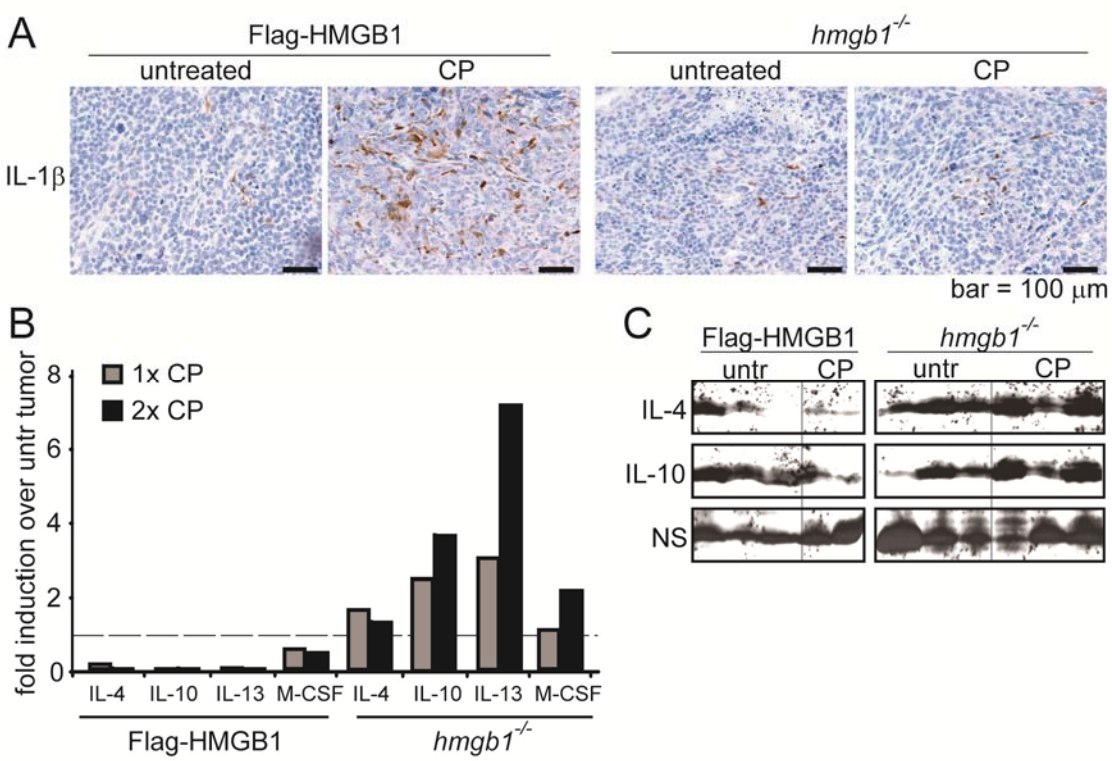

Figure 24. HMGB1 released during chemotherapy treatment mediates a pro-inflammatory response.

Mice bearing Flag-HMGB1 or *hmgb1*$^{-/-}$ tumors were either left untreated or treated with IP injections of 170 mg/kg of CP five days apart. (A) Tumor tissue sections were subjected to IHC using an anti-IL-1β antibody. (B and C) Tumors were excised at indicated time points and made into lysates. (B) The induction of cytokines was assessed with a mouse cytokine array panel in lysates from tumor in mice left untreated or treated 1x or 2x with CP. Results are shown as optical density normalized to values for each cytokine in untreated tumor tissue. The dashed line represents the untreated tumor value set to one. (C) Immunoblotting of IL-4 and IL-10 was used to confirm the cytokine array results in tumor cell lysates. Three independent Flag-HMGB1 and *hmgb1*$^{-/-}$ untreated tumors, three independent *hmgb1*$^{-/-}$ CP-treated tumors and two Flag-HMGB1 CP-treated were used.

A

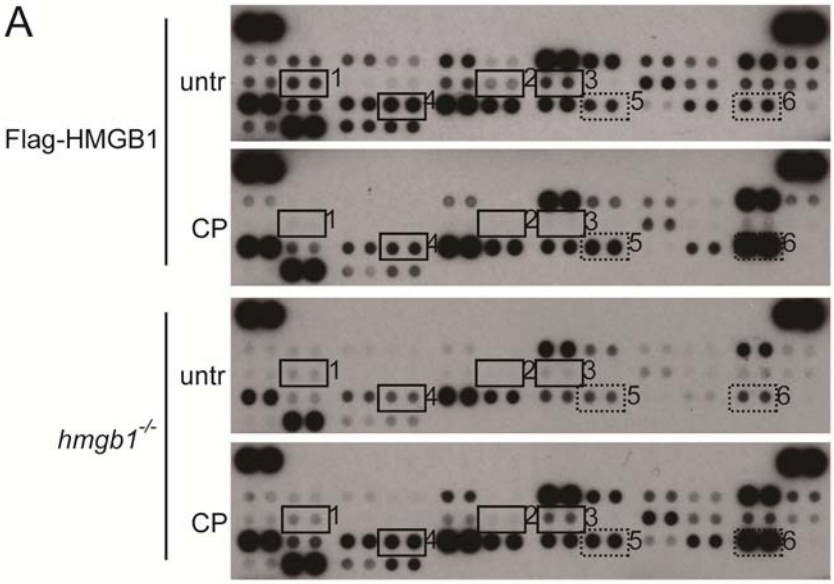

1	IL-4
2	IL-10
3	IL-13
4	M-CSF
5	MIP-1α
6	RANTES

B

	Flag-HMGB1		*hmgb1*$^{-/-}$	
	untr	CP	untr	CP
IL-4	29161	797	3815	7088
IL-10	9092	19	176	2116
IL-13	23250	610	1686	14578
M-CSF	62029	34295	13689	56665
MIP-1α	32933	57337	16773	54967
RANTES	43573	162594	18933	144230

Figure 25. HMGB1 suppresses the expression of anti-inflammatory cytokines in tumor tissue following chemotherapy.

(A-B) Mice bearing Flag-HMGB1 or *hmgb1*$^{-/-}$ tumors were either left untreated or treated with two IP injections of 170 mg/kg of CP five days apart. Tumors were removed from mice at indicated time points and lysed for tissue cytokine array analysis. (A) The cytokine array blots and (B) raw OD readings are shown for selected cytokines. Numbered rectangles highlight the duplicate spots of anti-inflammatory cytokines (solid lines) and pro-inflammatory cytokines (dashed lines) that are altered by the status of HMGB1 presence, as summarized in the table.

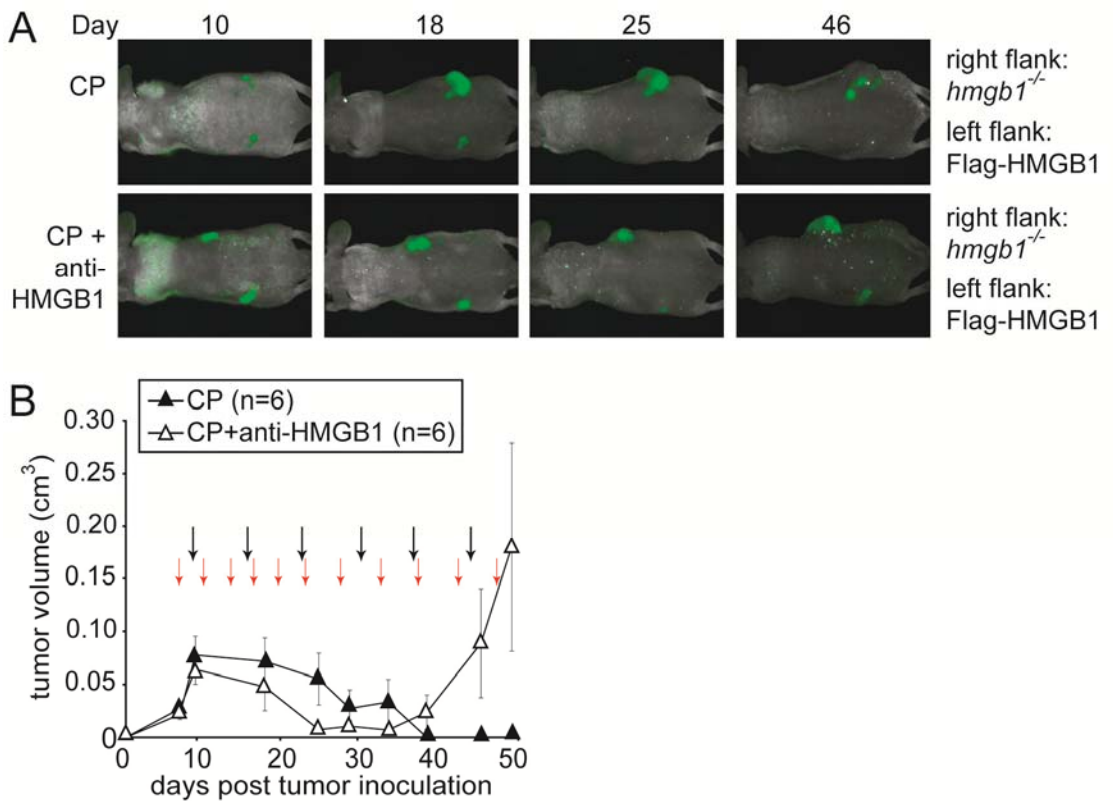

Figure 26. HMGB1 is required for tumor regression in response to chemotherapy.

Mice bearing Flag-HMGB1 or *hmgb1*$^{-/-}$ tumors were treated with IP injection of 170 mg/kg of CP every 5 days (black arrows) alone, or with 50 mg of an HMGB1 neutralizing antibody twice a week (red arrows). (A) Tumors were monitored by *in vivo* imaging and representative images of the animals from each group are shown. (B) Mice bearing tumors with endogenous HMGB1 were treated with CP alone or together with anti-HMGB1. Tumors were measured by caliper and the average tumor volume was plotted with S.E.M.

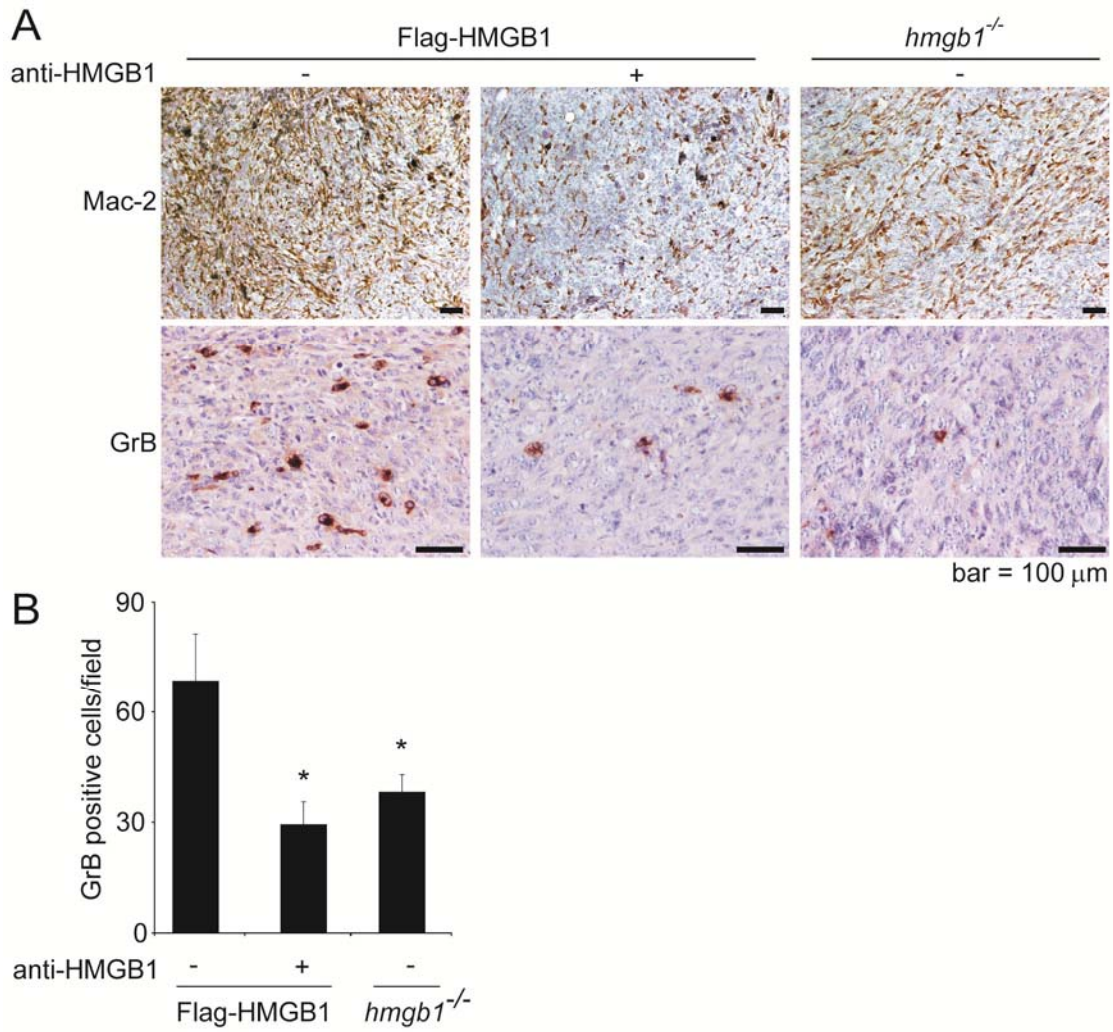

Figure 27. HMGB1 is required for activation of the innate immune response in response to chemotherapy.

Mice bearing Flag-HMGB1 or *hmgb1*$^{-/-}$ tumors were treated with IP injection of 170 mg/kg of CP every 5 days alone, or with 50 mg of an HMGB1 neutralizing antibody twice a week. (A) CP-treated tumors were excised and embedded in paraffin. Sections were made and subjected to IHC using an antibody against Mac-2 to assess the level of macrophage infiltration, and an antibody against granzyme B (GrB) to assess the level of activated NK cells. Note that similar to *hmgb1*$^{-/-}$ tumors, CP-treated tumors subjected to HMGB1 depletion (α-HMGB1) had reduced levels of macrophage and activated NK cell infiltration, compared to the Flag-HMGB1 CP-treated tumors. (B) Ten randomly selected microscope fields were counted for GrB positive cells. Data shown are average ± S.E.M. (*, $p<0.05$).

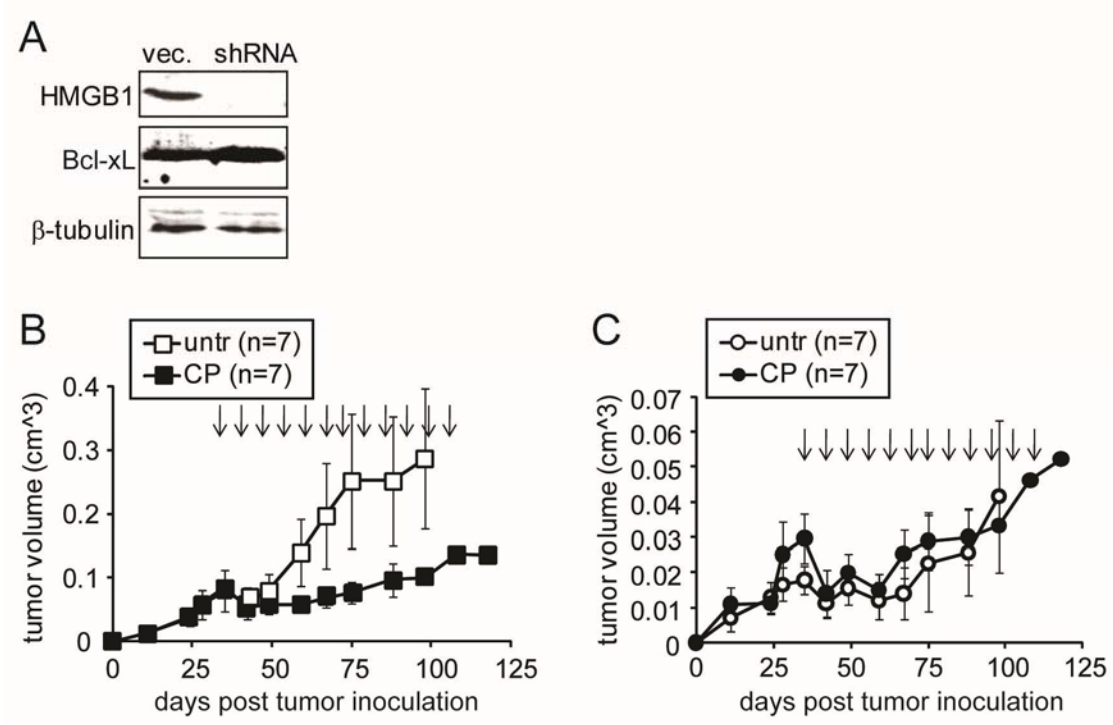

Figure 28. HMGB1 knockdown compromises the anti-tumoral activity of CP.

The anti-apoptotic protein Bcl-xL was expressed in the human breast cancer cells, MDA-MB-231. Subsequently a pool of these cells was transfected with a shRNA vector control or a construct targeted against HMGB1. (A) Cell lysates were subjected to immunoblot analysis using antibodies against HMGB1, Bcl-xL, and β-tubulin. (B) Fourteen athymic nude mice were injected with the Bcl-xL expressing MDA-MB-231 cells with shRNA vector control. When tumors formed mice were divided into two groups; untreated (n=7) and those treated every 5 days with 170 mg/kg of the DNA alkylating agent cyclophosphamide as indicated by the arrows (n=7). Tumor volume was determined by caliper measurement and the average tumor volume was plotted with S.E.M. (C) Fourteen athymic nude mice were injected with the Bcl-xL expressing MDA-MB-231 tumor cells that have HMGB1 knockdown. When tumors formed mice were divided into two groups; untreated (n=7) and those treated every 5 days with 170 mg/kg of the DNA alkylating agent cyclophosphamide as indicated by the arrows (n=7). Tumor volume was determined by caliper measurement and the average tumor volume was plotted with S.E.M.

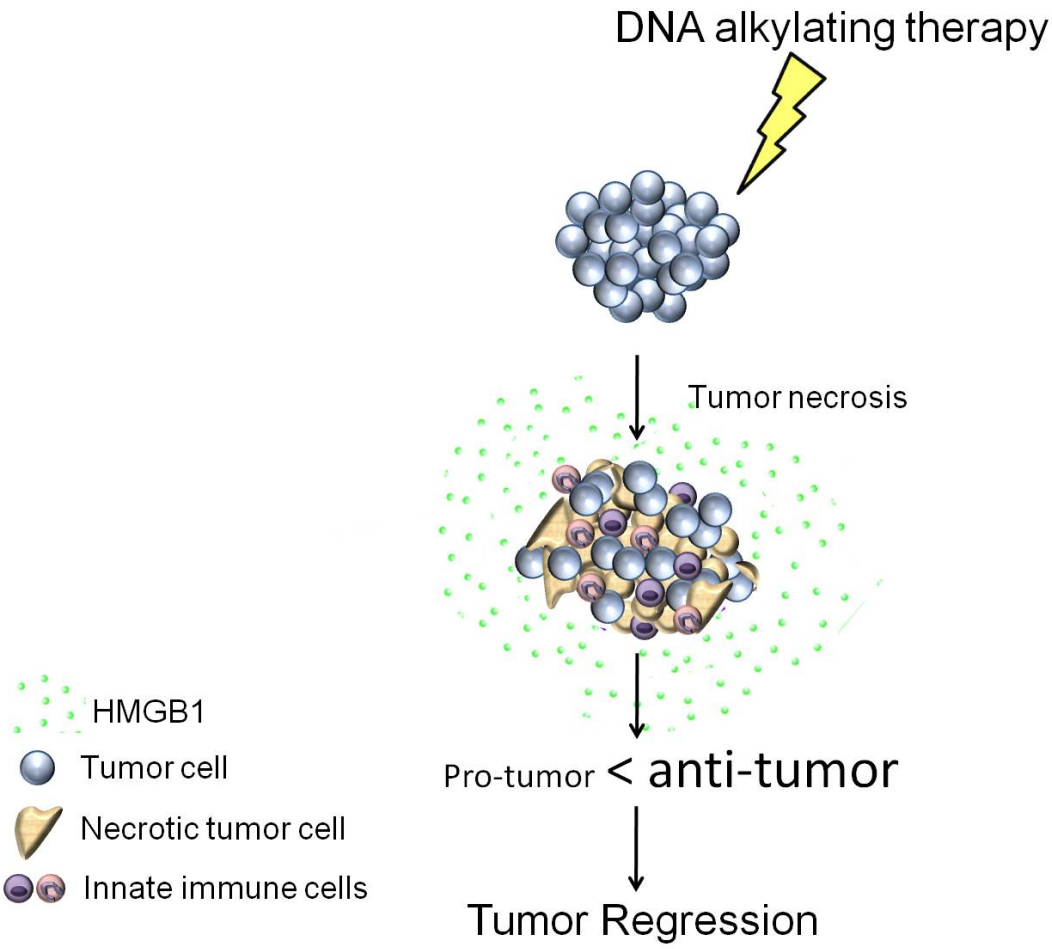

Figure 29. Proposed model for chemotherapy induced tumor regression.

Chemotherapy induces tumor cell necrosis which is associated with the release of HMGB1 from the necrotic tumor cells. HMGB1 is essential for recruiting innate immune cells into the treated tumor tissue. Activation of innate immune cells in the treated tumor tissue are essential for tumor regression. In the presence of HMGB1, the pro-tumor immune response is suppressed and the anti-tumor immune response predominates, leading to tumor regression.

V. Materials and Methods

1. Plasmids

Retroviral vectors for E1A (LPC-12S) and K-Ras (pBabe-Ras) were gifts of Dr. Scott Lowe. The Bcl-xL construct was generated in Dr. Craig Thompson's laboratory. The retroviral GFP-LC3 construct was generated using the EGFP-tagged LC3 excised from the pEGFP-C1-LC3 expression vector, a gift from Dr. Tamotsu Yoshimori (National Institute of Genetics, Japan). pBabeMN-IRES-GFP (Gary Nolan, Stanford University) was used for GFP expression, and RFP was used to replace GFP to generate the RFP retroviral construct. Flag-tagged HMGB1 was cloned into the LPC vector using a pEF6-Flag-HMGB1 construct as previously described [164]. shRNA contructs were obtained from Sigma (SHGLY-NM_002128).

2. Cell lines

Immortalized wild-type, *bax*$^{-/-}$*bak*$^{-/-}$, and *p53*$^{-/-}$ murine embryonic fibroblasts (MEFs) were generated as previously described [287]. Immortalized *hmgb1*$^{-/-}$ MEFs were a kind gift from Dr. Marco Bianchi (San Raffaele Scientific Institute, Milano, Italy).

3. Cell culture and tumor cell preparation

All cell lines were retrovirally transformed with E1A and K-Ras using 293T packaging cells via a calcium phosphate precipitation method in the presence of 10 μg/mL of polybrene (Sigma). When generating Bcl-xL-expressing tumors, a retroviral Bcl-xL construct was used together with E1A and K-Ras plasmids. The cells were subcutaneously injected into the back of 6-8 week old male athymic nude mice (Taconic Farms, New York). When tumors formed they were excised from the mice, minced, and digested with Trypsin-EDTA (0.05%) and collagenase A (10 μg/mL in trypsin) for 21 minutes at 37°C with brief vortexing every 7 minutes. The tumor cells were then strained through a 70 μm nylon filter to obtain a single cell suspension. The 293T, MDA-MB-231 and MEFs were maintained in Dulbecco's modified Eagle's medium (D-MEM) supplemented with 10% fetal bovine serum (FBS), 2 mM L-Glutamine, 100 units/mL of penicillin and 100 μg/mL of streptomycin at 37°C with 5.5% CO_2.

4. Immunoblotting

Cells were lysed in RIPA buffer (1% sodium deoxycholine, 0.1% SDS, 1% Triton X-100, 10 mM Tris at pH 8.0, 0.14 M NaCl) with protease inhibitor cocktail (G-Biosciences) plus EDTA. Sample concentration was determined by bicinchonic acid (BCA) protein analysis. To determine HMGB1 release from treated tumor cells, cell culture supernatant was collected from cells at indicated treatment points, centrifuged at low speed, and stored at -20°C. Twenty μg of protein or 20 μL of culture supernatant was resolved by SDS-PAGE, transferred to a nitrocellulose membrane, blocked for 1 hour at room temperature with 5% milk in PBS containing 0.05% Tween-20, and probed overnight at 4°C with primary antibodies diluted 1:1,000, unless otherwise noted, in the blocking solution. Blots were washed with PBS containing 0.05% Tween-20 and membranes were probed with the appropriate secondary antibodies diluted in block

solution for 1 hour at room temperature. The following primary antibodies were used: Bax (Santa Cruz Biotechnology, N-20), Bak (Upstate Biotechnology), p53 (Novocastra Laboratories, CM5), Tom40 (Santa Cruz Biotechnology, sc-11414), Bcl-xL (BD Pharmingen, 556361), cleaved Caspase 3 (Cell Signaling, 9661), γH2A.X (Cell Signaling, 2577), HMGB1 (Abcam, ab18256), β-tubulin (Sigma T4026), and Caspase 3 (Transducation Laboratories, C76920), Flag (Sigma F3165), Bcl-xL (BD Pharmingen 556361), IL-4 (BD Pharmingen 554386, 1:100), IL-10 (BD Pharmingen 551215, 1:100), and granzyme B (R&D systems AF1865, 1:100).

5. Xenograft mouse tumor experiments

Male nude mice, aged 6-8 weeks were obtained from Taconic Farms, Inc. (New York). Mice were housed and monitored at the Division of Laboratory Animal Resources (DLAR) at Stony Brook University. All experimental procedures and protocols were approved by the Institutional Animal Care and Use Committee. Tumors were established by resuspending $1x10^6$ tumor cells in 100 μL of PBS and injecting the cells into the mid flanks of mice using a 26 gauge needle. When palpable tumors formed (approximately 100 mm^3 in size), mice were placed randomly into treatment groups. Mice were treated via intraperitoneal injections of 170 mg/kg of cyclophosphamide monohydrate (CP) (Sigma-Aldrich, C0768). CP was made fresh for each treatment in sterile 0.9% sodium chloride every 5 days. Mice were treated via intravenous injections of 50 mg/kg of ortataxol every 5 days. Ortataxel was made to a concentration of 30 mg/mL in Tween 80 and ethanol at a 1:1 ratio, then diluted in sterile 0.9% sodium chloride for each treatment. Mice were treated via intravenous injections of 5 mg/kg of doxorubicin every 5 days. Doxorubicin was stored at 2 mg/mL and diluted in sterile 0.9% sodium chloride for each treatment. For each tumor, the tumor length (l) and width (w) was measured every 4-5 days with electronic calipers. Tumor volume (v), in mm^3, was calculated using the formula: $v = (lxw^2)/2$. The mice were imaged using the Maestro small animal imaging system (CRi). The animals bearing untreated tumors were sacrificed around day 30 post tumor inoculation, when tumors reached 2 cm^3 in size, in accordance with the Institutional Animal Care and Use Committee guidelines (IACUC).

6. Measurement of cell death

After treating cells for the indicated times, cells were collected, harvested, and trypan blue staining and propidium iodide (PI) exclusion were used to measure of cell death. Cells were stained with trypan blue (0.2%) and counted under a phase contrast light microscope, or resuspended in DMEM with PI (1 μg/mL) and cell viability was determined by flow cytometry using a FACSCalibur (BD Biosciences). Pictures of untreated and treated cells were taken with a Zeiss Axiovert S100 microscope using a 20x objective. Images were captured using an Infinity 3 camera (Lumen*era* Corporation) and analyzed with Infinity Analyze software.

7. Immunohistochemistry

Immunohistochemistry was performed according to standard protocol unless otherwise noted. Briefly, for paraffin-embedded sections, tissue was fixed in 10% neutral buffered formalin overnight, dehydrated in gradually increasing concentrations of ethanol, perfused overnight at 60°C with paraffin, and embedded in paraffin the next day. For cryosections, the tissue was embedded directly in O.C.T. media and stored at -80°C. Tissue was sectioned into 6 μm sections and paraffin tissue was dewaxed and rehydrated in decreasing concentrations of ethanol solutions. Following rehydration of tissue sections, antigen retrieval was performed using Citrate Buffer at pH 6.0. Frozen sections were warmed to room temperature for 15 minutes and then fixed in 4% paraformaldehyde. For both paraffin and frozen sections, endogenous peroxidase quenching was performed using 3% H_2O_2. Slides were blocked in 5% serum and the tissue was incubated with primary antibody overnight at 4°C. The following antibodies were used on paraffin embedded tissue: cleaved Caspase 3 (Cell Signaling Technology, 9661, 1:50), Ki67 (Dako, M7249, 1:50), HMGB1 (Abcam, ab18256, 1:100), IL-1β (R&D systems, AF-401-NA, 2 μg/mL), Flag (Sigma F3165, 1:100), Mac-2 (Cedarlane Laboratories 1:2000), Neutrophil allotypic marker (AbD Serotec MCA771G, 1:50), and granzyme B (R&D systems AF1865, 1:10). The following antibodies were used on frozen sections: F4/80 (AbD Serotec, MCA497GA, 1:100), Neutrophil (AbD Serotec, allotypic marker, MCA771G, 1:100), and perforin (Santa Cruz Biotechnology sc-58643, 1:500). Biotinylated secondary antibodies were used at a concentration of 1:1,000 for 1 hour at room temperature. Following a wash series, tissue was incubated with avidin/biotinylated HRP (ABC Elite kit from Vector Labs) according to manufacturer's instructions. Slides were submerged in diaminobenzidine (DAB)/H_2O_2 substrate solution until the desired staining intensity was obtained and slides were counterstained with hematoxylin. Natural killer cell marker NKp46 (BioLegend 137601, 1:37) was used on paraffin embedded sections and IHC analysis was performed by an automated processor (Discovery XT, Ventanna, Tuscon, AZ) using an alkaline protease antigen retrieval method. TUNEL staining was performed on paraffin embedded tissue according to manufacturer's instructions (Chemicon International, S7101). Quantitation of positive cells per field or percentage of positive cells was performed as indicated in the figure legends.

8. Electron Microscopy

Upon tumor extraction, the samples for TEM were collected immediately after sacrificing the mouse to ensure tissue integrity. Briefly, tissue was fixed with 4% paraformaldehyde and 2.5% EM grade glutaraldehyde in PBS. After fixation, samples were placed in 2% osmium tetroxide in PBS, dehydrated in a graded series of ethyl alcohol, and embedded in Durcupan resin. Ultrathin sections of 80 nm were cut with a Reichert-Jung UltracutE ultramicrotome and placed on formvar coated slot copper grids. Sections were then counterstained with uranyl acetate and lead citrate and viewed with a FEI Tecnai12 BioTwinG^2 electron microscope. Digital images were acquired with an AMT XR-60 CCD Digital Camera System.

9. Senescence and autophagy detection

For autophagy, frozen sections were examined with the Zeiss Axiovert Fluorescence microscope, using both 10x and the 63x oil objectives with tumors that expressed the GFP-LC3 construct. To quantify the percentage of autophagic cells, cells containing more than 3 green puncta were considered autophagic and expressed as a percentage of the total cells counted. For senescence, SA-β-gal detection was performed as previously described [288]. Briefly, frozen tumor sections were fixed for 1 minute in 1% formalin in PBS at room temperature, washed briefly in PBS and incubated with SA-ß-gal color solution (1 mg of 5-bromo-4-chloro-3-indolyl ß-D-galactosidase (X-gal) per mL, 40 mM citric acid, sodium phosphate pH 6.0, 5 mM potassium ferrocyanide, 5 mM potassium ferricyanide, and 150 mM NaCl, 2 mM $MgCl_2$) overnight in a humidified chamber at 37°C.

10. Preparation of samples for flow cytometry

Tumors were excised from mice and minced into small pieces. Tumor pieces were put in a microcentrifuge tube and digested with Trypsin-EDTA (0.05%) and collagenase A (10 μg/mL in trypsin) for 21 minutes at 37°C with brief vortexing every 7 minutes. Trypsin was stopped using normal cell culture media and the tumor cells were centrifuged. The media was removed and the red blood cells were lysed using a buffered ammonium chloride (ACK) solution (0.15 M NH_4Cl, 1.0 mM $KHCO_3$, 0.1 mM Na_2EDTA, pH 7.2-7.4). The tube was briefly vortexed and centrifuged at 1,000 rpm for 5 minutes. Lysing of the red blood cells was continued until the tumor cells were visibly clear of red blood cells. The cells were washed two times with PBS. After the last wash the microcentrifuge tube was allowed to sit at room temperature for 5 minutes so that the large pieces of tumor tissue would descend to the bottom of the tube. The cell suspension was collected and used for flow cytometry. To confirm macrophages, neutrophil, and NK cell depletion, blood was collected from mice via eye bleeds, red blood cells were lysed with ACK solution, washed twice with PBS plus 5% FBS, and subjected to flow cytometry.

11. Flow cytometry

Flow cytometry was performed using a FACSCalibur (BD Biosciences). The following antibodies were used to detect macrophages: Phycoerythrin (PE)-conjugated anti-mouse CD11b (Mac-1, BD Biosciences 553311), Alexa 488-conjugated anti-CD11b (Mac-1) (BD Biosciences 557672), and Allophycocyanin (APC)-conjugated anti-mouse F4/80, (BM8, eBiosciences 17-4801); neutrophils: PE-conjugated anti-Gr-1 (BD Biosciences 553128), Alexa 488-conjugated anti-mouse Gr-1 (Serotec MCA771A647T); and natural killer cells: fluorescein isothiocyanate (FITC)-conjugated anti-mouse NK1.1 (BD Biosciences 553164).

12. ELISA

One-hundred μg of tumor lysates were run on an enzyme-linked immuno sorbent assay (ELISA) to determine the levels of IL-1β and TNFα, using ELISA kits (R&D Systems).

13. Live cell imaging

hmgb1$^{-/-}$ MEFs were transfected with GFP-HMGB1 and treated with 100 μg/mL MAF in the presence of 0.5 μg/mL PI and 0.5 μg/mL Hoschst 33342. Live cell imaging was captured with a Zeiss LSM 510 META NLO Two-Photon Laser Scanning Confocal Microscope System using the time series function and processed using Zeiss Confocal microscope imaging software.

14. Depletion experiments

For macrophage depletion, IV injections of 10 mg/kg of gadolinium chloride ($GdCl_3$) (Alfa Aesar) were started at day 8 post tumor inoculation and occurred every day for two additional consecutive days (day 9, day 10) and then every 3 days (day 13, 16, 19, etc.). CP treatment was started on day 9 post tumor inoculation when tumor size was approximately 100 mm^3. $GdCl_3$ was dissolved in saline and stored in 100 mg/mL stocks. For neutrophil depletion, a neutrophil neutralizing antibody (Ly-6G, eBioscience 14-5931) was injected IP at a concentration of 150 μg/mouse/injection starting with the first CP treatment and continuing for the next 3 CP treatments for a total of 4 anti-neutrophil injections. For NK cell depletion, 25 μL of a NK neutralizing antibody (anti-Asialo GM1, Wako 98-1000) was diluted in 75 μL saline and injected IV with the first CP treatment and continued twice a week for a total of 6 treatments. To deplete circulating HMGB1in mice, an HMGB1 neutralizing antibody [221, 262] was injected 3 times a week for the first two weeks, starting 2 days before the first CP treatment, and two times a week thereafter at a concentration of 50 μg/mouse/injection.

15. Cytokine array

Tumors were extracted from untreated and treated animals and minced into small pieces. Tissue lysate was made with a glass tissue homogenizer and protein concentration was determined by BCA assay. A mouse cytokine array from R&D Systems (ARY006) was used to assess anti- and pro-inflammatory cytokines in the tumor tissue. All procedures were performed following manufacturer's instructions. The array blot was developed using enhanced chemiluminescent detection reagent and the density of each cytokine spot was analyzed using ImageJ Software (NIH). The amount of cytokines in the treated tumor was normalized to the untreated tumor and graphed.

16. Statistical analysis

Data were analyzed with Microsoft Excel and are represented as mean ± S.E.M. (standard error of the mean). Statistical analysis to generate p values was performed using Graph Pad Prism with Anova.

References

1. Adams, J.M. and S. Cory, *The Bcl-2 apoptotic switch in cancer development and therapy.* Oncogene, 2007. **26**(9): p. 1324-37.
2. Coultas, L. and A. Strasser, *The role of the Bcl-2 protein family in cancer.* Semin Cancer Biol, 2003. **13**(2): p. 115-23.
3. Blank, M. and Y. Shiloh, *Programs for cell death: apoptosis is only one way to go.* Cell Cycle, 2007. **6**(6): p. 686-95.
4. Okada, H. and T.W. Mak, *Pathways of apoptotic and non-apoptotic death in tumour cells.* Nat Rev Cancer, 2004. **4**(8): p. 592-603.
5. Haupt, S., et al., *Apoptosis - the p53 network.* J Cell Sci, 2003. **116**(Pt 20): p. 4077-85.
6. Greenblatt, M.S., et al., *Mutations in the p53 tumor suppressor gene: clues to cancer etiology and molecular pathogenesis.* Cancer Res, 1994. **54**(18): p. 4855-78.
7. Brown, J.M. and L.D. Attardi, *The role of apoptosis in cancer development and treatment response.* Nat Rev Cancer, 2005. **5**(3): p. 231-7.
8. Blagosklonny, M.V., *Prospective strategies to enforce selectively cell death in cancer cells.* Oncogene, 2004. **23**(16): p. 2967-75.
9. Pommier, Y., et al., *Apoptosis defects and chemotherapy resistance: molecular interaction maps and networks.* Oncogene, 2004. **23**(16): p. 2934-49.
10. Melino, G., R.A. Knight, and P. Nicotera, *How many ways to die? How many different models of cell death?* Cell Death Differ, 2005. **12 Suppl 2**: p. 1457-62.
11. Mathew, R., V. Karantza-Wadsworth, and E. White, *Role of autophagy in cancer.* Nat Rev Cancer, 2007. **7**(12): p. 961-967.
12. Linder, S., et al., *Determining tumor apoptosis and necrosis in patient serum using cytokeratin 18 as a biomarker.* Cancer Letters, 2004. **214**(1): p. 1-9.
13. Raymond, A.K., et al., *Osteosarcoma chemotherapy effect: a prognostic factor.* Semin Diagn Pathol, 1987. **4**(3): p. 212-36.
14. Bacci, G., et al., *Grade of chemotherapy-induced necrosis as a predictor of local and systemic control in 881 patients with non-metastatic osteosarcoma of the extremities treated with neoadjuvant chemotherapy in a single institution.* Eur J Cancer, 2005. **41**(14): p. 2079-85.
15. Delanian, S. and J.L. Lefaix, *Current management for late normal tissue injury: radiation-induced fibrosis and necrosis.* Semin Radiat Oncol, 2007. **17**(2): p. 99-107.
16. Schmitt, C.A. and S.W. Lowe, *Bcl-2 mediates chemoresistance in matched pairs of primary E(mu)-myc lymphomas in vivo.* Blood Cells Mol Dis, 2001. **27**(1): p. 206-16.
17. Thornberry, N.A. and Y. Lazebnik, *Caspases: enemies within.* Science, 1998. **281**(5381): p. 1312-6.
18. Petros, A.M., E.T. Olejniczak, and S.W. Fesik, *Structural biology of the Bcl-2 family of proteins.* Biochimica et Biophysica Acta (BBA) - Molecular Cell Research, 2004. **1644**(2-3): p. 83-94.

19. Hanahan, D. and R.A. Weinberg, *The hallmarks of cancer.* Cell, 2000. **100**(1): p. 57-70.
20. Bos, J.L., *ras oncogenes in human cancer: a review.* Cancer Res, 1989. **49**(17): p. 4682-9.
21. Weber, M.J., *Raffling off the effectors of Ras.* Cancer Biol Ther, 2003. **2**(1): p. 76-7.
22. Corominas, M., et al., *ras activation in human tumors and in animal model systems.* Environ Health Perspect, 1991. **93**: p. 19-25.
23. Velcich, A. and E. Ziff, *Adenovirus E1a ras cooperation activity is separate from its positive and negative transcription regulatory functions.* Mol Cell Biol, 1988. **8**(5): p. 2177-83.
24. Grand, R.J., et al., *Human cells arrest in S phase in response to adenovirus 12 E1A.* Virology, 1998. **244**(2): p. 330-42.
25. McGill, G. and D.E. Fisher, *Apoptosis in tumorigenesis and cancer therapy.* Front Biosci, 1997. **2**: p. d353-79.
26. Philchenkov, A., et al., *Caspases and cancer: mechanisms of inactivation and new treatment modalities.* Exp Oncol, 2004. **26**(2): p. 82-97.
27. Vogelstein, B. and K.W. Kinzler, *Cancer genes and the pathways they control.* Nat Med, 2004. **10**(8): p. 789-99.
28. Reed, J.C., et al., *BCL-2 family proteins: regulators of cell death involved in the pathogenesis of cancer and resistance to therapy.* J Cell Biochem, 1996. **60**(1): p. 23-32.
29. Ghavami, S., et al., *Apoptosis and cancer: mutations within caspase genes.* J Med Genet, 2009. **46**(8): p. 497-510.
30. Salvesen, G.S. and J.M. Abrams, *Caspase activation - stepping on the gas or releasing the brakes? Lessons from humans and flies.* Oncogene, 2004. **23**(16): p. 2774-84.
31. Reed, J.C., *Apoptosis mechanisms: implications for cancer drug discovery.* Oncology (Williston Park), 2004. **18**(13 Suppl 10): p. 11-20.
32. LaCasse, E.C., et al., *IAP-targeted therapies for cancer.* Oncogene, 2008. **27**(48): p. 6252-75.
33. Altieri, D.C., *New wirings in the survivin networks.* Oncogene, 2008. **27**(48): p. 6276-84.
34. Altieri, D.C., *Survivin, versatile modulation of cell division and apoptosis in cancer.* Oncogene, 2003. **22**(53): p. 8581-9.
35. Yamamoto, H., C.Y. Ngan, and M. Monden, *Cancer cells survive with survivin.* Cancer Sci, 2008. **99**(9): p. 1709-14.
36. Schimmer, A.D., et al., *Targeting XIAP for the treatment of malignancy.* Cell Death Differ, 2006. **13**(2): p. 179-88.
37. Huang, Y., M. Lu, and H. Wu, *Antagonizing XIAP-mediated caspase-3 inhibition. Achilles' heel of cancers?* Cancer Cell, 2004. **5**(1): p. 1-2.
38. Liston, P., W.G. Fong, and R.G. Korneluk, *The inhibitors of apoptosis: there is more to life than Bcl2.* Oncogene, 2003. **22**(53): p. 8568-80.
39. Zhou, X.D., et al., *Expression of cellular FLICE-inhibitory protein and its association with p53 mutation in colon cancer.* World J Gastroenterol, 2005. **11**(16): p. 2482-5.

40. Takakuwa, T., et al., *Frequent mutations of Fas gene in nasal NK/T cell lymphoma.* Oncogene, 2002. **21**(30): p. 4702-5.
41. Takakuwa, T., et al., *Frequent mutations of Fas gene in thyroid lymphoma.* Cancer Res, 2001. **61**(4): p. 1382-5.
42. Takayama, H., et al., *Frequent Fas gene mutations in testicular germ cell tumors.* Am J Pathol, 2002. **161**(2): p. 635-41.
43. Donehower, L.A., et al., *Mice deficient for p53 are developmentally normal but susceptible to spontaneous tumours.* Nature, 1992. **356**(6366): p. 215-21.
44. Vogelstein, B., *Cancer. A deadly inheritance.* Nature, 1990. **348**(6303): p. 681-2.
45. Vogelstein, B., D. Lane, and A.J. Levine, *Surfing the p53 network.* Nature, 2000. **408**(6810): p. 307-10.
46. Lowe, S.W. and A.W. Lin, *Apoptosis in cancer.* Carcinogenesis, 2000. **21**(3): p. 485-95.
47. DeLeo, A.B., et al., *Detection of a transformation-related antigen in chemically induced sarcomas and other transformed cells of the mouse.* Proc Natl Acad Sci U S A, 1979. **76**(5): p. 2420-4.
48. Tsujimoto, Y., et al., *Cloning of the chromosome breakpoint of neoplastic B cells with the t(14;18) chromosome translocation.* Science, 1984. **226**(4678): p. 1097-9.
49. Ricci, M.S. and W.X. Zong, *Chemotherapeutic approaches for targeting cell death pathways.* Oncologist, 2006. **11**(4): p. 342-57.
50. Rezuke, W.N., E.C. Abernathy, and G.J. Tsongalis, *Molecular diagnosis of B- and T-cell lymphomas: fundamental principles and clinical applications.* Clin Chem, 1997. **43**(10): p. 1814-23.
51. Rampino, N., et al., *Somatic frameshift mutations in the BAX gene in colon cancers of the microsatellite mutator phenotype.* Science, 1997. **275**(5302): p. 967-9.
52. Meijerink, J.P., et al., *Hematopoietic malignancies demonstrate loss-of-function mutations of BAX.* Blood, 1998. **91**(8): p. 2991-7.
53. Schuler, M., et al., *Adenovirus-mediated wild-type p53 gene transfer in patients receiving chemotherapy for advanced non-small-cell lung cancer: results of a multicenter phase II study.* J Clin Oncol, 2001. **19**(6): p. 1750-8.
54. Chen, L., et al., *Synergistic activation of p53 by inhibition of MDM2 expression and DNA damage.* Proc Natl Acad Sci U S A, 1998. **95**(1): p. 195-200.
55. Wasylyk, C., et al., *p53 mediated death of cells overexpressing MDM2 by an inhibitor of MDM2 interaction with p53.* Oncogene, 1999. **18**(11): p. 1921-34.
56. Vassilev, L.T., et al., *In vivo activation of the p53 pathway by small-molecule antagonists of MDM2.* Science, 2004. **303**(5659): p. 844-8.
57. Issaeva, N., et al., *Small molecule RITA binds to p53, blocks p53-HDM-2 interaction and activates p53 function in tumors.* Nat Med, 2004. **10**(12): p. 1321-8.
58. Dinnen, R.D., et al., *Activation of targeted necrosis by a p53 peptide: a novel death pathway that circumvents apoptotic resistance.* J Biol Chem, 2007. **282**(37): p. 26675-86.
59. Fesik, S.W., *Insights into Programmed Cell Death through Structural Biology.* Cell, 2000. **103**(2): p. 273-282.

60. Oltersdorf, T., et al., *An inhibitor of Bcl-2 family proteins induces regression of solid tumours.* Nature, 2005. **435**(7042): p. 677-81.
61. Vogler, M., et al., *Bcl-2 inhibitors: small molecules with a big impact on cancer therapy.* Cell Death Differ, 2009. **16**(3): p. 360-7.
62. Del Gaizo Moore, V. and A. Letai, *Rational design of therapeutics targeting the BCL-2 family: are some cancer cells primed for death but waiting for a final push?* Adv Exp Med Biol, 2008. **615**: p. 159-75.
63. Meiler, J. and M. Schuler, *Therapeutic targeting of apoptotic pathways in cancer.* Curr Drug Targets, 2006. **7**(10): p. 1361-9.
64. Sun, H., et al., *Design, synthesis, and characterization of a potent, nonpeptide, cell-permeable, bivalent Smac mimetic that concurrently targets both the BIR2 and BIR3 domains in XIAP.* J Am Chem Soc, 2007. **129**(49): p. 15279-94.
65. Petersen, S.L., et al., *Autocrine TNFalpha signaling renders human cancer cells susceptible to Smac-mimetic-induced apoptosis.* Cancer Cell, 2007. **12**(5): p. 445-56.
66. Varfolomeev, E., et al., *IAP antagonists induce autoubiquitination of c-IAPs, NF-kappaB activation, and TNFalpha-dependent apoptosis.* Cell, 2007. **131**(4): p. 669-81.
67. Vince, J.E., et al., *IAP antagonists target cIAP1 to induce TNFalpha-dependent apoptosis.* Cell, 2007. **131**(4): p. 682-93.
68. Lang, P., et al., *Osteogenic sarcoma: noninvasive in vivo assessment of tumor necrosis with diffusion-weighted MR imaging.* Radiology, 1998. **206**(1): p. 227-35.
69. Blakey, D.C., et al., *Antitumor activity of the novel vascular targeting agent ZD6126 in a panel of tumor models.* Clin Cancer Res, 2002. **8**(6): p. 1974-83.
70. Guerriero, J.L., et al., *Chemotherapy induces tumor clearance independent of apoptosis.* Cancer Res, 2008. **68**(23): p. 9595-600.
71. Schmitt, C.A., et al., *A senescence program controlled by p53 and p16INK4a contributes to the outcome of cancer therapy.* Cell, 2002. **109**(3): p. 335-46.
72. Kondo, Y. and S. Kondo, *Autophagy and cancer therapy.* Autophagy, 2006. **2**(2): p. 85-90.
73. Kanzawa, T., et al., *Role of autophagy in temozolomide-induced cytotoxicity for malignant glioma cells.* Cell Death Differ, 2004. **11**(4): p. 448-57.
74. Paglin, S., et al., *A novel response of cancer cells to radiation involves autophagy and formation of acidic vesicles.* Cancer Res, 2001. **61**(2): p. 439-44.
75. Falkvoll, K.H., *The occurrence of apoptosis, abnormal mitoses, cells dying in mitosis and micronuclei in a human melanoma xenograft exposed to single dose irradiation.* Strahlenther Onkol, 1990. **166**(7): p. 487-92.
76. Roninson, I.B., E.V. Broude, and B.-D. Chang, *If not apoptosis, then what? Treatment-induced senescence and mitotic catastrophe in tumor cells.* Drug Resistance Updates, 2001. **4**(5): p. 303-313.
77. Roninson, I.B., *Tumor cell senescence in cancer treatment.* Cancer Res, 2003. **63**(11): p. 2705-15.
78. Lock, R.B. and L. Stribinskiene, *Dual modes of death induced by etoposide in human epithelial tumor cells allow Bcl-2 to inhibit apoptosis without affecting clonogenic survival.* Cancer Res, 1996. **56**(17): p. 4006-12.

79. Torres, K. and S.B. Horwitz, *Mechanisms of Taxol-induced cell death are concentration dependent.* Cancer Res, 1998. **58**(16): p. 3620-6.
80. Chang, B.D., et al., *A senescence-like phenotype distinguishes tumor cells that undergo terminal proliferation arrest after exposure to anticancer agents.* Cancer Res, 1999. **59**(15): p. 3761-7.
81. Majno, G. and I. Joris, *Apoptosis, oncosis, and necrosis. An overview of cell death.* Am J Pathol, 1995. **146**(1): p. 3-15.
82. Proskuryakov, S.Y., V.L. Gabai, and A.G. Konoplyannikov, *Necrosis is an active and controlled form of programmed cell death.* Biochemistry (Mosc), 2002. **67**(4): p. 387-408.
83. Zong, W.X. and C.B. Thompson, *Necrotic death as a cell fate.* Genes Dev, 2006. **20**(1): p. 1-15.
84. Degterev, A. and J. Yuan, *Expansion and Evolution of Cell Death Programs.* Nat Rev Mol Cell Bio, 2008. **In press.**
85. Golstein, P. and G. Kroemer, *Cell death by necrosis: towards a molecular definition.* Trends Biochem Sci, 2007. **32**(1): p. 37-43.
86. Zong, W.X., et al., *Alkylating DNA damage stimulates a regulated form of necrotic cell death.* Genes Dev, 2004. **18**(11): p. 1272-82.
87. Moore, C.M., D. Pendse, and M. Emberton, *Photodynamic therapy for prostate cancer--a review of current status and future promise.* Nat Clin Pract Urol, 2009. **6**(1): p. 18-30.
88. Blitzer, A., et al., *Clinical-pathological determinants in prognosis of fibrous histiocytomas of head and neck.* Laryngoscope, 1981. **91**(12): p. 2053-70.
89. Olofsson, M.H., et al., *Cytokeratin-18 is a useful serum biomarker for early determination of response of breast carcinomas to chemotherapy.* Clin Cancer Res, 2007. **13**(11): p. 3198-206.
90. Hendershot, E., et al., *Tumor Necrosis in Pediatric Osteosarcoma: Impact of Modern Therapies.* Journal of Pediatric Oncology Nursing, 2006. **23**(4): p. 176-181.
91. Wunder, J.S., et al., *The histological response to chemotherapy as a predictor of the oncological outcome of operative treatment of Ewing sarcoma.* J Bone Joint Surg Am, 1998. **80**(7): p. 1020-33.
92. Reiser, M., et al., *Raynaud's phenomenon and acral necrosis after chemotherapy for AIDS-related Kaposi's sarcoma.* Eur J Clin Microbiol Infect Dis, 1998. **17**(1): p. 58-60.
93. Eilber, F.C., et al., *Treatment-induced pathologic necrosis: a predictor of local recurrence and survival in patients receiving neoadjuvant therapy for high-grade extremity soft tissue sarcomas.* J Clin Oncol, 2001. **19**(13): p. 3203-9.
94. Schmack, I., et al., *Ischemic necrosis and atrophy of the optic nerve after periocular carboplatin injection for intraocular retinoblastoma.* Am J Ophthalmol, 2006. **142**(2): p. 310-5.
95. Scott, L.C., et al., *Cytokeratin 18 in plasma of patients with gastrointestinal adenocarcinoma as a biomarker of tumour response.* Br J Cancer, 2009. **101**(3): p. 410-7.
96. Schutte, B., et al., *The caspase-9 derived C-terminal fragment of cytokeratin 18 modulates topoisomerase action.* Int J Oncol, 2009. **35**(3): p. 625-30.

97. Kramer, G., et al., *Differentiation between cell death modes using measurements of different soluble forms of extracellular cytokeratin 18.* Cancer Res, 2004. **64**(5): p. 1751-6.
98. Gridelli, C., et al., *Vascular disrupting agents: a novel mechanism of action in the battle against non-small cell lung cancer.* Oncologist, 2009. **14**(6): p. 612-20.
99. Siemann, D.W., D.J. Chaplin, and M.R. Horsman, *Vascular-targeting therapies for treatment of malignant disease.* Cancer, 2004. **100**(12): p. 2491-9.
100. Balkwill, F., *Tumour necrosis factor and cancer.* Nat Rev Cancer, 2009.
101. Fagnoni, F.F., et al., *Combination of radiofrequency ablation and immunotherapy.* Front Biosci, 2008. **13**: p. 369-81.
102. Vivarelli, M., et al., *Surgical resection versus percutaneous radiofrequency ablation in the treatment of hepatocellular carcinoma on cirrhotic liver.* Ann Surg, 2004. **240**(1): p. 102-7.
103. Cho, C.M., et al., *[The comparative results of radiofrequency ablation versus surgical resection for the treatment of hepatocellular carcinoma.].* Korean J Hepatol, 2005. **11**(1): p. 59-71.
104. Lu, C., et al., *NMDA receptor subtypes at autaptic synapses of cerebellar granule neurons.* J Neurophysiol, 2006. **96**(5): p. 2282-94.
105. Buytaert, E., M. Dewaele, and P. Agostinis, *Molecular effectors of multiple cell death pathways initiated by photodynamic therapy.* Biochim Biophys Acta, 2007. **1776**(1): p. 86-107.
106. Degterev, A., et al., *Identification of RIP1 kinase as a specific cellular target of necrostatins.* Nat Chem Biol, 2008. **4**(5): p. 313-21.
107. Han, W., et al., *Shikonin circumvents cancer drug resistance by induction of a necroptotic death.* Mol Cancer Ther, 2007. **6**(5): p. 1641-9.
108. Degterev, A., et al., *Chemical inhibitor of nonapoptotic cell death with therapeutic potential for ischemic brain injury.* Nat Chem Biol, 2005. **1**(2): p. 112-9.
109. Holler, N., et al., *Fas triggers an alternative, caspase-8-independent cell death pathway using the kinase RIP as effector molecule.* Nat Immunol, 2000. **1**(6): p. 489-95.
110. Lin, Y., et al., *Cleavage of the death domain kinase RIP by caspase-8 prompts TNF-induced apoptosis.* Genes Dev, 1999. **13**(19): p. 2514-26.
111. Feng, S., et al., *Cleavage of RIP3 inactivates its caspase-independent apoptosis pathway by removal of kinase domain.* Cell Signal, 2007. **19**(10): p. 2056-67.
112. Xu, Y., et al., *Poly(ADP-ribose) polymerase-1 signaling to mitochondria in necrotic cell death requires RIP1/TRAF2-mediated JNK1 activation.* J Biol Chem, 2006. **281**(13): p. 8788-95.
113. Chan, F.K., et al., *A role for tumor necrosis factor receptor-2 and receptor-interacting protein in programmed necrosis and antiviral responses.* J Biol Chem, 2003. **278**(51): p. 51613-21.
114. Amaravadi, R.K. and C.B. Thompson, *The roles of therapy-induced autophagy and necrosis in cancer treatment.* Clin Cancer Res, 2007. **13**(24): p. 7271-9.
115. Shen, H.M., et al., *Essential roles of receptor-interacting protein and TRAF2 in oxidative stress-induced cell death.* Mol Cell Biol, 2004. **24**(13): p. 5914-22.

116. Temkin, V., et al., *Inhibition of ADP/ATP exchange in receptor-interacting protein-mediated necrosis.* Mol Cell Biol, 2006. **26**(6): p. 2215-25.
117. Vanlangenakker, N., et al., *Molecular mechanisms and pathophysiology of necrotic cell death.* Curr Mol Med, 2008. **8**(3): p. 207-20.
118. Thon, L., et al., *Ceramide mediates caspase-independent programmed cell death.* FASEB J, 2005. **19**(14): p. 1945-56.
119. Henriquez, M., et al., *Cell death by necrosis, a regulated way to go.* Curr Mol Med, 2008. **8**(3): p. 187-206.
120. Cho, Y.S., et al., *Phosphorylation-driven assembly of the RIP1-RIP3 complex regulates programmed necrosis and virus-induced inflammation.* Cell, 2009. **137**(6): p. 1112-23.
121. He, S., et al., *Receptor interacting protein kinase-3 determines cellular necrotic response to TNF-alpha.* Cell, 2009. **137**(6): p. 1100-11.
122. Zhang, D.W., et al., *RIP3, an Energy Metabolism Regulator that Switches TNF-Induced Cell Death from Apoptosis to Necrosis.* Science, 2009.
123. Chakraborty, M., et al., *Irradiation of tumor cells up-regulates Fas and enhances CTL lytic activity and CTL adoptive immunotherapy.* J Immunol, 2003. **170**(12): p. 6338-47.
124. de Murcia, G. and J. Menissier de Murcia, *Poly(ADP-ribose) polymerase: a molecular nick-sensor.* Trends Biochem Sci, 1994. **19**(4): p. 172-6.
125. Ha, H.C. and S.H. Snyder, *Poly(ADP-ribose) polymerase is a mediator of necrotic cell death by ATP depletion.* Proc Natl Acad Sci U S A, 1999. **96**(24): p. 13978-82.
126. Kirkegaard, T. and M. Jaattela, *Lysosomal involvement in cell death and cancer.* Biochim Biophys Acta, 2009. **1793**(4): p. 746-54.
127. Tu, H.C., et al., *The p53-cathepsin axis cooperates with ROS to activate programmed necrotic death upon DNA damage.* Proc Natl Acad Sci U S A, 2009. **106**(4): p. 1093-8.
128. Sun, Y. and Z.L. Peng, *Programmed cell death and cancer.* Postgrad Med J, 2009. **85**(1001): p. 134-40.
129. Lum, J.J., R.J. DeBerardinis, and C.B. Thompson, *Autophagy in metazoans: cell survival in the land of plenty.* Nat Rev Mol Cell Biol, 2005. **6**(6): p. 439-48.
130. Mizushima, N., *Autophagy: process and function.* Genes Dev, 2007. **21**(22): p. 2861-73.
131. Shintani, T. and D.J. Klionsky, *Autophagy in health and disease: a double-edged sword.* Science, 2004. **306**(5698): p. 990-5.
132. Klionsky, D.J. and S.D. Emr, *Autophagy as a regulated pathway of cellular degradation.* Science, 2000. **290**(5497): p. 1717-21.
133. Klionsky, D.J., et al., *A unified nomenclature for yeast autophagy-related genes.* Dev Cell, 2003. **5**(4): p. 539-45.
134. Levine, B. and D.J. Klionsky, *Development by self-digestion: molecular mechanisms and biological functions of autophagy.* Dev Cell, 2004. **6**(4): p. 463-77.
135. Cuervo, A.M., *Autophagy: in sickness and in health.* Trends Cell Biol, 2004. **14**(2): p. 70-7.

136. Elmore, S.P., et al., *The mitochondrial permeability transition initiates autophagy in rat hepatocytes.* FASEB J, 2001. **15**(12): p. 2286-7.
137. Liang, X.H., et al., *Induction of autophagy and inhibition of tumorigenesis by beclin 1.* Nature, 1999. **402**(6762): p. 672-6.
138. Yue, Z., et al., *Beclin 1, an autophagy gene essential for early embryonic development, is a haploinsufficient tumor suppressor.* Proc Natl Acad Sci U S A, 2003. **100**(25): p. 15077-82.
139. Aita, V.M., et al., *Cloning and genomic organization of beclin 1, a candidate tumor suppressor gene on chromosome 17q21.* Genomics, 1999. **59**(1): p. 59-65.
140. Ahn, C.H., et al., *Expression of beclin-1, an autophagy-related protein, in gastric and colorectal cancers.* APMIS, 2007. **115**(12): p. 1344-9.
141. Alva, A.S., S.H. Gultekin, and E.H. Baehrecke, *Autophagy in human tumors: cell survival or death?* Cell Death Differ, 2004. **11**(9): p. 1046-8.
142. Bursch, W., et al., *Active cell death induced by the anti-estrogens tamoxifen and ICI 164 384 in human mammary carcinoma cells (MCF-7) in culture: the role of autophagy.* Carcinogenesis, 1996. **17**(8): p. 1595-607.
143. Mizushima, N., et al., *In vivo analysis of autophagy in response to nutrient starvation using transgenic mice expressing a fluorescent autophagosome marker.* Mol Biol Cell, 2004. **15**(3): p. 1101-11.
144. Okada, H. and T.W. Mak, *PATHWAYS OF APOPTOTIC AND NON-APOPTOTIC DEATH IN TUMOUR CELLS.* Nature Reviews Cancer, 2004. **4**(8): p. 592-603.
145. Collado, M., et al., *Tumour biology: senescence in premalignant tumours.* Nature, 2005. **436**(7051): p. 642.
146. Morse, D.L., et al., *Docetaxel induces cell death through mitotic catastrophe in human breast cancer cells.* Mol Cancer Ther, 2005. **4**(10): p. 1495-504.
147. Fadok, V.A., et al., *A receptor for phosphatidylserine-specific clearance of apoptotic cells.* Nature, 2000. **405**(6782): p. 85-90.
148. McDonald, P.P., et al., *Transcriptional and translational regulation of inflammatory mediator production by endogenous TGF-beta in macrophages that have ingested apoptotic cells.* J Immunol, 1999. **163**(11): p. 6164-72.
149. Sauter, B., et al., *Consequences of cell death: exposure to necrotic tumor cells, but not primary tissue cells or apoptotic cells, induces the maturation of immunostimulatory dendritic cells.* J Exp Med, 2000. **191**(3): p. 423-34.
150. Edinger, A.L. and C.B. Thompson, *Death by design: apoptosis, necrosis and autophagy.* Curr Opin Cell Biol, 2004. **16**(6): p. 663-9.
151. Festjens, N., T. Vanden Berghe, and P. Vandenabeele, *Necrosis, a well-orchestrated form of cell demise: signalling cascades, important mediators and concomitant immune response.* Biochim Biophys Acta, 2006. **1757**(9-10): p. 1371-87.
152. Zitvogel, L., et al., *Immune response against dying tumor cells.* Adv Immunol, 2004. **84**: p. 131-79.
153. Savill, J. and V. Fadok, *Corpse clearance defines the meaning of cell death.* Nature, 2000. **407**(6805): p. 784-8.
154. Chen, W., et al., *TGF-beta released by apoptotic T cells contributes to an immunosuppressive milieu.* Immunity, 2001. **14**(6): p. 715-25.

155. Fadok, V.A., et al., *Macrophages that have ingested apoptotic cells in vitro inhibit proinflammatory cytokine production through autocrine/paracrine mechanisms involving TGF-beta, PGE2, and PAF.* J Clin Invest, 1998. **101**(4): p. 890-8.
156. Voll, R.E., et al., *Immunosuppressive effects of apoptotic cells.* Nature, 1997. **390**(6658): p. 350-1.
157. Fournier, T., V. Fadok, and P.M. Henson, *Tumor necrosis factor-alpha inversely regulates prostaglandin D2 and prostaglandin E2 production in murine macrophages. Synergistic action of cyclic AMP on cyclooxygenase-2 expression and prostaglandin E2 synthesis.* J Biol Chem, 1997. **272**(49): p. 31065-72.
158. Erwig, L.P. and P.M. Henson, *Immunological consequences of apoptotic cell phagocytosis.* Am J Pathol, 2007. **171**(1): p. 2-8.
159. Huynh, M.L., V.A. Fadok, and P.M. Henson, *Phosphatidylserine-dependent ingestion of apoptotic cells promotes TGF-beta1 secretion and the resolution of inflammation.* J Clin Invest, 2002. **109**(1): p. 41-50.
160. Kim, S., K.B. Elkon, and X. Ma, *Transcriptional suppression of interleukin-12 gene expression following phagocytosis of apoptotic cells.* Immunity, 2004. **21**(5): p. 643-53.
161. Gallucci, S., M. Lolkema, and P. Matzinger, *Natural adjuvants: endogenous activators of dendritic cells.* Nat Med, 1999. **5**(11): p. 1249-55.
162. Kariko, K., et al., *mRNA is an endogenous ligand for Toll-like receptor 3.* J Biol Chem, 2004. **279**(13): p. 12542-50.
163. Marenholz, I., C.W. Heizmann, and G. Fritz, *S100 proteins in mouse and man: from evolution to function and pathology (including an update of the nomenclature).* Biochem Biophys Res Commun, 2004. **322**(4): p. 1111-22.
164. Ditsworth, D., W.X. Zong, and C.B. Thompson, *Activation of poly(ADP)-ribose polymerase (PARP-1) induces release of the pro-inflammatory mediator HMGB1 from the nucleus.* J Biol Chem, 2007. **282**(24): p. 17845-54.
165. Ferrari, D., et al., *Purinergic modulation of interleukin-1 beta release from microglial cells stimulated with bacterial endotoxin.* J Exp Med, 1997. **185**(3): p. 579-82.
166. Shi, Y., J.E. Evans, and K.L. Rock, *Molecular identification of a danger signal that alerts the immune system to dying cells.* Nature, 2003. **425**(6957): p. 516-21.
167. Basu, S., et al., *Necrotic but not apoptotic cell death releases heat shock proteins, which deliver a partial maturation signal to dendritic cells and activate the NF-kappa B pathway.* Int Immunol, 2000. **12**(11): p. 1539-46.
168. Dunn, G.P., et al., *Cancer immunoediting: from immunosurveillance to tumor escape.* Nat Immunol, 2002. **3**(11): p. 991-8.
169. Swann, J.B. and M.J. Smyth, *Immune surveillance of tumors.* J Clin Invest, 2007. **117**(5): p. 1137-46.
170. Duan, F., et al., *Immune Rejection of Mouse Tumors Expressing Mutated Self.* Cancer Res, 2009.
171. Lu, B. and O.J. Finn, *T-cell death and cancer immune tolerance.* Cell Death Differ, 2008. **15**(1): p. 70-9.
172. Buell, J.F., T.G. Gross, and E.S. Woodle, *Malignancy after transplantation.* Transplantation, 2005. **80**(2 Suppl): p. S254-64.

173. Coussens, L.M. and Z. Werb, *Inflammation and cancer.* Nature, 2002. **420**(6917): p. 860-7.
174. Zitvogel, L., et al., *Immunological aspects of cancer chemotherapy.* Nat Rev Immunol, 2008. **8**(1): p. 59-73.
175. Xue, W., et al., *Senescence and tumour clearance is triggered by p53 restoration in murine liver carcinomas.* Nature, 2007. **445**(7128): p. 656-60.
176. Lin, W.W. and M. Karin, *A cytokine-mediated link between innate immunity, inflammation, and cancer.* J Clin Invest, 2007. **117**(5): p. 1175-83.
177. Vakkila, J. and M.T. Lotze, *Inflammation and necrosis promote tumour growth.* Nat Rev Immunol, 2004. **4**(8): p. 641-8.
178. Karin, M., T. Lawrence, and V. Nizet, *Innate immunity gone awry: linking microbial infections to chronic inflammation and cancer.* Cell, 2006. **124**(4): p. 823-35.
179. Degenhardt, K., et al., *Autophagy promotes tumor cell survival and restricts necrosis, inflammation, and tumorigenesis.* Cancer Cell, 2006. **10**(1): p. 51-64.
180. Banchereau, J., et al., *Immunobiology of dendritic cells.* Annu Rev Immunol, 2000. **18**: p. 767-811.
181. Aspord, C., et al., *Breast cancer instructs dendritic cells to prime interleukin 13-secreting CD4+ T cells that facilitate tumor development.* J Exp Med, 2007. **204**(5): p. 1037-47.
182. Rettig, M.B., et al., *Kaposi's sarcoma-associated herpesvirus infection of bone marrow dendritic cells from multiple myeloma patients.* Science, 1997. **276**(5320): p. 1851-4.
183. Bell, D., et al., *In breast carcinoma tissue, immature dendritic cells reside within the tumor, whereas mature dendritic cells are located in peritumoral areas.* J Exp Med, 1999. **190**(10): p. 1417-26.
184. Mantovani, A., et al., *Infiltration of tumours by macrophages and dendritic cells: tumour-associated macrophages as a paradigm for polarized M2 mononuclear phagocytes.* Novartis Found Symp, 2004. **256**: p. 137-45; discussion 146-8, 259-69.
185. Coca, S., et al., *The prognostic significance of intratumoral natural killer cells in patients with colorectal carcinoma.* Cancer, 1997. **79**(12): p. 2320-8.
186. Orange, J.S. and Z.K. Ballas, *Natural killer cells in human health and disease.* Clin Immunol, 2006. **118**(1): p. 1-10.
187. Hicks, A.M., et al., *Transferable anticancer innate immunity in spontaneous regression/complete resistance mice.* Proc Natl Acad Sci U S A, 2006. **103**(20): p. 7753-8.
188. Cui, Z., et al., *Spontaneous regression of advanced cancer: identification of a unique genetically determined, age-dependent trait in mice.* Proc Natl Acad Sci U S A, 2003. **100**(11): p. 6682-7.
189. Yamazaki, M., M. Ikenami, and T. Sugiyama, *Cytolytic heterogeneity of polymorphonuclear leukocytes in killing of murine tumor cells.* Jpn J Cancer Res, 1988. **79**(11): p. 1217-23.
190. Ackermann, M.F., et al., *Antitumor activity of murine neutrophils demonstrated by cytometric analysis.* Cancer Res, 1989. **49**(3): p. 528-32.

191. Zivkovic, M., et al., *Oxidative burst and anticancer activities of rat neutrophils.* Biofactors, 2005. **24**(1-4): p. 305-12.
192. Balkwill, F., K.A. Charles, and A. Mantovani, *Smoldering and polarized inflammation in the initiation and promotion of malignant disease.* Cancer Cell, 2005. **7**(3): p. 211-7.
193. de Visser, K.E., A. Eichten, and L.M. Coussens, *Paradoxical roles of the immune system during cancer development.* Nat Rev Cancer, 2006. **6**(1): p. 24-37.
194. Lin, E.Y., et al., *Colony-stimulating factor 1 promotes progression of mammary tumors to malignancy.* J Exp Med, 2001. **193**(6): p. 727-40.
195. Aharinejad, S., et al., *Colony-stimulating factor-1 blockade by antisense oligonucleotides and small interfering RNAs suppresses growth of human mammary tumor xenografts in mice.* Cancer Res, 2004. **64**(15): p. 5378-84.
196. Leek, R.D., et al., *Association of macrophage infiltration with angiogenesis and prognosis in invasive breast carcinoma.* Cancer Res, 1996. **56**(20): p. 4625-9.
197. Imada, A., et al., *Mast cells correlate with angiogenesis and poor outcome in stage I lung adenocarcinoma.* Eur Respir J, 2000. **15**(6): p. 1087-93.
198. Ribatti, D., et al., *Tumor vascularity and tryptase-positive mast cells correlate with a poor prognosis in melanoma.* Eur J Clin Invest, 2003. **33**(5): p. 420-5.
199. Mai, H.Q., et al., *Endoscopic microwave coagulation therapy for early recurrent T1 nasopharyngeal carcinoma.* Eur J Cancer, 2009.
200. Landsberg, R., et al., *Laser-induced hyperthermia for treatment of granulation tissue growth in rats.* Otolaryngol Head Neck Surg, 2009. **140**(4): p. 480-486.
201. Lotfi, R., J.J. Lee, and M.T. Lotze, *Eosinophilic granulocytes and damage-associated molecular pattern molecules (DAMPs): role in the inflammatory response within tumors.* J Immunother, 2007. **30**(1): p. 16-28.
202. Seino, K., et al., *Antitumor effect of locally produced CD95 ligand.* Nat Med, 1997. **3**(2): p. 165-70.
203. Cormier, S.A., et al., *Pivotal Advance: eosinophil infiltration of solid tumors is an early and persistent inflammatory host response.* J Leukoc Biol, 2006. **79**(6): p. 1131-9.
204. Reiter, I., B. Krammer, and G. Schwamberger, *Cutting edge: differential effect of apoptotic versus necrotic tumor cells on macrophage antitumor activities.* J Immunol, 1999. **163**(4): p. 1730-2.
205. Banchereau, J. and R.M. Steinman, *Dendritic cells and the control of immunity.* Nature, 1998. **392**(6673): p. 245-52.
206. Liu, K., et al., *Innate NKT lymphocytes confer superior adaptive immunity via tumor-capturing dendritic cells.* J Exp Med, 2005. **202**(11): p. 1507-16.
207. Bonifaz, L.C., et al., *In vivo targeting of antigens to maturing dendritic cells via the DEC-205 receptor improves T cell vaccination.* J Exp Med, 2004. **199**(6): p. 815-24.
208. Dhodapkar, M.V., K.M. Dhodapkar, and A.K. Palucka, *Interactions of tumor cells with dendritic cells: balancing immunity and tolerance.* Cell Death Differ, 2008. **15**(1): p. 39-50.
209. Steinman, R.M., et al., *Dendritic cell function in vivo during the steady state: a role in peripheral tolerance.* Ann N Y Acad Sci, 2003. **987**: p. 15-25.

210. Hawiger, D., et al., *Dendritic cells induce peripheral T cell unresponsiveness under steady state conditions in vivo.* J Exp Med, 2001. **194**(6): p. 769-79.
211. Buttiglieri, S., et al., *Influence of drug-induced apoptotic death on processing and presentation of tumor antigens by dendritic cells.* Int J Cancer, 2003. **106**(4): p. 516-20.
212. Pietra, G., et al., *Phases of apoptosis of melanoma cells, but not of normal melanocytes, differently affect maturation of myeloid dendritic cells.* Cancer Res, 2001. **61**(22): p. 8218-26.
213. Brusa, D., et al., *Post-apoptotic tumors are more palatable to dendritic cells and enhance their antigen cross-presentation activity.* Vaccine, 2008. **26**(50): p. 6422-32.
214. Rovere-Querini, P., et al., *HMGB1 is an endogenous immune adjuvant released by necrotic cells.* EMBO Rep, 2004. **5**(8): p. 825-30.
215. Apetoh, L., et al., *Toll-like receptor 4-dependent contribution of the immune system to anticancer chemotherapy and radiotherapy.* Nat Med, 2007. **13**(9): p. 1050-9.
216. Ellerman, J.E., et al., *Masquerader: high mobility group box-1 and cancer.* Clin Cancer Res, 2007. **13**(10): p. 2836-48.
217. Bianchi, M.E. and A.A. Manfredi, *High-mobility group box 1 (HMGB1) protein at the crossroads between innate and adaptive immunity.* Immunol Rev, 2007. **220**: p. 35-46.
218. Scaffidi, P., T. Misteli, and M.E. Bianchi, *Release of chromatin protein HMGB1 by necrotic cells triggers inflammation.* Nature, 2002. **418**(6894): p. 191-5.
219. Trisciuoglio, L. and M.E. Bianchi, *Several nuclear events during apoptosis depend on caspase-3 activation but do not constitute a common pathway.* PLoS One, 2009. **4**(7): p. e6234.
220. Jiang, W., et al., *The effects of CpG DNA on HMGB1 release by murine macrophage cell lines.* J Leukoc Biol, 2005. **78**(4): p. 930-6.
221. Wang, H., et al., *HMG-1 as a late mediator of endotoxin lethality in mice.* Science, 1999. **285**(5425): p. 248-51.
222. Andersson, U., et al., *High mobility group 1 protein (HMG-1) stimulates proinflammatory cytokine synthesis in human monocytes.* J Exp Med, 2000. **192**(4): p. 565-70.
223. Wang, H., et al., *Proinflammatory cytokines (tumor necrosis factor and interleukin 1) stimulate release of high mobility group protein-1 by pituicytes.* Surgery, 1999. **126**(2): p. 389-92.
224. Sparatore, B., et al., *Extracellular high-mobility group 1 protein is essential for murine erythroleukaemia cell differentiation.* Biochem J, 1996. **320 (Pt 1)**: p. 253-6.
225. Bonaldi, T., et al., *Monocytic cells hyperacetylate chromatin protein HMGB1 to redirect it towards secretion.* EMBO J, 2003. **22**(20): p. 5551-60.
226. Ito, I., J. Fukazawa, and M. Yoshida, *Post-translational methylation of high mobility group box 1 (HMGB1) causes its cytoplasmic localization in neutrophils.* J Biol Chem, 2007. **282**(22): p. 16336-44.
227. Lotze, M.T. and K.J. Tracey, *High-mobility group box 1 protein (HMGB1): nuclear weapon in the immune arsenal.* Nat Rev Immunol, 2005. **5**(4): p. 331-42.

228. Gardella, S., et al., *The nuclear protein HMGB1 is secreted by monocytes via a non-classical, vesicle-mediated secretory pathway.* EMBO Rep, 2002. **3**(10): p. 995-1001.
229. Bell, C.W., et al., *The extracellular release of HMGB1 during apoptotic cell death.* Am J Physiol Cell Physiol, 2006. **291**(6): p. C1318-25.
230. Youn, J.H. and J.S. Shin, *Nucleocytoplasmic shuttling of HMGB1 is regulated by phosphorylation that redirects it toward secretion.* J Immunol, 2006. **177**(11): p. 7889-97.
231. Kang, H.J., et al., *Non-histone nuclear factor HMGB1 is phosphorylated and secreted in colon cancers.* Lab Invest, 2009. **89**(8): p. 948-59.
232. Oh, Y.J., et al., *HMGB1 is phosphorylated by classical protein kinase C and is secreted by a calcium-dependent mechanism.* J Immunol, 2009. **182**(9): p. 5800-9.
233. Tang, D., et al., *Hydrogen peroxide stimulates macrophages and monocytes to actively release HMGB1.* J Leukoc Biol, 2007. **81**(3): p. 741-7.
234. Kazama, H., et al., *Induction of immunological tolerance by apoptotic cells requires caspase-dependent oxidation of high-mobility group box-1 protein.* Immunity, 2008. **29**(1): p. 21-32.
235. Yu, M., et al., *HMGB1 signals through toll-like receptor (TLR) 4 and TLR2.* Shock, 2006. **26**(2): p. 174-9.
236. Yang, H., et al., *A critical cysteine is required for HMGB1 binding to Toll-like receptor 4 and activation of macrophage cytokine release.* Proc Natl Acad Sci U S A, 2010.
237. Tang, D., et al., *High-mobility group box 1 and cancer.* Biochim Biophys Acta, 2010. **1799**(1-2): p. 131-140.
238. Sims, G.P., et al., *HMGB1 and RAGE in inflammation and cancer.* Annu Rev Immunol, 2010. **28**: p. 367-88.
239. Andersson, U.G. and K.J. Tracey, *HMGB1, a pro-inflammatory cytokine of clinical interest: introduction.* J Intern Med, 2004. **255**(3): p. 318-9.
240. Palumbo, R. and M.E. Bianchi, *High mobility group box 1 protein, a cue for stem cell recruitment.* Biochem Pharmacol, 2004. **68**(6): p. 1165-70.
241. Kim, M.Y., T. Zhang, and W.L. Kraus, *Poly(ADP-ribosyl)ation by PARP-1: 'PAR-laying' NAD+ into a nuclear signal.* Genes Dev, 2005. **19**(17): p. 1951-67.
242. Taguchi, A., et al., *Blockade of RAGE-amphoterin signalling suppresses tumour growth and metastases.* Nature, 2000. **405**(6784): p. 354-60.
243. Curtin, J.F., et al., *HMGB1 mediates endogenous TLR2 activation and brain tumor regression.* PLoS Med, 2009. **6**(1): p. e10.
244. Apetoh, L., et al., *The interaction between HMGB1 and TLR4 dictates the outcome of anticancer chemotherapy and radiotherapy.* Immunol Rev, 2007. **220**: p. 47-59.
245. Apetoh, L., et al., *Molecular interactions between dying tumor cells and the innate immune system determine the efficacy of conventional anticancer therapies.* Cancer Res, 2008. **68**(11): p. 4026-30.
246. Chabner, B.A. and D.L. Longo, *Cancer Chemotherapy and Biotherapy. Principles and Practice*. Fourth ed. 2006, Philadelphia: Lippincott Williams & Wilkins.

247. Castedo, M., et al., *Cell death by mitotic catastrophe: a molecular definition.* Oncogene, 2004. **23**(16): p. 2825-37.
248. Rhodin, J.A.G., *Histology. A Text and Atlas*. 1974, Oxford University Press: New York, NY. p. 371-398.
249. Kabeya, Y., et al., *LC3, a mammalian homologue of yeast Apg8p, is localized in autophagosome membranes after processing.* EMBO J, 2000. **19**(21): p. 5720-8.
250. Kwon, C.H., et al., *Activation mechanisms of mafosfamide and the role of thiols in cyclophosphamide metabolism.* J Med Chem, 1987. **30**(2): p. 395-9.
251. Zeh, H.J., 3rd and M.T. Lotze, *Addicted to death: invasive cancer and the immune response to unscheduled cell death.* J Immunother, 2005. **28**(1): p. 1-9.
252. Calogero, S., et al., *The lack of chromosomal protein Hmg1 does not disrupt cell growth but causes lethal hypoglycaemia in newborn mice.* Nat Genet, 1999. **22**(3): p. 276-80.
253. Hattori, K., et al., *Quantitative in vivo assay of human granulocyte colony-stimulating factor using cyclophosphamide-induced neutropenic mice.* Blood, 1990. **75**(6): p. 1228-33.
254. Chowdhury, D. and J. Lieberman, *Death by a thousand cuts: granzyme pathways of programmed cell death.* Annu Rev Immunol, 2008. **26**: p. 389-420.
255. MacDonald, G., et al., *Mitochondria-dependent and -independent regulation of Granzyme B-induced apoptosis.* J Exp Med, 1999. **189**(1): p. 131-44.
256. Hardonk, M.J., et al., *Heterogeneity of rat liver and spleen macrophages in gadolinium chloride-induced elimination and repopulation.* J Leukoc Biol, 1992. **52**(3): p. 296-302.
257. Mizgerd, J.P., et al., *Gadolinium induces macrophage apoptosis.* J Leukoc Biol, 1996. **59**(2): p. 189-95.
258. Lamagna, C., M. Aurrand-Lions, and B.A. Imhof, *Dual role of macrophages in tumor growth and angiogenesis.* J Leukoc Biol, 2006. **80**(4): p. 705-13.
259. Mantovani, A. and A. Sica, *Macrophages, innate immunity and cancer: balance, tolerance, and diversity.* Curr Opin Immunol, 2010.
260. Qian, B.Z. and J.W. Pollard, *Macrophage diversity enhances tumor progression and metastasis.* Cell, 2010. **141**(1): p. 39-51.
261. Rao, D.A., K.J. Tracey, and J.S. Pober, *IL-1alpha and IL-1beta are endogenous mediators linking cell injury to the adaptive alloimmune response.* J Immunol, 2007. **179**(10): p. 6536-46.
262. Yang, H., et al., *Reversing established sepsis with antagonists of endogenous high-mobility group box 1.* Proc Natl Acad Sci U S A, 2004. **101**(1): p. 296-301.
263. Ueno, T., M. Toi, and S. Linder, *Detection of epithelial cell death in the body by cytokeratin 18 measurement.* Biomed Pharmacother, 2005. **59 Suppl 2**: p. S359-62.
264. Gonzalez, V.M., et al., *Is cisplatin-induced cell death always produced by apoptosis?* Mol Pharmacol, 2001. **59**(4): p. 657-63.
265. Wood, L.J., et al., *Cancer chemotherapy-related symptoms: evidence to suggest a role for proinflammatory cytokines.* Oncol Nurs Forum, 2006. **33**(3): p. 535-42.
266. Marnett, L.J., *Oxyradicals and DNA damage.* Carcinogenesis, 2000. **21**(3): p. 361-70.

267. Schmitt, C.A., C.T. Rosenthal, and S.W. Lowe, *Genetic analysis of chemoresistance in primary murine lymphomas.* Nat Med, 2000. **6**(9): p. 1029-35.
268. Shimizu, S., et al., *Role of Bcl-2 family proteins in a non-apoptotic programmed cell death dependent on autophagy genes.* Nat Cell Biol, 2004. **6**(12): p. 1221-8.
269. Cao, C., et al., *Inhibition of mammalian target of rapamycin or apoptotic pathway induces autophagy and radiosensitizes PTEN null prostate cancer cells.* Cancer Res, 2006. **66**(20): p. 10040-7.
270. Amaravadi, R.K., et al., *Autophagy inhibition enhances therapy-induced apoptosis in a Myc-induced model of lymphoma.* J Clin Invest, 2007. **117**(2): p. 326-36.
271. Katayama, M., et al., *DNA damaging agent-induced autophagy produces a cytoprotective adenosine triphosphate surge in malignant glioma cells.* Cell Death Differ, 2007. **14**(3): p. 548-58.
272. Apel, A., et al., *Blocked autophagy sensitizes resistant carcinoma cells to radiation therapy.* Cancer Res, 2008. **68**(5): p. 1485-94.
273. Ding, W.X., et al., *Differential effects of endoplasmic reticulum stress-induced autophagy on cell survival.* J Biol Chem, 2007. **282**(7): p. 4702-10.
274. Ullman, E., et al., *Autophagy promotes necrosis in apoptosis-deficient cells in response to ER stress.* Cell Death Differ, 2008. **15**(2): p. 422-5.
275. Albert, M.L., *Death-defying immunity: do apoptotic cells influence antigen processing and presentation?* Nat Rev Immunol, 2004. **4**(3): p. 223-31.
276. Tesniere, A., et al., *Molecular characteristics of immunogenic cancer cell death.* Cell Death Differ, 2008. **15**(1): p. 3-12.
277. Morelli, A.E., et al., *Internalization of circulating apoptotic cells by splenic marginal zone dendritic cells: dependence on complement receptors and effect on cytokine production.* Blood, 2003. **101**(2): p. 611-20.
278. Muller, S., et al., *New EMBO members' review: the double life of HMGB1 chromatin protein: architectural factor and extracellular signal.* EMBO J, 2001. **20**(16): p. 4337-40.
279. Park, J.S., et al., *Involvement of toll-like receptors 2 and 4 in cellular activation by high mobility group box 1 protein.* J Biol Chem, 2004. **279**(9): p. 7370-7.
280. Yang, D., et al., *High mobility group box-1 protein induces the migration and activation of human dendritic cells and acts as an alarmin.* J Leukoc Biol, 2007. **81**(1): p. 59-66.
281. Orlova, V.V., et al., *A novel pathway of HMGB1-mediated inflammatory cell recruitment that requires Mac-1-integrin.* EMBO J, 2007. **26**(4): p. 1129-39.
282. Grivennikov, S.I., F.R. Greten, and M. Karin, *Immunity, inflammation, and cancer.* Cell, 2010. **140**(6): p. 883-99.
283. Stockman, G.D., et al., *Differential effects of cyclophosphamide on the B and T cell compartments of adult mice.* J Immunol, 1973. **110**(1): p. 277-82.
284. Lerman, S.P. and W.P. Weidanz, *The effect of cyclophosphamide on the ontogeny of the humoral immune response in chickens.* J Immunol, 1970. **105**(3): p. 614-9.
285. Kuniyasu, H., et al., *Colon cancer cell-derived high mobility group 1/amphoterin induces growth inhibition and apoptosis in macrophages.* Am J Pathol, 2005. **166**(3): p. 751-60.

286. Ishiguro, H., et al., *Receptor for advanced glycation end products (RAGE) and its ligand, amphoterin are overexpressed and associated with prostate cancer development.* Prostate, 2005. **64**(1): p. 92-100.
287. Wei, M.C., et al., *Proapoptotic BAX and BAK: a requisite gateway to mitochondrial dysfunction and death.* Science, 2001. **292**(5517): p. 727-30.
288. Dimri, G.P., et al., *A biomarker that identifies senescent human cells in culture and in aging skin in vivo.* Proc Natl Acad Sci U S A, 1995. **92**(20): p. 9363-7.